

Edinburgh Napier University

Polymer Microspheres for Microbial Detection

Wisrutta Atthakor

A thesis submitted in partial fulfilment of the requirements of
Edinburgh Napier University for the degree of
Doctor of Philosophy

October 2009

I certify that the work carried out and presented in this thesis is my own, except where acknowledgements have been made, and that the material presented here has not been previously presented for assessment as part of any degree.

Wisrutta Atthakor

Abstract

Microspheres have become an important material in the biomedical and environmental sciences, particularly for use in the detection of pathogenic microorganisms and toxins as well as for use as carriers in drug delivery. In this study, their use in microbial detection, with particular emphasis on immunochromatographic assays, was investigated. Two main types of microspheres were studied: colloidal gold and polymeric. The original plan to combine the use of colloidal gold and fluorescent-dye-labelled PMMA microspheres as a signal generator, in order to enhance detection signals and improve detection limit, was abandoned when preliminary detection experiments showed that the use of colloidal gold was not so beneficial after all, taking into account the amount of light lost to absorption by the gold particles. Therefore, it was decided to use Rhodamine B-labelled PMMA microspheres. PMMA particles, both unlabelled and internally labelled with Rhodamine B, were synthesised by emulsion polymerisation and yielded monodisperse particles of around 200 nm and 300 nm, respectively. An attempt to co-polymerise MMA with HEMA to form 200 nm-sized monodisperse P(MMA-HEMA) microspheres in order to create functional –OH groups on the microsphere surface to be used in chemical covalent coupling with monoclonal antibodies resulted in aggregated microspheres and non-uniform particles, and were therefore not used for covalent coupling. Attachment of monoclonal antibodies onto the surface of Rhodamine-B labelled PMMA microspheres by passive adsorption also resulted in aggregated particles. Diffusion and detection experiments were carried out on the Rhodamine-B labelled PMMA microspheres. Diffusion of PMMA microspheres along a nitrocellulose strip was found to be 42% slower than the diffusion of colloidal gold along a nitrocellulose strip. Using a spectrophotometer, detection experiments were performed on dilutions of an original stock solution of 1% w/v PMMA in distilled water. The detection limit was found to be of the order of 10^{-3} .

This study has investigated the materials that constitute an immunochromatographic assay and has illustrated some of the complications associated with the synthesis of copolymer microspheres and immobilisation of antibodies onto their surfaces. Further work on how to improve on the methods discussed in this study have also been recommended.

Contents

Acknowledgements	i
Abbreviations and Notation	ii
List of Figures	v
List of Tables	viii

Chapter 1 Introduction 1

Chapter 2 Review of Literature 4

2.1	Developments in Microbial Detection Methods	4
2.1.1	Rapid Detection and Biosensors	4
2.2	Developments in Lateral Flow Technology	10
2.3	Lateral Flow Technology	12
2.3.1	Configurations and Assay Protocol	12
2.3.2	Materials	18
2.4	Principles of Immunology	19
2.4.1	Structure and Function of Antibodies	19
2.4.2	Monoclonal Antibodies	22
2.4.3	Antibody-Antigen Interaction	29
2.5	Antibodies and Antigens in Lateral Flow Technology	31
2.6	Microspheres	34
2.6.1	Colloidal Gold Microspheres	35
2.6.2	Polymer Microspheres	40
2.6.3	Polymerisation Mechanisms and Kinetics	41
2.6.4	Polymerisation Techniques and Processes	48
2.6.5	Polymer Microspheres in Bioconjugation and Protein Immobilisation	55
2.6.6	Microsphere Surface Chemistry and Surface Modification	64
2.6.7	Cleaning and Separation of Microspheres	65
2.6.8	Microspheres Imaging	70
2.7	Adhesion Mechanisms and Theories	77
2.7.1	Mechanical Interlocking	77
2.7.2	Electrostatic or Electronic Adhesion	78
2.7.3	Diffusive Adhesion	79
2.7.4	Adsorption or Dispersive Adhesion	79

2.7.5	Chemisorption or Chemical Adhesion	81
2.8	Conjugation of Monoclonal Antibodies to Polymer Microspheres	83
2.8.1	Simple or Passive Adsorption	83
2.8.2	Complex Adsorption	85
2.8.3	Covalent Chemical Coupling	86
2.9	Principles of Fluorescence	88
2.9.1	The Three Stages of the Fluorescence Process	89
2.9.2	Absorption and Emission Spectra	91
2.9.3	Quantum Yield	93
2.9.4	Fluorescence Lifetime	95
2.10	Detection and Signal Recovery	97
2.10.1	Signal Measurements and Noise	97
2.10.2	Phase Sensitive Detection and the Lock-In Amplifier	99

Chapter 3 Experimental Methods **103**

3.1	Preliminary Studies	103
3.1.1	Preliminary Experiment	103
3.1.2	Design of cubic sample holder to house cylindrical vial	103
3.1.3	White Light Experiment on Colloidal Gold and Colloidal Gold Conjugate	104
3.1.4	Fluorescence Experiments	105
3.2	PMMA Synthesis	107
3.2.1	Preparation of Microspheres	107
3.3	Copolymerisation of P(MMA-HEMA)	111
3.4	Preparation of Monoclonal Antibody	113
3.4.1	Purification of IgG	113
3.5	Conjugation of Antibody to PMMA Microspheres	116
3.5.1	Preparation of Microspheres in Adsorption Buffer: Phosphate Buffer pH 8.0	116
3.5.2	Passive Adsorption	116
3.5.3	Determination of Bound/Unbound Proteins	117
3.6	Microsphere Analyses using Imaging Technology	118
3.6.1	Scanning Electron Microscopy	118
3.6.2	Atomic Force Microscopy	118
3.6.3	Confocal Microscopy	119
3.7	Diffusion of Microspheres	119
3.8	Detection Experiments	120
3.8.1	Preparation of 1% w/v PMMA Solution	120
3.8.2	Preparation of Dilutions of PMMA from a Common Stock	121
3.8.3	Design and set-up of Detection Experiments	122
3.8.4	Detection Limit	123

Chapter 4 Results **124**

4.1	Preliminary Studies	124
4.1.1	Preliminary Experiment	124
4.1.2	White Light Experiment on Colloidal Gold and Colloidal Gold Conjugate	125
4.1.3	Fluorescence Experiment	125
4.2	PMMA Synthesis	128
4.2.1	AFM Imaging of PMMA Microspheres	128
4.2.2	SEM Imaging of PMMA Microspheres	132
4.2.3	Confocal Microscope Imaging of PMMA Microspheres	133
4.3	Copolymerisation of P(MMA-HEMA)	134
4.3.1	SEM Imaging of P(MMA-HEMA)	134
4.4	Preparation of Monoclonal Antibody	135
4.4.1	Purification of IgG	135
4.5	Conjugation of Antibody to Microspheres	136
4.6	Diffusion of Microspheres	138
4.7	Detection Experiments	139

Chapter 5 Discussion **147**

5.1	Preliminary Studies	147
5.2	Polymer Microspheres	151
5.3	Antibody-Microsphere Conjugation	155
5.4	Imaging Techniques	158
5.5	Detection Limits	159

Chapter 6 Conclusions **160**

Chapter 7 Recommendations for Future Work **162**

7.1	Recommendation for production of P(MMA-HEMA)	163
7.2	Recommendation for covalent chemical coupling	164
7.3	Recommendation for microsphere cleaning and separation	164
7.4	Recommendation for lock-in amplification	165

References **166**

APPENDIX I Sample Calculations **173**

Acknowledgements

I would like to express my sincerest gratitude for all who have been involved with my PhD, both directly and indirectly. First and foremost, I would like to thank my Director of Studies, Mr Colin Hindle, for his continuing supervision, guidance and support and his indefatigable confidence in me even through my own periods of self-doubt. I would also like to thank my second supervisor, Prof Nick Christofi, for his support and patience throughout my studies, as well as Prof Janos Hajto, my original supervisor, for getting me started on my PhD studies.

In addition to my current and past supervisors, I would like to thank Dr Keith Guy and Dr Martin Wilson for their help on antibodies, Dr Vasileios Koutsos of Edinburgh University for kindly teaching me how to use an AFM and allowing me access to his department's AFM. I would also like to thank Dr Neil Shearer and Mr Bill Brownlee for their help on the SEM. I would particularly like to thank all the technical staff at Napier University, especially Mr Derek Cogle, Ms Kim Kellet, Mr Bill Young and Dr John Kinross, all of whom have greatly assisted me in the accommodation of laboratory space and equipment.

To all my fellow researchers at Napier University, I would like to thank you for making my time here a most pleasant and enjoyable one. It has been a pleasure working alongside you and socialising with you. For those who have yet to complete their PhDs, I wish you all the very best.

Last, but most definitely not least, I would like to say a special thanks to all my friends and family, especially my parents, my sister Platima and my boyfriend-turned-husband George who have all been incredible in their support and encouragement.

Abbreviations and Notation

A	absorbance
Ab	antibody
AC	alternating current
AFM	atomic force microscope
Ag _x	antigen X
AIBN	2,2'-azobisisobutyronitrile
Au	gold
<i>c</i>	speed of light (m s ⁻¹)
<i>c</i>	concentration of fluorophore (mol l ⁻¹)
C _b	component concentration in bulk solution (g l ⁻¹)
CDR	complementary determining region
C _f	component concentration in filtrate stream (g l ⁻¹)
C _H	constant heavy chain
C _L	constant light chain
Cl	chlorine
cmc	critical micelle concentration
C _w	component concentration in membrane surface (g l ⁻¹)
DC	direct current
DNA	deoxyribonucleic acid
E	energy (J)
ε	molar absorptivity coefficient (l mol ⁻¹ cm ⁻¹)
EIS	electrolyte-insulator-semiconductor
ELISA	enzyme-linked immunosorbent assay
F	fluorescence
Fab	fragment, antigen-binding
Fc	fragment, crystallisable
FITC	fluorescein isothiocyanate
FR	framework region
FTIR	Fourier transform infrared
G ₀	ground state

h	Planck's constant (J s)
HAT	hypoxanthine and thymidine
hCG	human Choriogonadotropin
HEMA	2-hydroxyethyl methacrylate
HIV	human immunodeficiency virus
HVR	hypervariable region
I	light intensity
I_0	intensity of incident light
Ig	immunoglobulin
IgA	immunoglobulin A
IgD	immunoglobulin D
IgE	immunoglobulin E
IgG	immunoglobulin G
IgM	immunoglobulin M
IUPAC	International Union of Pure and Applied Chemistry
k_i	internal conversion
k_p	phosphorescence
k_q	quenching
λ_A	excitation (or absorption) wavelength (m)
LAPS	light-addressable potentiometric sensors
LAT	latex agglutination test
LED	light emitting diode
mAb	monoclonal antibody
MES	2-(N-morpholino)ethanesulphonic acid
MMA	methyl methacrylate
μsph	microsphere
ν_A	frequency of incoming photon at excitation wavelength (Hz)
NFF	normal flow filtration
NMR	nuclear magnetic resonance
PBS	phosphate buffer saline
P_F	feed pressure (bar)
PHEMA	poly(2-hydroxyethyl methacrylate)

pI	isoelectric point
P_L	filtrate pressure (bar)
PMMA	polymethyl methacrylate
poly(MMA-HEMA)	poly(methyl methacrylate-co-2-hydroxyethyl methacrylate)
P_R	retentate pressure (bar)
PS	polystyrene
PSD	phase sensitive detector
P(S-HEMA)	poly(styrene-co-2-hydroxyethyl methacrylate)
PVC	polyvinyl chloride
Q	quantum yield
Q_F	feed flow rate ($l\ h^{-1}$)
Q_f	filtrate flow rate ($l\ h^{-1}$)
Q_R	retentate flow rate ($l\ h^{-1}$)
SEM	scanning electron microscope
S_n	excited singlet states ($n = 1, 2, \dots$)
SPR	surface plasmon resonance
t	time
τ	fluorescence lifetime
T_1	transition state
TFF	tangential flow filtration
TMP	applied pressure across membrane surface (bar)
ν	vibrational energy state
V_H	variable heavy chain
V_L	variable light chain
ω	frequency in lock-in amplifier
x	pathlength of light beam through solution (cm)
$x(t)$	incident light in lock-in amplifier
$x(t+\Delta)$	phase-adjusted signal
$y(t)$	output signal in lock-in amplifier
z	magnified output signal in lock-in amplifier

List of Figures

Figure 2.1 Basic biosensor. A schematic diagram showing the main components of a typical biosensor.	5
Figure 2.2 Schematic diagram of a lateral flow test strip	12
Figure 2.3 Snapshot view of the progressive flow of a lateral flow assay	13
Figure 2.4 Step-by-step process of a lateral flow assay	16
Figure 2.5 Structure of an IgG	20
Figure 2.6 General protocol for the production of monoclonal antibodies. Production of monoclonal antibodies derived from fusion of normal antibody-producing B cell and myeloma cell, based on the original methods developed by Köhler and Milstein (1975).	25
Figure 2.7 Macroscopic representation of the steps of purification by affinity chromatography	27
Figure 2.8 Absorbance spectrum at 280 nm of an affinity chromatography	27
Figure 2.9 Formation of colloidal gold particle by reduction of Au ³⁺ ions. Adapted from Chandler (2000).	36
Figure 2.10 Individual colloidal gold particle in solution. Adapted from Weiser (1933).	37
Figure 2.11 Interaction of white light with colloidal gold microspheres in solution	38
Figure 2.12 Free-radical initiators. Organic compounds containing a labile group.	42
Figure 2.13 Thermal dissociation of benzoyl peroxide to form two benzoyloxy radicals	43
Figure 2.14 Thermal dissociation of AIBN to form two cyanoisopropyl radicals	43
Figure 2.15 Representation of an emulsion polymerisation system	51
Figure 2.16 General mechanism of surfactant-free emulsion polymerisation	53
Figure 2.17 Polymerisation of styrene to form polystyrene	55
Figure 2.18 Polymerisation of styrene: initiation using benzoyl peroxide	56
Figure 2.19 Polymerisation of styrene: propagation	57
Figure 2.20 Polymerisation of styrene: termination by combination	57
Figure 2.21 Polymerisation of methyl methacrylate to form polymethyl methacrylate	58
Figure 2.22 Surfactant-free emulsion polymerisation of methyl methacrylate: initiation using a persulphate initiator	59
Figure 2.23 Surfactant-free emulsion polymerisation of methyl methacrylate: propagation	60
Figure 2.24 Surfactant-free emulsion polymerisation of methyl methacrylate: termination by disproportionation	60
Figure 2.25 Polymerisation of 2-hydroxyethyl methacrylate to form poly(2-hydroxyethyl methacrylate)	61
Figure 2.26 Copolymerisation of styrene and HEMA to form P(S-HEMA): one possible outcome in the form -ABAB-	62
Figure 2.27 Copolymerisation of MMA and HEMA to form P(MMA-HEMA): one possible outcome in the form -ABAB-	63

Figure 2.28 Schematic diagram of a tangential flow filtration system. Adapted from (Millipore 2003).	67
Figure 2.29 Flows and forces in a tangential flow filtration channel. Adapted from (Millipore 2003).	68
Figure 2.30 Pressure profile in a TFF channel. Adapted from (Millipore 2003).	68
Figure 2.31 Comparison of Normal Flow Filtration and Tangential Flow Filtration separation mechanisms	69
Figure 2.32 SEM column	71
Figure 2.33 Schematic diagram of how an AFM operates. Adapted from Lehenkari <i>et al</i> (2000).	73
Figure 2.34 Contact mode AFM. Adapted from West (2007). (a) Potential diagram showing the region of the probe while scanning in contact mode. (b) In contact mode the probe glides over the surface.	74
Figure 2.35 Tapping mode AFM. Adapted from West (2007). (a) Potential diagram showing the motion of the probe in tapping mode. (b) The probe vibrates as it scans across the surface.	75
Figure 2.36 Jabłoński diagram	88
Figure 2.37 Multippeak absorption spectrum	92
Figure 2.38 Absorption and emission spectra depicting Mirror Image Rule and Stokes Shift	92
Figure 2.39 Excitation and emission spectrum of a fluorophore	93
Figure 2.40 Signal buried in noise	98
Figure 2.41 Introduction of low pass filter	99
Figure 2.42 Schematic diagram of an experimental set-up using a lock-in amplifier	101
Figure 3.1 Aluminium sample holder to house cylindrical vial containing sample	103
Figure 3.2 Fibre-optic white light (cold) source	104
Figure 3.3 Set up of first fluorescence experiment. Illumination source and detector are aligned in a straight line.	105
Figure 3.4 Set up of second fluorescence experiment. Detection unit is at a right angle to the illumination source.	106
Figure 3.5 Set-up of equipment for PMMA synthesis	107
Figure 3.6 Set-up of equipment for P(MMA-HEMA) synthesis	111
Figure 3.7 Purification of MAb by affinity chromatography	114
Figure 3.8 Aluminium sample holder to house a 1 cm pathlength cuvette	122
Figure 4.1 Result of preliminary experiment. Reflectance spectra of colloidal gold and colloidal gold-antibody conjugate using a 60 W desk lamp as a light source.	124
Figure 4.2 Result of white light experiment on dilutions of colloidal gold and colloidal gold-antibody conjugate	125
Figure 4.3 Result of the first fluorescence experiment without the use of a filter	126
Figure 4.4 Result of the first fluorescence experiment, using a red filter	126
Figure 4.5 Result of second fluorescence experiment. Spectra of dilutions of Lumogen Red illuminated by varying intensities of green LED source.	127
Figure 4.6 AFM Images of unlabelled PMMA microspheres: reaction 3	128

Figure 4.7 AFM images of unlabelled PMMA microspheres: reaction 4	128
Figure 4.8 AFM images of unlabelled PMMA microspheres: reaction 5	129
Figure 4.9 AFM images of unlabelled PMMA microspheres: reaction 6	129
Figure 4.10 AFM image of unlabelled PMMA microspheres: reaction 7	130
Figure 4.11 AFM image of PMMA microspheres, internally labelled with the fluorescent dye Rhodamine B	130
Figure 4.12 Cross-sectional line analyses of PMMA image shown in Figure 4.11	131
Figure 4.13 SEM image of unlabelled PMMA microspheres: images obtained using a Cambridge Instruments StereoScan Mk II SEM	132
Figure 4.14 Zoomed in image taken from an area of the sample shown in Figure 4.13	132
Figure 4.15 Images of PMMA microspheres obtained using a Carl Zeiss AG, LSM 510 META confocal microscope	133
Figure 4.16 Zoomed image of PMMA microspheres obtained on a confocal microscope	133
Figure 4.17 SEM images of P(MMA-HEMA) using a cold field emission SEM	134
Figure 4.18 Absorbance spectrum for purification of anti-Phycoerythrin	135
Figure 4.19 SEM images of PMMA in phosphate buffer, pH 8.0	136
Figure 4.20 SEM images of PMMA-IgG conjugate in phosphate buffer	137
Figure 4.21 Rate of diffusion of PMMA along nitrocellulose strips as compared to colloidal gold and its conjugate	138
Figure 4.22 Emission spectra of dilutions of Rhodamine B-labelled PMMA	139
Figure 4.23 Emission spectra for 10^{-3} dilution subjected to varying LED intensities, compared to the Blank	140
Figure 4.24 Emission spectra for 10^{-4} dilution subjected to varying LED intensities, compared to the Blank	141
Figure 4.25 Emission spectra for 10^{-5} dilution subjected to varying LED intensities, compared to the Blank	141
Figure 4.26 Emission spectra for 10^{-6} dilution subjected to varying LED intensities, compared to the Blank	142
Figure 4.27 Emission spectra for dilutions 10^{-3} to 10^{-6} subjected to an LED intensity of 215 mA, compared to the Blank	142
Figure 4.28 Emission spectra for dilutions 10^{-3} to 10^{-6} subjected to an LED intensity of 420 mA, compared to the Blank	143
Figure 4.29 Emission spectra for dilutions 10^{-3} to 10^{-6} subjected to an LED intensity of 645 mA, compared to the Blank	143
Figure 4.30 Comparison of peak emission intensities for dilutions at varying source intensities	144
Figure 4.31 Comparison of peak emission intensities for increasing source intensities	145
Figure 4.32 Comparison of peak emission intensities at increasing source intensities	145
Figure 4.33 Comparison of peak emission intensities at increasing source intensities	146

List of Tables

Table 2.1 A summary of the comparison of the AFM to the SEM (West 2007).	76
Table 3.1 Dimensions for aluminium sample holder used to house cylindrical vial	104
Table 3.2 PMMA Synthesis Reaction Conditions	109
Table 3.3 Volume of stock solution required to make up each dilution	121
Table 3.4 Dimensions used for aluminium sample holder used to house a 1 cm pathlength cuvette	122

Chapter 1 Introduction

Microorganisms form a ubiquitous part of all ecosystems on Earth. From the depths of the arctic seas, to the high-rise metropolises of America and China, the environment teems with a near infinite array of bacteria, viruses, and fungal spores. These microbes permeate their environments completely, flourishing even inside larger, more complex organisms such as humans and other mammals.

Most microorganisms are harmless; in fact, many are vital to the proper functioning of their habitats. Be it phytoplankton forming the foundation of a marine food chain, and hence the basis of an aquatic and terrestrial food web, or harmless strains of *Escherichia coli* producing Vitamin K₂, which is required for blood coagulation, in the human gastrointestinal tract, life as we know it could not be sustained, or even have evolved, without them.

However, within this vast array exist a sizeable number of microorganisms that can have a considerably less benign effect on their surroundings. These effects can range from merely being mildly pathogenic, causing unpleasant but otherwise curable diseases, to being potentially lethal, even in small quantities. Such harmful microorganisms can exist in all the same media as their less dangerous cousins, be it blood, food, soil, air or water, and the effects of their presence could be catastrophic. For example, despite its normal beneficial role, even a very small amount of a pathogenic strain of *E. coli*, for example *E. coli* O157:H7, could represent the start of a very serious outbreak if it were to go unchecked and unnoticed. Under the right conditions, the bacteria would be able to reproduce at an exponential rate, and a small colony could multiply and spread alarmingly rapidly. This example illustrates why it is imperative that such harmful pathogens are detected in the early stages of multiplication, as this would allow suitable preventative measures to be put in place to stop the bacteria from spreading. The swift application of such measures could, in this case, prevent a large scale, and possibly fatal, public health issue from arising.

In the past, the process of determining the presence of a microorganism in a medium was a long and costly process. A small sample of the medium would need to be gathered from the location under investigation, packaged for transport, and then taken to a suitable laboratory site (often many miles from the sample's point of origin). Chemical and biochemical analyses would then be performed on the sample, and assays would have to be carried out. The laboratory testing alone could take hours or even days, and this, coupled with the transportation time from potentially remote locations meant that a result could take quite a considerable time to be returned. As such, in the time taken to confirm the presence of a particular microorganism in an environment, that organism might have had the opportunity to multiply and spread. What may have been small scale contamination could easily now effect a much wider area. If, for example, it were a dangerous pathogen this could have been enough time for a major outbreak to be triggered. Controlling and stopping the spread would have then become extremely difficult. In serious cases many fatalities could have occurred, which may have been preventable had the presence of the pathogens been detected earlier. For example, were a dangerous pathogen to be carried into the water supply of a major urban area by agricultural run-off the effects of this not being detected quickly could be devastating.

Another situation where such microorganisms can be dangerous to human health is in the effects of biological warfare and bioterrorism. Recent threats of *Bacillus anthracis* – bacteria that cause the disease anthrax – in the US have greatly raised fears and led to a state of heightened security alert (Bell 2003). Even false alarms can have a seriously detrimental effect on populations as unnecessary panic leads to heightened levels of anxiety and loss of productivity.

Of approximately 50 million total annual deaths worldwide, it is estimated that about 40% of these are caused by infectious diseases alone (Leonard *et al* 2003). Although the majority of such deaths are currently restricted to the developing world, especially countries where level of water treatment for domestic use is inadequate, it was within the last century that large proportions of the populations of Western Europe were wiped out by the H1N1 type A influenza pandemic, which killed upwards of 50 million people worldwide (Cox *et al* 2003). Recently, Britain experienced an outbreak of foot-and-mouth disease, a highly contagious disease in cattle and other hoofed

animals caused by *Apthovirus spp.* While the effects of this outbreak on human health were minimal, those on agriculture and the economy have been profound. Present fears regarding new strains of avian influenza being potentially passed between humans raise the spectre of another outbreak, potentially comparable in scale to the H1N1 pandemic (Capua and Alexander 2002; Kristensson 2006).

All of the above examples illustrate the need for an ability to rapidly detect *in situ* even small amounts of a particular microorganism in a given environment. However, in addition to being able to do this quickly, it is also equally important that the detection is accurate and sensitive. The capacity to quickly detect large quantities of pathogens, but not to be able to spot the presence of a low quantity of cells if it is there, is insufficient. Furthermore, it is equally useless to be able to quickly detect the presence of microorganisms in minute quantities but to discover later that the microorganisms detected are not the harmful type and not cause for concern. This could lead to unnecessary alarm and panic when what is really there is just background bacteria. In addition to the parameters mentioned, in order to be able to acquire rapid results *in situ*, it is important that the instrument used for detection is easily transportable into the field. For this to be possible, it needs to be small enough in size to not be bulky and inconvenient and should ideally, therefore, be hand-held.

Taking into account all the specifications, the detection device should be small and ergonomic whilst being capable of detecting, accurately and precisely, the smallest quantities of harmful microorganisms in the shortest time possible.

At the outset, the aim of this research project was to create a detection device that combines the properties of larger, more cumbersome biosensors and lateral flow technology into a fully portable optical lateral flow detection device, one that would be an improvement on currently available systems. In this endeavour, existing detection technology is examined and evaluated, through completion of a literature review, which investigates the developments in the fields of microbial detection and, more specifically, lateral flow technology. Colloidal gold microspheres are compared to polymer latex microspheres for use as detection materials in lateral flow technology. Investigations into detection limits and means for improving detection limits are carried out.

Chapter 2 Review of Literature

2.1 Developments in Microbial Detection Methods

The widespread need for rapid and inexpensive detection of microbial contamination in food, clinical samples and aquatic environments, examples of which were illustrated in Chapter 1, has led to a large number of microbial detection methods being developed. As a result, considerable progress has been made in the development of microbial detection devices, commonly known as biological sensors or biosensors (Hobson *et al* 1996).

Conventional methods for microbial detection often involve long and complicated processes. One established and widely used method for determining the presence of and identifying a species of microorganisms is the bacterial cell culture. This method involves growing bacteria in a suitable culture medium such as agar, which is derived from red algae, followed by isolation and then identification. In conventional bacterial monitoring in water samples, for instance, the water samples would be obtained from the site of interest and then transported to a laboratory. They would then be passed through a standard membrane filtration and the filtration membrane would be placed onto a culture medium, where the bacteria, if present, would grow into colonies. Bacteria enumeration and identification can then be carried out. This method can be time-consuming and requires some expertise in microbiological laboratory practices in order to carry out the procedures.

2.1.1 Rapid Detection and Biosensors

When the term rapid detection is referred to, it is generally implied that the time taken to produce a result – from the collection of to the processing of the sample in question – is less than 24 hours. However, this 24-hour time window is considered to be a threshold in terms of “rapid” detection time, meaning that most rapid detection systems strive to fall well within this time limit.

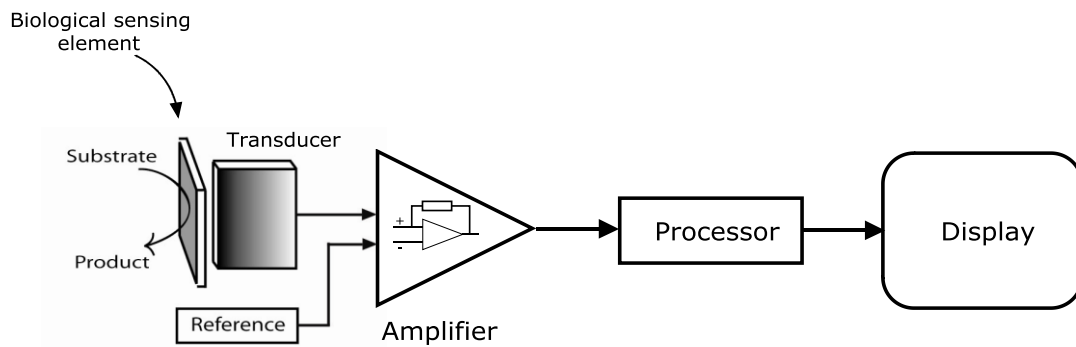


Figure 2.1 Basic biosensor. A schematic diagram showing the main components of a typical biosensor.

It is perhaps evident that the term biosensor comes from the terms bio (or biological) and sensor. However, it would be beneficial to briefly look at the term *sensor* in isolation in order to fully appreciate the biosensor’s meaning and uses, as discussed later on in this section.

A sensor, by its most basic definition, is “a device that receives and responds to a signal or stimulus” (dictionary.com 2007). Sensors range from simple pieces of testing apparatus to complex systems. Take pH tests, for example. The litmus paper test for acids and alkalis is a common and perhaps one of the best known types of sensor available, yet extremely user-friendly. By means of a colour reaction, it gives a qualitative indication of whether a substance is an acid or alkali. More sophisticated methods of determining the degree of acidity include the use of pH papers or a range of indicator solutions such as phenolphthalein or methyl orange. However, the most advanced method of measuring acidity is the use of a pH meter, which is an electrochemical sensor that monitors chemical changes and then produces an electrical response which can be displayed digitally or inputted into a microprocessor.

The insight into the various means by which acidity can be measured and determined gives an indication as to the uses of sensors, and hence biosensors.

A biosensor can be defined as “any of a variety of types of biomolecular probes which measures the presence or concentration of biological molecules, biological structures,

microorganisms, etc. by translating a biochemical interaction at the probe surface into a quantifiable physical signal” (University of Newcastle upon Tyne 1999). It is an analytical device used to detect or monitor biological material or activity, usually by incorporating some form of biological or biologically derived sensing element coupled with a transducer to produce a signal proportional to the analyte concentration.

Biomolecules used as biological sensing elements may include antibodies or other proteins, enzymes, DNA, microorganisms and animal and plant cells or tissues. Upon contact and interaction with a biological or chemical species, the biological sensing component of the device undergoes a physicochemical change. The change, be it a change in optical property, the absorption or emission of light, the uptake or release of gases, density, mass or resistance, is detected by the transducer, which then converts the biological or chemical signal into an electronic signal for processing. The transducers themselves may be of several types, including electrochemical, optical, piezoelectric and thermal.

There are many advantages to using biosensor technology as a microbial detection method. Because the biological recognition molecule is typically immobilised onto or near the transducer, only small amounts are needed. Also, there is a high degree of specificity when using biological sensing elements as they are able to differentiate between the analyte under investigation and other similar molecules. A prime example of this highly specific recognition is that of antibodies, which is discussed in Section 2.4. In addition, biosensors have rapid response times, many of which are capable of obtaining results in real-time. Furthermore, biosensors boast the capacity to provide continuous data without unduly disturbing the analyte, hence minimising the risk of sample contamination.

There are, however, certain notable disadvantages to many commercially available biosensors and attention is drawn to them later on in this section; prior to discussing their disadvantages, several types of biosensor are examined.

Biosensor types are usually labelled by their transducer type and not by the biological sensing element. For example, by definition supplied by IUPAC (Thévenot *et al*

1999), an electrochemical biosensor is a biosensor with an electrochemical transducer, which means that it uses a chemical change to determine the input parameter and produces an output, which is a varying electrical signal proportional to the input parameter.

In general, electrochemical biosensors are based on enzymatic catalysis of a redox reaction – a reaction in which electrons are produced or consumed. Hence, the enzymes used are called redox enzymes. Electrochemical biosensors can be potentiometric or amperometric and the sensor substrate usually contains a number of electrodes. When electrons are produced or consumed during the redox reaction on an active electrode involving the target analyte, ions are produced, creating a potential which is subtracted from the potential from a reference electrode to give a signal. The rate of flow of electrons is proportional to the analyte concentration and the current can either be measured at a fixed potential or the potential can be measured at zero current, which would give a logarithmic result. An example of a commercially successful electrochemical biosensor is the electrochemical glucose biosensor, which monitors glucose concentration by detecting the decrease in oxygen tension, or oxygen bound to red blood cells, as a result of enzymatic oxidation of glucose to gluconic acid and hydrogen peroxide (Magner 1998).

Potentiometric biosensors measure change in ion concentration during a reaction and are typically based on ion-selective electrodes, which convert this activity into an electrical potential that can be measured by a voltmeter or pH meter. They usually contain an immobilised enzyme membrane surrounding the probe of a pH meter where the catalysed reaction generates or absorbs hydrogen ions, leading to a change in pH to be read by the pH meter.

There has been extensive use of potentiometric biosensors for bacterial analyses, including the detection of bacterial contamination in milk, using an L-lactate biosensor, and sequence-specific biosensing of DNA. It was reported by Ercole *et al* (2002) that 10 bacterial cells ml⁻¹ were detected in 1.5 hours, in a recent study using a technique based on light-addressable potentiometric sensors (LAPS) – semiconductor-based systems with an electrolyte-insulator-semiconductor (EIS) – to detect *E. coli* in potable water.

Amperometric biosensors, as the name suggests, use enzymatic catalysts to generate a current between two electrodes. Like potentiometric biosensors, they have been used for the detection of *E. coli* in water and for monitoring bacterial contamination, as well as the detection of *B. anthracis*, an agent used in biological warfare, and neurotoxins such as *E. coli* heat-labile enterotoxin, which is a neurotoxin related to cholera.

Optical biosensors utilise fluorescent or colorimetric molecules to relate changes in light intensity to changes in mass or concentration. They can be based on optical fibres, surface plasmon resonance (SPR), luminescence, fluorescence or absorbance. Many optical fibre biosensors utilise the property of total internal reflection and are based on the use of immobilised antibodies for the specific recognition of the pathogen and have been used in the detection of bacteria such as *Salmonella spp.*, *E. coli* and *Listeria spp.*

Optical biosensors using surface plasmon resonance, like optical fibres, use total internal reflection in its operation but in a somewhat different manner to optical fibres. SPR is having a huge influence on biosensor development and its technology is briefly discussed below.

At an interface between two transparent media of different refractive indices, such as a water-air or glass-water interface, light travelling through from the higher refractive index medium to the one of lower refractive index is mostly refracted and partly reflected, provided the angle of incidence to the normal is less than a particular angle known as the critical angle. If the angle of incidence is greater than the critical angle of incidence, no light is refracted across the interface. In other words, all the light will be reflected back into the medium of higher refractive index; this is known as total internal reflection. If the interface surface is coated with a thin film of a noble metal such as gold, total reflection is prevented due to light being absorbed by the metal film, causing the intensity of reflected light to be reduced. Because of this effect and in addition to the critical angle, there exists another angle known as the surface plasmon resonance angle, greater than the critical angle, at which the loss of light intensity to the metal film is greatest and therefore the reflected light intensity reaches a minimum, or dip. Plasmons are the collective oscillations of the delocalised

electrons (or plasma) at the metal film surface; surface plasmon resonance refers to the resonating of the delocalised electrons when the wave vector, which represents the magnitude and direction, of the incident wave matches the wavelength of the surface plasmons. The change in SPR signal is proportional to the mass of the immobilised biological material on the film and the SPR measures the interactions of the biomolecules with interfaces as a result of changes in the refractive index.

Reported uses of SPR include real-time detection of *E. coli* O157:H7 using antibodies immobilised onto the sensor surface, detection of bacteria in the marine environment and sequence-specific binding of human immunodeficiency virus (HIV) type I (Rich and Myszka 2003; Taylor *et al* 2005; Wu *et al* 2007). Commercially available biosensors based on SPR technology are the Biacore systems (Biacore 2001; Leonard *et al* 2003), which are used in some academic and industrial laboratories.

The major downsides of many of the biosensors discussed thus far are that they tend to be expensive and large; as a result, many laboratories are unable to obtain such specialised equipment and some machines are simply too big to be considered portable. Another disadvantage, despite the sophistication of these biosensors and their ability for rapid detection, is that considerable technical knowledge and skill are often needed to operate the large systems. When designing a compact and portable detection device, it is important to consider the ease with which a sample analysis may be performed. As discussed in Chapter 1, areas most affected by pathogenic contamination and infectious diseases are areas in which funds and technological expertise may be limited. Therefore, a compact, low-cost and user-friendly device capable of performing microbial detection rapidly and accurately would be an extremely useful instrument in this field.

Lateral flow assays, the technology of which is discussed in the next section, are extremely compact, relatively inexpensive to produce compared to larger more complex systems, easy to use and can produce a result in less than ten minutes.

2.2 Developments in Lateral Flow Technology

Lateral flow technology is a “logical extension” (Bangs Labs 1999b) of the latex agglutination tests (LAT), first developed by Singer and Plotz in 1956 for the diagnosis of rheumatoid arthritis (Plotz and Singer 1956a, 1956b). Following the discovery of the LATs, the developments in this technique continued to grow. In 1988, a novel solid-phase sandwich chromatographic strip test called the Clearblue One Step Pregnancy Test was introduced by Unipath Ltd. in Bedford – then part of the Unilever portfolio of companies – for the rapid determination of pregnancy for women by the detection of human Choriogonadotropin (hCG) – a hormone produced by the placenta during pregnancy. The technology was patented (Unilever PLC GB 1988) and launched under the brand name ClearView® which came to include tests for the detection of diseases such as Strep A, Chlamydia, *Clostridium difficile* Toxin A and infectious mononucleosis.

Some of the key advantages of lateral flow techniques, as previously mentioned, are ease of use and low-cost production (and hence relatively low cost to supply); this makes the technology extremely attractive for home or point-of-care use but also incredibly valuable for environmental monitoring, especially in developing countries or areas that are not easy to access. To date, there are several reaction schemes and numerous developments and patents pertaining to lateral flow technology (Unilever PLC GB 1988; Bangs Labs 1999b; Paek *et al* 2000; Shyu *et al* 2002), all of which stem from the original works of Singer and Plotz (1956a, 1956b). Some are more widely used than others; they are appropriate for different types of detections, depending on the subject to be detected. In addition to the different reaction schemes, there are several different configurations on the test strip.

Two main reaction schemes currently used are the Non-Competitive (or direct) and Competitive (or Competitive Inhibition) reaction schemes (Bangs Labs 1999b). The Non-Competitive Scheme – also known as the Double Antibody Sandwich Scheme – is usually used for detecting large macromolecular, multivalent analytes. Multivalency is discussed in Section 2.4.3. Protein and bacterial antigen are usually detected via this method. The Double Antibody Sandwich Scheme uses the appearance of colour on a



detection line as well as on a control line to depict a positive result. Section 2.3 describes the basic principles of lateral flow technology, based on the Non-Competitive Reaction Scheme.

The Competitive Reaction Scheme, on the other hand, is primarily used for detecting small, monovalent molecules and requires an amount of free antigen in the sample that is in excess of the antibody bound to the microsphere. Contrary to the Non-Competitive Scheme, the Competitive Reaction Scheme uses the appearance of only a control line to depict a positive result. The appearance of colour on a second line would mean a negative result.

To date, lateral flow technology is only available for qualitative and semi-quantitative results (Bangs Labs 1999b). However, due to the versatility of the system the race to develop a fully quantitative lateral flow test is ever more appealing. Should there exist a fully quantitative portable detection device, it would be a very powerful tool indeed. Some of the challenges that would need to be overcome are signal-to-noise ratio and detection limit, which are discussed in Section 2.10.

2.3 Lateral Flow Technology

Symbols used in lateral flow diagrams Figure 2.2 to Figure 2.4:

- Y_1 mAb₁: e.g. mouse anti-Ag IgG
- Y_2 mAb₂: e.g. goat anti-Ag IgG
- Y_3 mAb₃: anti-mAb₁ IgG e.g. sheep anti-mouse IgG
-  Y_1 μ sph-mAb₁ conjugate
-  Antigen X (Ag)

2.3.1 Configurations and Assay Protocol

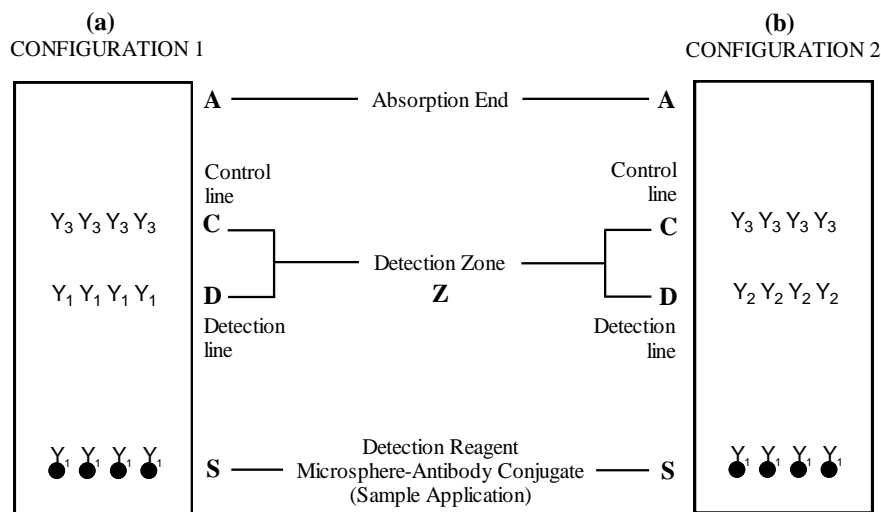


Figure 2.2 Schematic diagram of a lateral flow test strip

Lateral flow assay (or test) is known by several names: immunochromatographic assay or strip test; the different names to which it is referred are used interchangeably. The reasons for the various names by which this method of detection is known become apparent when the technology is more fully understood. Lateral flow technology is based on a chromatographic method developed for the latex

agglutination tests (Plotz and Singer 1956a, 1956b) as previously mentioned. The technology used and being developed in this research is based on the Non-Competitive (or Double Antibody Sandwich) Reaction Scheme, introduced earlier in Section 2.2. There are two basic configurations for the Non-Competitive Reaction Scheme, depicted by Figure 2.2 and discussed later on in this section.

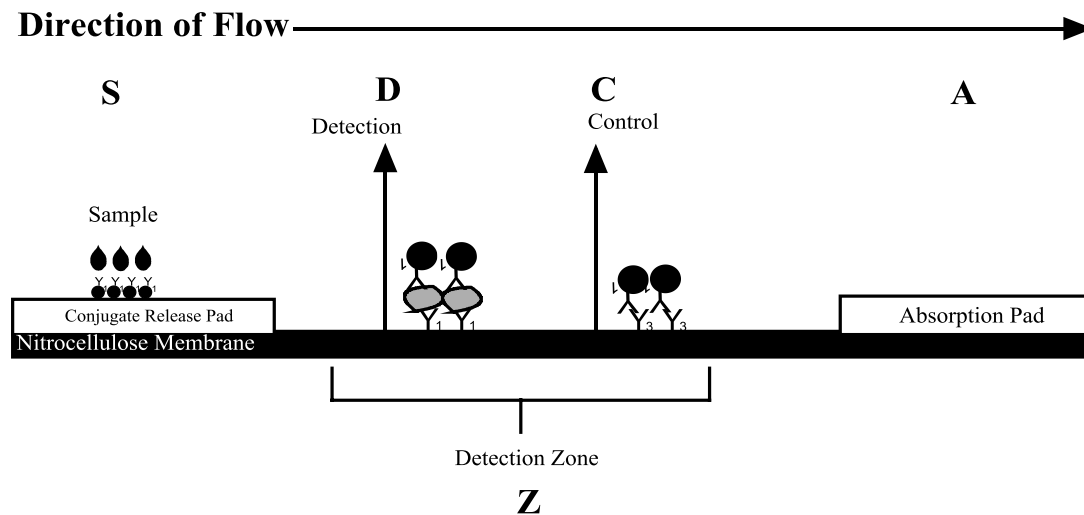


Figure 2.3 Snapshot view of the progressive flow of a lateral flow assay

A lateral flow test is a one-step process, which is essentially the application of a sample to the apparatus and, after a short time interval, a result is obtained. However, in order to illustrate the performance of such a test for the understanding of the technology, it needs to be broken down into a number of steps. The basic process of a lateral flow test can be summarised in a few steps, as illustrated by Figure 2.3: a snapshot diagram showing the progressive flow, from left to right, of an assay. The configuration of the strip assay shown in Figure 2.3 is based on Configuration 1 of the Double Antibody Sandwich Assay (Figure 2.2(a)).

In summary, a liquid analyte is applied to a conjugate release pad (at point S as shown in Figure 2.3) located at one end of the test strip, and is allowed to permeate, by capillary action, through the strip material towards an absorption pad (point A as shown in Figure 2.3) located at the opposite end of the test strip to the conjugate release pad. In doing so, the sample passes into or through a detection zone (Z) –

comprised of a detection line and a control line (denoted by D and C, respectively, in Figure 2.3) – and is trapped by specific binding reagents pre-immobilised on the test strip. The result is determined by the colouration or lack of colouration of one or both of the detection and control lines.

Further dissection of the brief summary described above is needed in order to fully provide a thorough insight into the technology. However, in order to describe the process fully, a more detailed explanation of the basic layout of a test strip is necessary. Thus, a detailed account of the principles, concentrating particularly on the importance of flow from points S through points D and C, is given after a more detailed explanation of the basic layout of a test strip.

As mentioned previously in this section, there are two basic configurations for a lateral flow test strip based on the Non-Competitive Reaction Scheme; they are shown in Figure 2.2 and described as follows.

An immunochromatographic test strip is made up of a reaction pad (usually a nitrocellulose membrane), a conjugate release pad (usually a glass fibre membrane) and an absorption pad (usually a cellulose membrane) as shown in Figure 2.3. Monoclonal antibody (mAb_1) specific to the target antigen (to be detected using this test) is bound to the surface of a visually or optically detectable solid support (by one of several methods discussed in Section 2.8) to form a microsphere-antibody ($\mu\text{sph-}mAb_1$) conjugate. A colloidal solution of this conjugate is dried onto the conjugate release pad, positioned at point S, as shown in Figure 2.2 and Figure 2.3. The antibody used here is one that is specific to the target antigen. For example, if the test is for the detection of *Salmonella spp.*, then an antibody (mAb_1) that may be used could be mouse anti-*Salmonella* monoclonal antibody.

Perhaps the most important area of the test strip is the detection zone (Z), shown in Figure 2.2. The detection zone is comprised of a detection line (D) and a control line (C). Both the detection and control lines are made up of monoclonal antibodies immobilised onto the nitrocellulose reaction pad. The difference in antibody type at the detection line between test strips is what makes the difference between the two

configurations. In Configuration 1 (shown in Figure 2.2(a)) the antibody immobilised at the detection line is of the same type as the antibody conjugated onto the solid support: mAb_1 . This antibody (mAb_1), as previously mentioned, is a monoclonal antibody specific to the target antigen. In Configuration 2 (shown in Figure 2.2(b)) the antibody (mAb_2) immobilised at the detection line is of a different type from the antibody (mAb_1) conjugated to the solid support. Although mAb_2 is different to that used in Configuration 1, it follows that it performs the same function as that used in Configuration 1. Thus, it also follows that mAb_2 is also a monoclonal antibody specific to the target antigen, although one that comes from a different source animal. An example of mAb_2 used in Configuration 2 may be goat anti-*Salmonella* monoclonal antibody – again, in the case that the target antigen is *Salmonella*). The reasons why both configurations work become clear when the principles of antibodies and their interactions with antigens are further discussed in Section 2.4.

Moving along the strip from the detection line is the control line (C), shown in Figure 2.2. The monoclonal antibody immobilised onto the nitrocellulose reaction pad at the control line is of a third type of antibody: mAb_3 . This third type of antibody (mAb_3) is a species-specific anti-immunoglobulin antibody, specific for the conjugate antibody (mAb_1) on the microsphere surface. In other words, it is an antibody against the first type of antibody: $mAb_3 = \text{anti-}mAb_1$. An example of mAb_3 is goat anti-mouse monoclonal antibody (provided that mAb_1 used is a mouse antibody). Again, the details of these interactions are discussed in Section 2.4.

In the detailed account of the principles of a lateral flow test that follows, the discussions will be based on Configuration 1 of the Double Antibody Sandwich Reaction Scheme, illustrated in Figure 2.2 and Figure 2.3.

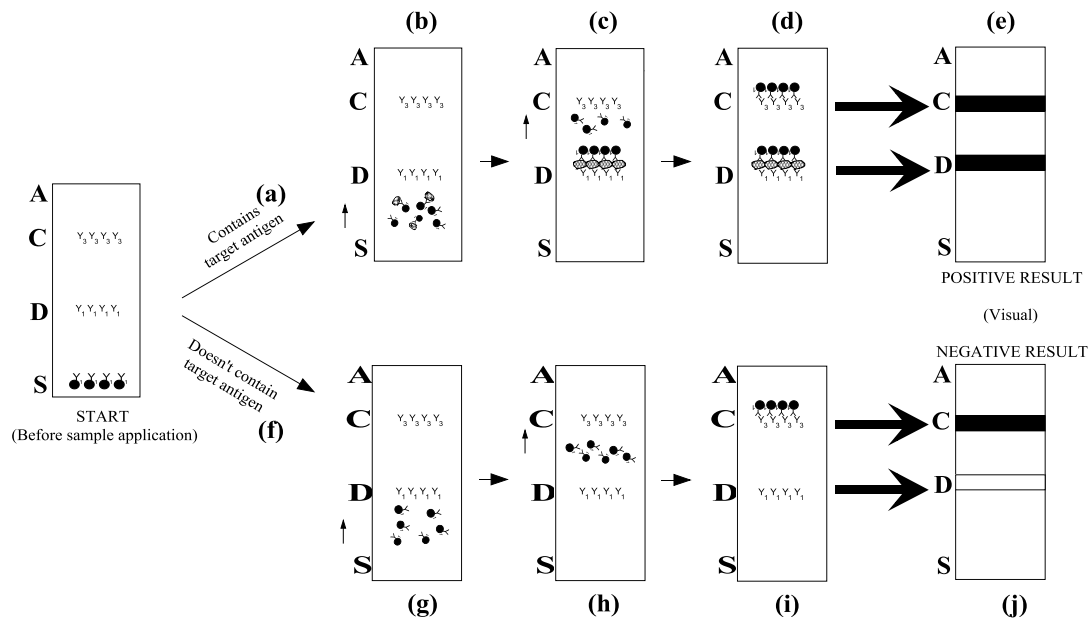


Figure 2.4 Step-by-step process of a lateral flow assay

At the start of an analysis, a liquid analyte – blood, water or other fluid – is applied to the conjugate release pad at point S, as shown in Figure 2.3. The liquid dislodges the $\mu\text{sph-mAb}_1$ conjugate, previously dried on the conjugate release pad, and the $\mu\text{sph-mAb}_1$ enters into a mixed solution with the analyte. Figure 2.4 shows a step-by-step process of the analysis for the case of a positive assay (following route (a) in Figure 2.4) and a negative assay (following route (f)), showing the movements of the particles of the mixed solution along the test strip.

The step-by-step process of a positive assay is described thus:

In a positive assay, the analyte contains the target antigen (Ag_x). Once the liquid sample has been applied and the $\mu\text{sph-mAb}_1$ conjugate has entered into solution, the antibody (mAb_1) on the surface of the microsphere support will bind to the target antigen via its antigenic recognition site (described in Section 2.4). There is an excess of $\mu\text{sph-mAb}_1$ conjugate compared to the number of antigen present; thus, some of the $\mu\text{sph-mAb}_1$ conjugate will not contain a bound antigen. The liquid mixture thus contains a mixture of bound and unbound particles, as shown in Figure 2.4(b). These continue to diffuse along the nitrocellulose reaction strip towards the detection line (D) – the first area of the detection zone (Z). When the mixture reaches the detection

line (D) containing the immobilised antibody (mAb_1), any $\mu\text{sph-mAb}_1\text{-Ag}_x$ macromolecule will get trapped by the antibody (mAb_1) on the reaction pad: the antibody (mAb_1) on the reaction pad binds to the antigen in the macromolecule and thus traps everything else bound to the antigen. This is shown at point D in Figure 2.4(c). The remaining unbound $\mu\text{sph-mAb}_1$ conjugate continues to travel along the test strip towards the control line (C), as shown in Figure 2.4(c). When the excess $\mu\text{sph-mAb}_1$ conjugate reaches the control line (C), the antibody (mAb_3) immobilised at this line will trap the $\mu\text{sph-mAb}_1$ conjugate (Figure 2.4(d)): the Fab fragment of mAb_3 binds to the Fab fragment of the mAb_1 antibody on the microsphere. This interaction is further discussed in Section 2.4.

The step-by-step process of a negative assay is described thus:

In a negative assay, the analyte does not contain the target antigen (Ag_x). When the liquid sample has been applied and the $\mu\text{sph-mAb}_1$ conjugate has entered into solution, there will be no target antigen for the antibody (mAb_1) on the surface of the microsphere support to bind to. Thus, the $\mu\text{sph-mAb}_1$ conjugate diffuses, unbound, along the nitrocellulose reaction strip towards the detection line (D) as shown in Figure 2.4(g). When the mixture reaches the detection line (D) containing the immobilised antibody (mAb_1), the $\mu\text{sph-mAb}_1$ conjugate will not get trapped by the antibody (mAb_1) on the reaction pad: the antibody (mAb_1) on the reaction pad binds to the target antigen only, and will therefore not bind to anything else if there is no target antigen present. The unbound $\mu\text{sph-mAb}_1$ conjugate continues to travel along the test strip towards the control line (C), as shown in Figure 2.4(h). When the $\mu\text{sph-mAb}_1$ conjugate reaches the control line (C), the antibody (mAb_3) immobilised at this line will trap the $\mu\text{sph-mAb}_1$ conjugate (Figure 2.4(i)) as it does in a positive assay.

It can thus be seen that in a positive assay, biological interaction occurs at both the detection line (D) and the control line (C). In a negative assay, biological interaction occurs only at the control line (C). As previously mentioned, the solid support used would be a visually or optically detectable microsphere particle. Hence, the result that can be seen either visually or optically is shown in Figure 2.4(e) for the positive result and in Figure 2.4(j) for the negative result. It follows that if the appearance of colour

occurred only at the detection line, the test is considered void. Likewise, if no colour appears, then the test is also void.

There are several reasons for a test becoming void. One reason is that the particles did not diffuse properly down the length of the strip and thus did not pass through the appropriate regions of the strip to be trapped by the antibodies immobilised on the detection and control lines. Another reason could be that there were not enough $\mu\text{sph-mAb}_1$ conjugate molecules in excess of the target antigen to diffuse through to the control line to be trapped by the antibody immobilised there.

2.3.2 Materials

There are two main types of material that constitute the components and functioning of a lateral flow assay. One of the most important ingredients of a lateral flow assay is the antibody to the antigen. Monoclonal antibody specific to the antigen is normally used; reasons for the use of monoclonal antibodies are discussed in sections 2.4.2 and 2.5. A second type of antibody may be used for the detection line or the same type of antibody as that bound to the solid support may be used. A control antibody, usually an antibody to the first monoclonal antibody, is needed for the control line. The solid support – microspheres of uniform size – is required for the conjugation with the monoclonal antibody but also as an important component of the detection process.

In order to fully understand and demonstrate the simplicity of this technology, it is first necessary to comprehend the complexities behind this technique that allow it to be thus. The principles, mechanisms and properties of the materials that make up this detection method must therefore be explained and acknowledged. Sections 2.4 to 2.8 discuss in detail the materials that make up the core of an immunochromatographic assay.

2.4 Principles of Immunology

In order to understand the chemistry of antibody-antigen binding and its relevance in lateral flow technology, it is essential to first understand the chemical structure of antibodies. The chemistry of antibodies determines three important functions. Firstly, it determines the versatility in antigen binding. Antibodies will bind to an infinite number of antigens, including artificial antigens that do not exist naturally. Antibody molecules are incredibly diverse; they respond to a vast array of determinants. Secondly, the chemical structure determines the specificity of antibodies. A particular antibody will only react to a specific determinant and will not react to unrelated determinants. Thirdly, the chemical structure determines the biological effector mechanisms. Section 2.4.1 discusses the chemistry of antibodies in greater detail and Section 2.4.3 provides a brief account of antibody-antigen interaction.

2.4.1 Structure and Function of Antibodies

Antibodies, also known as immunoglobulins (Ig), are a type of soluble glycoproteins belonging to the class of proteins called globulins due to their globular structure. There are three types of globulins: alpha (α -globulin), beta (β -globulin) and gamma (γ -globulin). Elvin Kabat *et al* (Abbas 2000) showed that most antibodies are found in the third-fastest migrating group of globulins: the γ -globulins. The term immunoglobulin refers to the immunity-conferring portion of the gamma globulin portion and thus, the terms immunoglobulin and antibody are used interchangeably. Found in the serum, expressed as secreted and membrane-bound forms, they are produced in the lymphoid tissues by a type of lymphocyte called B-cells.

Immunoglobulins have been shown by electron microscopy to have a common symmetrical globular structure consisting of four polypeptide chains: two identical heavy (H) chains and two identical light (L) chains, joined together by disulphide bridges to form a Y-shaped macromolecule, shown in Figure 2.5. The light and heavy chains have relative molecular masses of about 25 kDa and 50-70 kDa respectively. They are further divided into the amino terminal (N-terminal) variable (V) and

carboxy terminal constant (C) regions. The regions are composed of repeating and homologous segments called domains, each approximately 110 amino acid residues in length and folded independently in a globular motif. An immunoglobulin domain contains two layers of β -pleated sheet, each layer composed of three to five strands of antiparallel polypeptide chain. Each light chain consists of one variable (V_L) and one constant (C_L) domain, while most heavy chains consist of one variable (V_H) and three constant (C_H) domains. One V_H is juxtaposed with one V_L to form an antigen-binding site; since there are two heavy chains and two light chains on the core structure of each antibody there are also two antigen-binding sites, thus making it divalent.

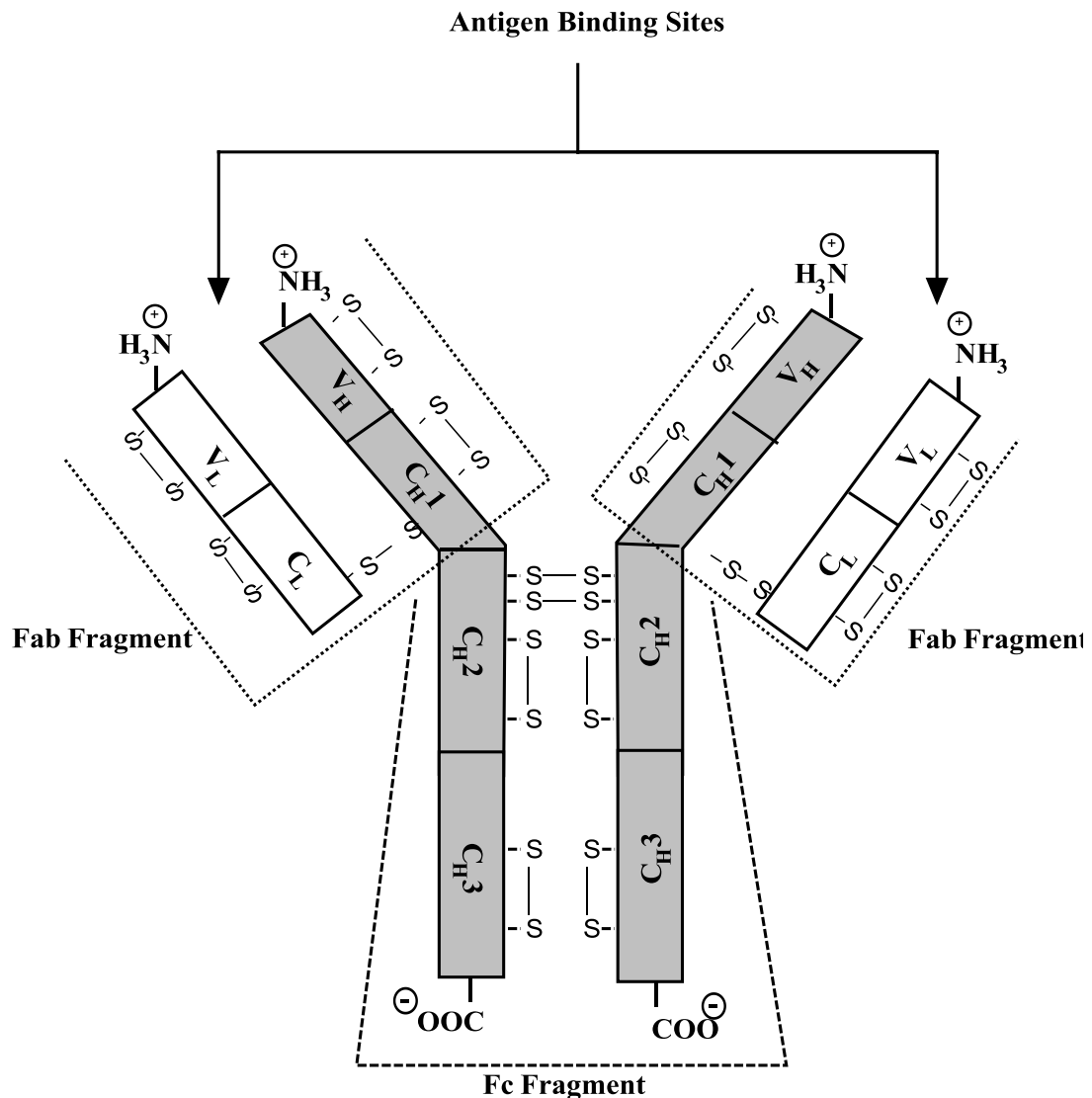


Figure 2.5 Structure of an IgG

Human antibodies are divided into five major Immunoglobulin Classes or isotypes – IgG, IgM, IgA, IgD and IgE – based on their constant region structure and immune function, and differentiated mainly by their heavy chains. IgM is the primary antibody response to most antigens. However, IgG is the predominant and most abundant class of antibodies, constituting approximately 75% of the total immunoglobulin and distributed equally within the intravascular and extravascular pools. It is also the only antibody that can be transferred from the mother to the foetus, providing the infant with immunologic protection in the early stages of birth. In addition, it is the primary antibody induced by protein antigens and is the main antibody in the secondary antibody response to antigens: very little IgG is produced during the early stages of the primary response to antigen, but it is the major form of antibody produced during the secondary response – it has a higher affinity for antigen than IgM, and is therefore more suited for detection purposes. For this reason, for the purpose of this research, only IgG will be discussed.

In the 1950s, Rodney Porter treated IgG with protease papain – a protein-cleaving enzyme derived from papaya – to yield two Fab (fragment, antigen binding) and one Fc (fragment, crystallisable) for each whole IgG molecule. The Fc fragment was named thus, due to its readiness to crystallise when chilled. It was noted that the Fab fragments could precipitate antigen; hence, the Fab fragment contained the antigen-combining region of the Ig molecule and included the variable ends of the antibody, as shown in Figure 2.5.

The remarkable specificity of antibodies is due to the variable antigen binding regions, which are unique to each type of antigen. The variable region is further subdivided into hypervariable regions (HVR) and framework regions (FR). Much of the variation found between immunoglobulins of different antigenic specificities is located within three HVRs, which lie in close proximity to each other within the folded structure of the variable domain. Thus, the most variable parts of this domain are brought together to form the antigen-combining site, or antigen binding site. The HVRs lining the combining site are also referred to as complementary determining regions (CDRs) – short polypeptide segments – since the specific chemistry and shape of the combining site are complementary to the specific chemistry and shape of the

antigenic determinant or epitope. The antigen binding site consists of three CDRs from the light chain and a further three from the adjacent heavy chain. The HVRs have a high ratio of different amino acids in a given position, relative to the most common amino acid in that position. Four FRs, which have more stable amino acid sequences, separate the HVRs. The FRs form the β -sheet structure, which serves as a scaffold for holding the HVRs in position to contact antigen.

The constant-region domains are separate from the antigen-binding site and do not participate in antigen recognition. The carboxy-terminal end of the heavy chain constant regions forms the Fc portion of the Ig molecule; the Fc region is responsible for the biological functions of the antibody such as complement activation and binding to cell surface receptors, interacting with other effector molecules and cells of the immune system. The constant regions of the light chains, on the other hand, do not participate in effector functions. It is important to note that the amino acid sequence of the Fc portion of an antibody varies between the antibody classes and subclasses but is identical within the class. For example, the Fc portion of an anti-*E. coli* IgG is identical to the Fc portion of an anti-*Clostridium spp.* IgG; the Fc portion of an anti-*E. coli* IgG is different from the Fc portion of the IgM antibody to the same antigen. This is important for the preparation of antibody-microsphere conjugates, which is discussed in sections 2.5 and 2.8.

Different isotypes and subtypes of antibodies perform different effector functions. The reason for this is that most of the effector functions of antibodies are mediated by the binding of heavy chain C regions to different cell surface receptors and macromolecules such as complement proteins. Antibody isotypes and subtypes differ in their C regions and therefore in the effector functions they perform.

2.4.2 Monoclonal Antibodies

A monoclonal antibody (mAb) is a standardised antibody, which is derived from a single clone and recognises a specific antigen. It is highly homogeneous, usually reacting with only one molecule and with a single antigenic determinant (epitope) on the molecule. It is produced artificially from a clone of cells obtained by fusing a specific antibody-producing plasma cell with a myeloma cell. All monoclonal

antibodies of the same type are identical since they are produced by one type of immune cell, all clones of a single parent cell. Owing to the most widely used method of production, first illustrated by Georges Köhler and Cesar Milstein in 1975 (Köhler and Milstein 1975), monoclonal antibodies of known specificity can be produced in potentially unlimited amounts. Polyclonal antibodies, on the other hand, are a mixture of a number of antibodies that will recognise and attack a number of different targets. The specific antibodies present in the mixture are highly heterogeneous in antigen-binding affinity and are usually directed at a number of different epitopes on the immunising antigen. Unlike monoclonal antibodies, polyclonal preparations are much more difficult to standardise; preparation and purification of satisfactory polyclonal reagents require considerable time and effort.

Production of Monoclonal Antibodies

Köhler and Milstein (1975) described a method of producing cultures of fused cells that secreted an antibody of predefined specificity, i.e. monoclonal antibody, that has not only revolutionised immunology but has also had an incredible impact on a diverse field of research, including medicine and environmental studies (Abbas 2000). In this method, normal antibody-producing B cells from a mouse that has been immunised with a particular antigen are fused with the mouse myelomas: “immortal” or cancer cells from the mouse bone marrow. The result is immortalised monoclonal antibody-producing cell lines called hybridomas.

To produce a monoclonal antibody specific for a predefined antigen, a mouse is immunised with that antigen, and the produced B cells are isolated from the spleen or lymph nodes of the mouse (Figure 2.6). The B cells are then fused with the immortalised myeloma cells. This creates a mixture of both fused (hybrid) and non-fused cells. *In vitro* growth of the hybrids is performed in hypoxanthine and thymidine (HAT) medium. Non-fused myeloma cells die in HAT medium and non-fused B cells cannot survive for more than one or two weeks. However, immortalised hybrids can grow in the HAT medium, making it the medium of choice for selective growth of hybridomas. The supernatant is then screened for the presence of antibody reactive with the designated antigen by enzyme-linked immunosorbent assay (ELISA) or another screening method. Positive hybridomas are cloned in semisolid agar or by

limiting dilution and then subjected to further screening. Once the hybridoma line is selected, it is injected into a healthy mouse, causing a tumour to grow inside the host mouse. When the tumour grows, it produces ascites, a fluid that is rich in monoclonal antibodies. The ascites fluid containing the monoclonal antibodies can then be collected for further processing.

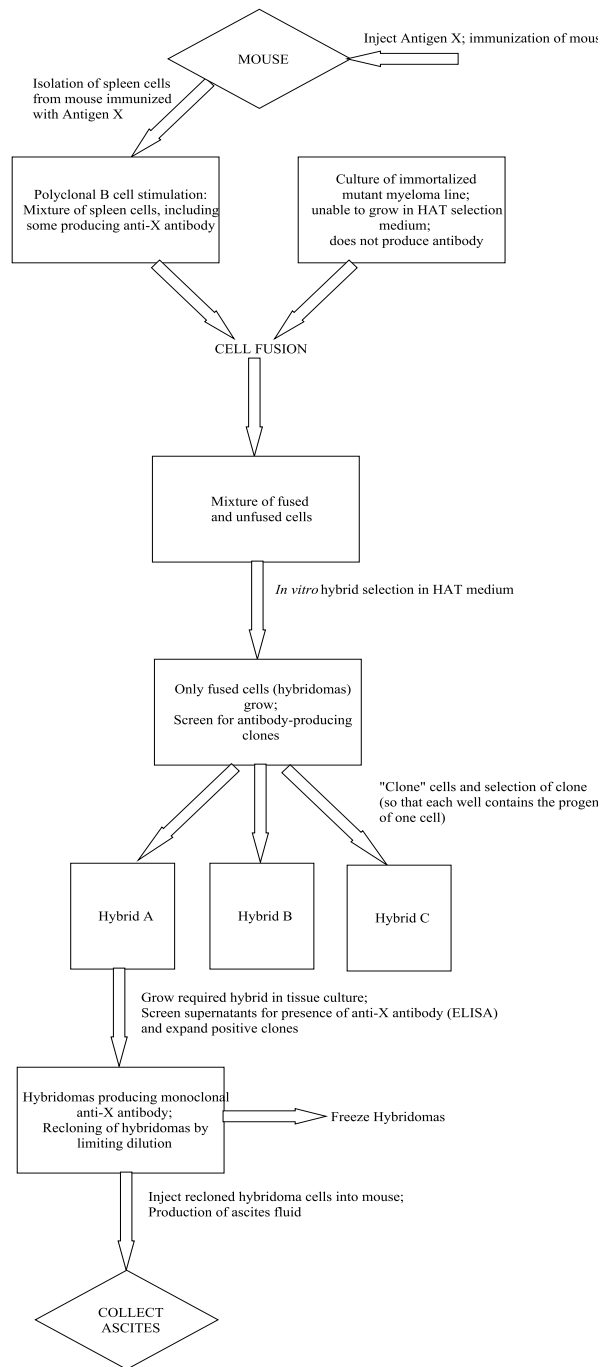


Figure 2.6 General protocol for the production of monoclonal antibodies. Production of monoclonal antibodies derived from fusion of normal antibody-producing B cell and myeloma cell, based on the original methods developed by Köhler and Milstein (1975).

Purification of Monoclonal Antibodies by Affinity Chromatography

Once the monoclonal antibodies are produced they need to be purified as the ascites fluid or other supernatants that they are in will contain a number of unwanted

proteins; considerable care needs to be taken in their purification in order to avoid adverse effects that may affect their use. Although each protein purification method is unique and there aren't standard procedures like those for the purification of nucleic acids, many purification methods resemble each other (Huse *et al* 2002).

Affinity chromatography is a chromatography method used for purifying a particular protein from a mixed sample by reversible interaction between a protein, or group of proteins, and a specific ligand coupled to an insoluble support, known as the chromatography matrix. Purification levels in the order of several thousand-fold with high recovery of active material is achievable because of high selectivity, and hence high resolution, and high capacity for the protein of interest.

Affinity chromatography is unique in purification technology because it is the only technique that enables purification of a biomolecule on the basis of its biological function or individual chemical structure. It is also considered the most powerful technique available because it is the only technique that can potentially allow a one-step purification of the target molecule.

Successful separation by affinity chromatography requires a biospecific ligand to be available and able to be covalently attached to the chromatography matrix. The coupled ligand – the biospecific ligand, which could be an antibody, enzyme or receptor protein – must retain its specific binding affinity for the target molecules – the antigen, substrate or hormone.

A typical purification by affinity chromatography occurs in a few simple steps, as shown in Figure 2.7. Firstly, a binding buffer is passed through the affinity column to equilibrate the affinity medium (Figure 2.7(a)). Then the sample containing the target protein is applied to the column, under conditions that favour the specific binding of the target protein to the ligand (Figure 2.7(b)). Unwanted non-target particles do not bind to the ligand and are washed through the column, leaving the target molecules

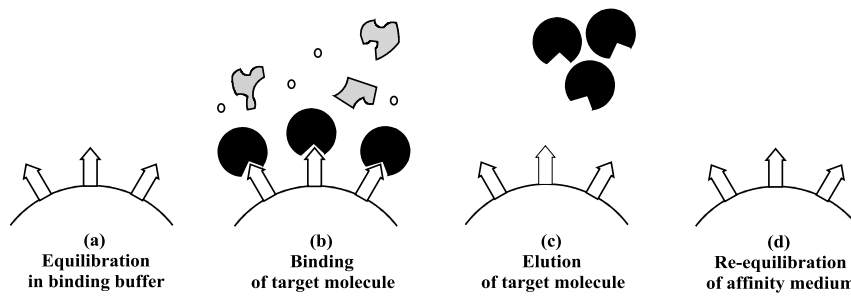


Figure 2.7 Macroscopic representation of the steps of purification by affinity chromatography

bound to the ligand. When the washing of the unwanted particles is complete, an elution buffer is applied to the column to detach the target protein from the ligand (Figure 2.7(c)). The target protein that is eluted from the column is collected in a purified and concentrated form. Figure 2.8 shows a typical absorbance spectrum at 280 nm of protein purification by affinity chromatography.

The matrix of an affinity chromatography packing should possess a number of key characteristics. Firstly, it should have a low affinity for non-target molecules so that it does not bind with unwanted molecules. Secondly, it should be porous so that proteins and other molecules can pass through. Thirdly, it should be chemically inert so that unwanted reactions do not occur. Finally, it should be mechanically stable so that it can undergo washing whilst maintaining physical support. It should also be easily modifiable for ease of attachment of the ligand. There are two basic types of materials used to make the gels in the chromatography matrix: agarose and polyacrylamide.

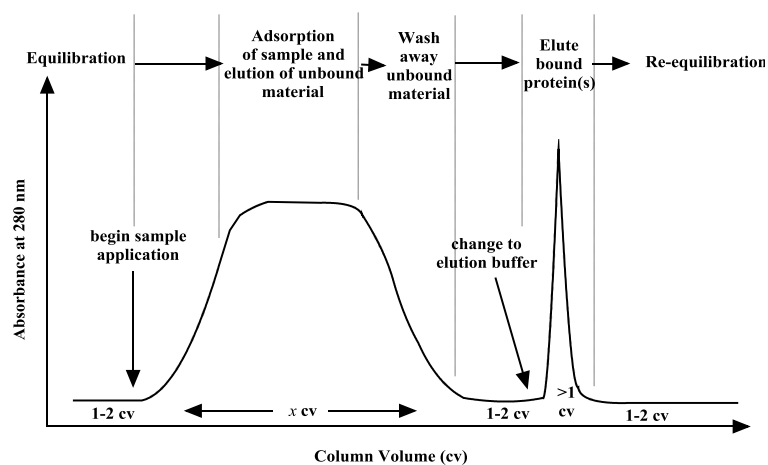


Figure 2.8 Absorbance spectrum at 280 nm of an affinity chromatography

Despite its cost, agarose is the most commonly used substance for the matrix. It is a natural colloid extracted from seaweed and is extremely fragile, susceptible to destruction when handling. It is a linear polysaccharide made from the basic repeating unit agarobiose, which in turn is comprised of alternating units of galactose and 3,6-anhydrogalactose. Agarose gels are formed by suspending dry agarose in an aqueous buffer and then boiling the mixture to achieve a clear solution. The solution is then allowed to cool to room temperature to form a rigid gel. Although agarose gels can be processed more quickly than polyacrylamide gels, their resolutions appear to be inferior to that of polyacrylamide.

Sepharose is a bead form of agarose, which displays virtually all of the features required of a successful matrix for immobilising biologically active molecules. The hydroxyl groups on the sugar residues can be easily derivatised for the covalent attachment of a ligand. The bead form of the gel also provides good flow properties with minimal channelling in the bed, which ensures that rapid separations are obtained. The MAb Trap Kit (Amersham Biosciences) column, for instance, is packed with Protein G Sepharose High Performance.

The selection of ligand for affinity chromatography is influenced by two factors. Firstly, the ligand should exhibit specific and reversible binding affinity for the target protein to be purified. Secondly, it should have chemically modifiable groups that allow it to be covalently attached to the matrix without destroying its binding activity and capability. It is also important to consider the region of ligand that is attached to the matrix. If several functional groups are available, the ligand should be coupled via the group that is least likely to be involved in its specific interaction with the target protein. The ligand is generally attached to the matrix by covalent bonds via a linker. Common ligands used for the purification of antibodies by affinity chromatography are the antigen to the antibody, Protein A and Protein G.

Protein A, a cell surface protein from *Staphylococcus aureus*, and Protein G, a cell surface protein from *Streptococcus spp.*, are bacterial Fc receptors which are important tools for the affinity purification of immunoglobulins, used as ligands in many affinity applications (Huse *et al* 2002). They bind specifically to the Fc region of IgG. Protein G binds to IgG with high affinity; it has three highly homologous IgG-

binding domains. Protein G is the column of choice, over Protein A, for purifying mouse IgGs from ascites fluid because mouse IgG₁ binds much better to Protein G. It is also a preferred choice for general capture of antibodies because it binds to a broader range of IgG from eukaryotic species and binds more classes of IgG. Compared to Protein A, Protein G usually has a higher affinity for IgG and has minimal binding to albumin, resulting in cleaner preparations and greater yields.

An ideal binding buffer used in affinity chromatography for the purification of a target protein should have a pH that encourages the binding of the target protein to the ligand. It should also have a low ionic strength to prevent the buffer components from competing with the target protein for binding sites and should not denature the ligand binding site of the target protein. Buffer conditions are optimised to ensure the effective interaction and retention of the target protein with the ligand and affinity medium whilst unwanted non-target molecules are washed through the column.

Elution is performed specifically using a competitive ligand, or non-specifically by changing the pH, ionic strength or polarity. With ionic elution strategies, the ions in a concentrated buffer solution are used to compete with the ionic binding sites on the ligand. The ionic strength of the elution buffer will generally be higher than that of the binding buffer. With pH elution strategies, the elution buffer pH changes the charge and/or the conformation of the protein, thus weakening the bond between the protein and the ligand. The elution buffer in a pH elution strategy contains a high concentration of buffers, which compete with the protein for the ligand, and the pH of the buffer will generally be different from that of the binding buffer. In general, the elution buffer may contain a compound that binds to the ligand and has a higher affinity for the ligand than the bound protein or a compound that binds to the target protein and has a higher affinity for the protein than the ligand.

2.4.3 Antibody-Antigen Interaction

An antigen is any substance or molecule that can be specifically bound by an antibody. Antibodies can recognise almost every kind of biological molecule. However, only macromolecules are capable of stimulating B lymphocytes to initiate humoral immune response. An immunogen is a macromolecule that induces immune

cells to generate an immune response, which includes the production of specific antibodies. Although the terms antigen and immunogen are often used interchangeably, it should be noted that an immunogen is an antigen: an antigen is not necessarily an immunogen. An antigen that can bind to an antibody but does not evoke an immune response unless combined with a carrier protein is specifically termed a hapten. The recognition of antigen by antibody involves non-covalent, reversible binding; these may include hydrogen bonds, van der Waals forces, electrostatic forces or hydrophobic interactions.

Macromolecules are generally larger than the antigen-binding region of an antibody molecule, so an antibody would only bind to a part of the macromolecule called the determinant (epitope). The macromolecules themselves are usually polyvalent or multivalent, having multiple identical epitopes, each of which can be bound by an antibody or by an antibody with more than one binding site. IgG is divalent and, due to its flexibility provided by the hinge region, can therefore bind to two epitopes on one antigen macromolecule. The significance of multivalency of the antigen macromolecules in lateral flow technology is discussed in Section 2.5.

Because of the nature of the immune response system, when introduced into a foreign host, an antibody can itself become an antigen, thus eliciting the production of anti-antibodies. It is therefore possible to obtain anti-antibodies specific for one Ig class or subclass. Lateral flow technology exploits these properties, as discussed in Section 2.5.

2.5 Antibodies and Antigens in Lateral Flow Technology

Recalling the schematic diagram in Figure 2.2, which shows the two configurations of a lateral flow test strip based on the Double Antibody Sandwich reaction scheme, it was discussed that the two configurations were made possible due to the principles of antibodies and their interactions with antigens. Configuration 1 (shown in Figure 2.2(a)) shows that the antibody (mAb_1) at the detection line is the same type as the antibody (mAb_1) conjugated onto the surface of the microsphere support. On the other hand, in Configuration 2 (shown in Figure 2.2(b)) the antibody (mAb_2) at the detection line is of a different type as the antibody (mAb_1) on the microsphere surface.

As shown by the examples given, mAb_1 and mAb_2 are both monoclonal antibodies that specifically target one particular antigen type (Ag_x), such as *Salmonella spp.* However, these antibodies are from different sources: they are produced by different organisms. mAb_1 , for instance, may be one produced by a mouse whereas mAb_2 may be one produced by a goat. The fact that they are from different sources is irrelevant since they both specifically target the same antigen; therefore, either may be used.

Looking more closely at Configuration 1, an explanation for using the same type of antibody (mAb_1) on both the microsphere surface and on the detection line is warranted. Recalling the structure of the Fc portion of antibodies, previously discussed in Section 2.4.1, the Fc portion of all IgG molecules are identical – regardless of the source where the antibodies are produced and regardless of whether they are specific to the same antigen or not. In other words, the Fc portion of the mAb_1 IgG is identical to the Fc portions of the mAb_2 and mAb_3 IgGs.

Also discussed in Section 2.4.1, the Fc region of antibodies is responsible for biological functions such as binding to cell surface receptors. It is therefore via the Fc region that the antibody (mAb_1) is conjugated to the microsphere surface. It is also via the Fc region that the antibody (either mAb_1 or mAb_2) is immobilised onto the nitrocellulose strip at the detection line. Likewise, the Fc region of mAb_3 is attached onto the nitrocellulose strip at the detection line. Because of the immobilisation via

the Fc region, the antigen-binding sites on the antibody molecules are then in an optimised position for capturing and binding the target antigen.

As discussed in Section 2.3.1 (regarding the description of the step-by-step process of a positive strip test) and in Section 2.4.3, the multivalency of antigen macromolecules plays a significant role in immunochromatographic assays. Recalling Figure 2.3 and Figure 2.4(b to d) in Section 2.3.1, the antigen binds to the monoclonal antibody (mAb₁) on the microsphere surface as well as to the monoclonal antibody (mAb₁) immobilised at the detection line of the test strip. This is due to the multiple determinants on the antigen macromolecule. Hence, in a positive immunochromatographic assay, when the mixture containing the combined $\mu\text{sph-mAb}_1\text{-Ag}_x$ macromolecular complex reaches the detection line, the mechanism for the capture of this macromolecule by the Fab region of the antibody on the nitrocellulose strip is via the unoccupied epitope of the antigen (Ag_x) in the macromolecular complex. Once the complex is captured by the detection antibodies it remains bound in an 'upside-down' position, as shown in Figure 2.3 (point D) and Figure 2.4 (c and d), for the duration of the assay. This orientation is important in the detection process since the microsphere becomes exposed and is thus easily detectable by visual or optical methods. Visual versus optical detection methods are discussed later on in Section 2.10.

Following the discussions in Section 2.3.1, regarding the antibody (mAb₃) immobilised onto the nitrocellulose strip at the control line, and Section 2.4.3, regarding antibodies acting as antigens and eliciting the production of anti-antibodies, it has been illustrated that, because of the nature of the immune response to produce antibodies to target all types of immunogens, if an antibody produced by one type of organism were introduced into a second organism, that second organism's immune response would be to produce an antibody against that foreign molecule: the anti-antibody. In the example illustrated in Section 2.3.1, the anti-antibody used is goat anti-mouse monoclonal antibody. This means that during the production stage, an antibody produced in a mouse immune system is introduced as a foreign molecule into a goat. The goat's immune response then produces an antibody to the mouse antibody: a goat anti-mouse immunoglobulin. It is this goat anti-mouse

immunoglobulin that can be used as the control antibody on the lateral flow test strip – immobilised at the control line – in order to capture the antigen-free $\mu\text{sph-mAb}_1$ conjugate. The interaction between the mAb_3 antibody and the mAb_1 antibody on the microsphere surface abides by the same principles as those described in sections 2.4.1 and 2.4.3: the Fab region of mAb_3 recognises mAb_1 as its target antigen; likewise, the Fab region on mAb_1 acts as its determinant. Thus, the Fab region of mAb_3 binds to the Fab region of mAb_1 , again orientating the $\mu\text{sph-mAb}_1$ conjugate in an ‘upside-down’ position as shown in Figure 2.3 (point C) and Figure 2.4 (d and i). This exposes the microsphere, allowing it to be easily detected either by visible or optical means.

2.6 Microspheres

The term *microsphere* has a number of different definitions and needs to be specified for the purpose of this work. It can refer to any small particle that is spherical in shape. *Microsphere* is also termed because of a spherical particle's microscopic nature, which in itself can be unspecific. These uses can be ambiguous and somewhat of a misnomer because they encompass a large range of particle sizes. In order to be precise, it should refer to spherical particles with a diameter (d) that falls within the micrometer range ($1 \times 10^{-6} m \leq d < 1 \times 10^{-3} m$). In actuality, however, it usually also includes particles of submicron sizes ($d < 1 \times 10^{-6} m$) – particles in the nanometre range, which are also referred to as nanospheres or nanoparticles. Similarly, microspheres are also referred to as microparticles, although this could also be unclear since not all microparticles are spherical in shape. In this thesis, the term *microsphere* is taken to include spherical particles of both micrometer and nanometre ranges.

Microspheres referred to in this thesis are colloidal in nature, which means that they exist as single entities dispersed in a liquid medium. Undergoing Brownian motion, their small sizes enable them to overcome the effects of gravity and remain in colloidal suspension for a long period of time (months or years).

Microspheres perform an integral function in microbial detection using the immunochromatographic method. Not only are they one of the substrates onto which the detection antibodies are immobilised but, in addition to their role as a support, they themselves are used directly in the detection process. In fact, it is through their detection that the presence of the microorganism in question is determined.

Certain factors need to be considered when determining the type of microspheres to be used in a detection method. Particle size affects ease of detection, antibody immobilisation and mobility. The method by which the microspheres are detected (visual versus optical as well as light reflectance and scattering versus fluorescence) is also an important factor when considering microspheres. Finally, affinity for proteins and non-specific binding as a result of surface chemistry should be taken into account.

In this project, materials falling into two main types of microspheres are considered. Colloidal gold microspheres (a metal colloid) and PMMA and P(MMA-HEMA) (polymer microspheres) are investigated and discussed in turn.

2.6.1 Colloidal Gold Microspheres

Colloidal gold has become widely used as a marker and signal generator in immunochromatographic assays and other biochemical and immunological applications (Beesley 1989; Paek *et al* 2000). Certain properties of colloidal gold have made it an attractive material for use in microbial detection. Gold is considered a noble metal due to its resistance to corrosion and its reluctance to react with most chemicals, making it a highly stable metal. In addition, good quality colloidal gold appears red in colour, which is highly visible and ideal for chromatographic tests.

The preparation of monodisperse colloidal gold of uniform shape and size by the chemical reduction of Au^{3+} present in tetrachloroauric acid occurs in three distinct steps, and can be represented by the chemical equation (2.6.1) and the graph in Figure 2.9 (Chandler 2000):



Gold tetrachloric acid + reducing agent \longrightarrow gold colloid

Prior to the addition of the reducing agent, gold exists as positively charged Au^{3+} ions in solution. Immediately after the reducing agent is added, reduction occurs, in which the reducing agent donates electrons to the positively charged Au^{3+} ions to rapidly produce gold atoms in solution until a supersaturated molecular Au solution is reached. This is followed by a process called nucleation, in which aggregation of the gold atoms at nucleation sites occur to form nuclei. Following nucleation, particle growth takes place, in which the remaining molecular Au in solution continue to be deposited onto the nuclei until all the atoms are used up.

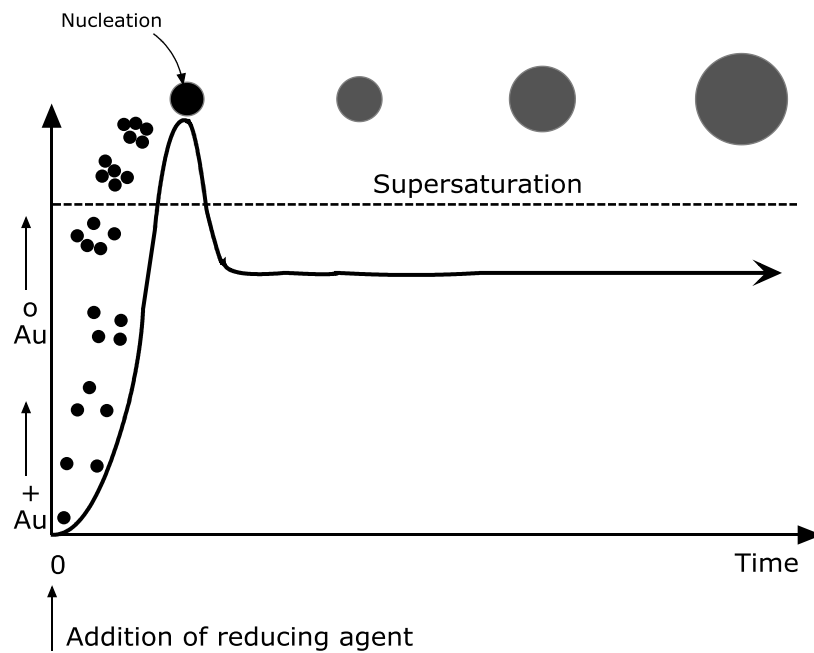


Figure 2.9 Formation of colloidal gold particle by reduction of Au^{3+} ions. Adapted from Chandler (2000).

Some commonly used reducing agents include an ether solution of white phosphorous, sodium citrate, yellow phosphorous, sodium borohydride or sodium thiocyanate. Particle size ranges from 1 nm to 100 nm, and is carefully controlled by the type and concentration of reducing agent used. For instance, if white phosphorous, sodium thiocyanate or potassium thiocyanate is used as the reducing agent, the reduction of Au^{3+} is rapid and many small gold particles of around 2-3 nm or 5-12 nm are formed. On the other hand, if sodium citrate is used as the reducing agent, the reduction of chloroauric acid is slow and fewer but larger particles, ranging from around 15 nm to around 150 nm, are formed, depending on the amount of sodium citrate added (Beesley 1989).

The small particles sizes of colloidal gold allow for ease of transport along the nitrocellulose strip in an immunochromatographic assay. However, larger sized colloidal gold particles result in greater visibility because of the greater surface area. With regards to particle size, there is a trade-off between required visibility and steric hindrance but it has been reported that the optimum size for most immunoassay applications is 40 nm (Chandler 2000).

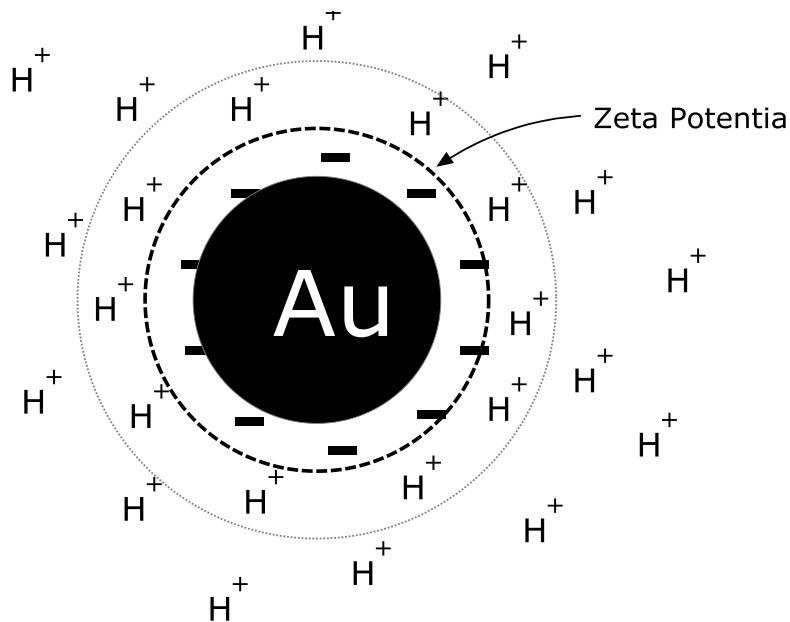


Figure 2.10 Individual colloidal gold particle in solution. Adapted from Weiser (1933).

An individual colloidal gold particle, shown in Figure 2.10, is surrounded by what is known as a zeta potential – a negative charge layer resulting from residual negative ions in solution – which causes an electrostatic repulsion between the particles and causes the particles to undergo Brownian motion, enabling them to remain in colloidal suspension for an indefinite period. And depending on the total ionic concentration of the surrounding solution, the zeta potential can either be compressed or expanded.

Colloidal gold’s overall negative surface charge gives it an affinity for antibodies and allows it to be “coated” with antibodies via passive adsorption to form a colloidal gold-antibody conjugate, as discussed in Section 2.8.1. However, due to its readiness to bind to proteins, unspecific binding can occur and a blocking agent would need to be added to prevent unwanted proteins from being adsorbed onto the gold surface.

Adsorption of the antibodies onto the gold surface is due to electrostatic interaction between the negatively charged surface of the gold particle and positively charged amino groups (e.g. lysine) within the Fc region of the protein, followed by hydrophobic adsorption to the particle surface due to van der Waals-London forces. Because the gold binds to the Fc region of the antibodies, the Fab regions at the tip of

the 'arms' of the Y-shaped proteins are then free to bind with antigens that are to be detected.

As previously mentioned, high quality colloidal gold appears red in colour. Good quality colloidal gold refers to colloidal gold suspensions that contain monosize, monodisperse particles. This red colour is detected by means of light reflectance and scattering. The interaction of light with a colloidal gold particle in solution is shown in Figure 2.11 and described as follows.

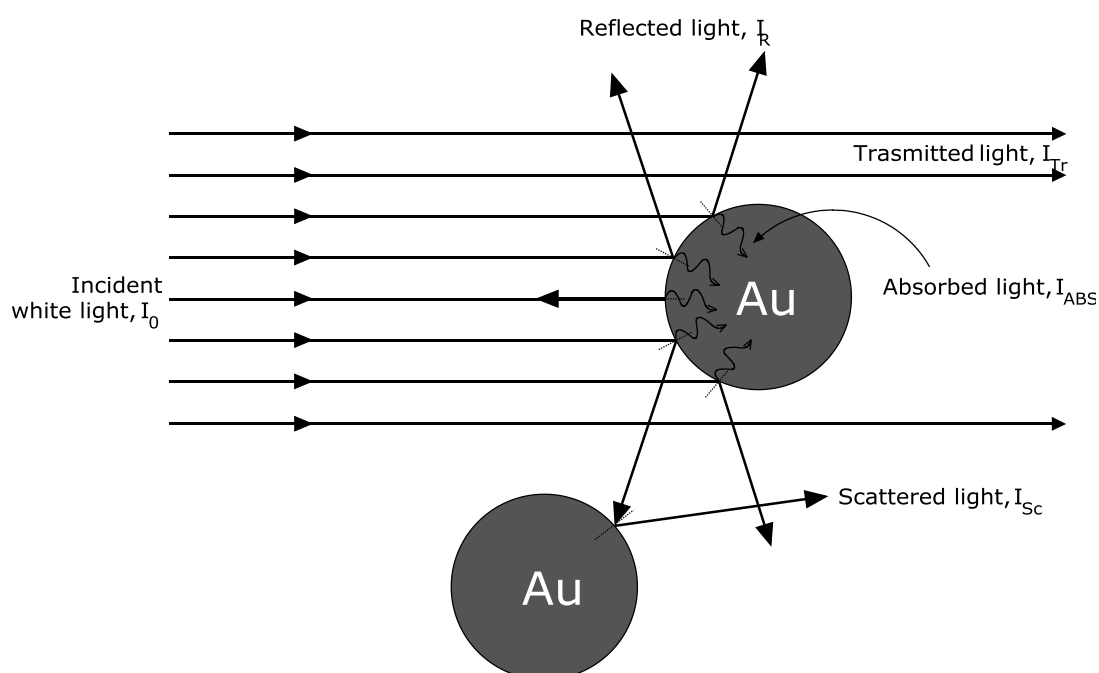


Figure 2.11 Interaction of white light with colloidal gold microspheres in solution

When white light is shone onto a colloidal gold suspension, several things occur. White light propagates in a straight line and therefore, if a beam of light does not come into contact with a gold particle, it merely carries on through the solution and is called transmitted light. However, when the incident light interacts with a gold particle, several things occur. The gold particle partially reflects and partially absorbs some of the red component of white light, and absorbs all the other components. The reflected light travels in a straight line and passes out of the solution, which can be detected. However, because there is more than one particle in a solution containing colloidal gold microspheres, not all of the reflected light from a particle will make it

through the solution without encountering another particle. When the reflected light encounters another particle, it is forced to deviate from its straight trajectory. This light, upon coming to contact with another gold particle is in turn reflected from the second particle's surface in the form of scattered light. The reflectance of the red component of white light from the gold surface is the reason why colloidal gold appears red in colour, as viewed by the naked eye. The intensity of the red colour is greater at greater concentrations of gold particles or, as previously mentioned, if the particle sizes are larger, due to greater surface area.

Because gold is a metal, and because metals both reflect and absorb light, colloidal gold is also, therefore, light absorbing and a significant amount of light could be lost to absorption by the particle, especially at lower concentrations, making the detection of reflected or scattered signal a relatively low efficiency process. At high concentrations of gold, there is enough reflectance and scattering of light from the surface of the spheres to overcome the loss of light due to absorption. However, when the concentration of gold is low, light lost due to absorption becomes more significant. In addition, because of the low number of particles much of the white light is transmitted through the solution without coming into contact with any gold particle, making it even more difficult to detect the small amount of red light that does manage to get through. In an attempt to overcome the disadvantages of using colloidal gold in the detection of low concentrations of microorganisms, the feasibility of incorporating a fluorescent molecule onto the surface of the signal generator in order to increase the sensitivity of light detection at low concentrations was investigated.

2.6.2 *Polymer Microspheres*

Polymer microspheres, also known as latex particles, are spherical polymer particles that can be synthesised from a variety of monomers by a number of different polymerisation methods, as discussed in sections 2.6.3 and 2.6.4. The particles are dispersed in aqueous, as well as non-aqueous, media to form suspensions that are, in most cases, colloidal in nature.

Over the past half century a great deal of work has been done on the formation and properties of polymer latexes and much of this work has been dedicated to the study of the process of formation of polymer particles in a latex and to the characterisation of the particles once formed (Piirma 1982; Boury *et al* 1997). In addition, since the works of Singer and Plotz (1956a, 1956b) on latex agglutination tests, much of the work done on polymer latexes has been devoted to their use in immunoassays and biological sciences, including a number of work on their interaction with proteins and the immobilisation of proteins onto their surfaces (Olal 1990; Wong 1993; Hermanson 1996; Ortega-Vinuesa J. L. *et al* 1998). From these extensive studies has emerged the general recognition that the majority of latex particles in dispersion media have diameters in the range of 0.01 μm to 1 μm (i.e. 1 nm to 1 μm), which falls within the size range defined at the start of Section 2.6. It is this size range that designates them as colloidal. In a stable colloidal suspension, as previously mentioned, the particles in the dispersion will remain for long periods of time dispersed as single entities in Brownian motion.

Polymer latexes can be classified as homopolymers or heteropolymers. Homopolymers are formed by the polymerisation of a single type of monomer. Examples of homopolymers include polymethyl methacrylate (PMMA), polystyrene (PS) and polyvinyl chloride (PVC). Heteropolymers, also known as copolymers, are formed from the copolymerisation of two or more different types of monomer. Examples of heteropolymer latexes include polymethyl methacrylate-co-hydroxyethyl methacrylate (P(MMA-HEMA)) and styrene-butadiene copolymers.

Polymer particles have been used in a wide variety of applications in many fields and industries. Because of their perfect spherical shape and uniform size distribution

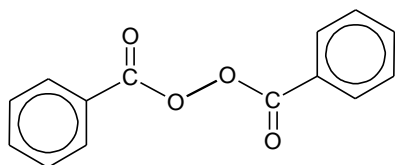
polymer latexes have been used as size calibration standards for optical and electron microscopes, light scattering instruments and particle counting devices, and for the determination of pore sizes (Campbell and Bartlett 2002). They are also having increasingly significant applications in the biomedical field such as drug delivery systems, flow cytometry standards and detection systems (Hall *et al* 1999; Freiberg and Zhu 2004).

Polymer microspheres can be produced by polymerisation from their monomers via a variety of polymerisation and copolymerisation mechanisms and techniques. There are two distinct mechanisms by which polymer molecules are formed: 1) step-growth polymerisation, which involves a stepwise increase in molecular weight by the random combination of monomer molecules containing reactive functional groups, and 2) chain-growth polymerisation, which involves the successive addition of monomer molecules onto the reactive ends of a growing polymer chain. Polymerisation techniques include bulk, solution, suspension and emulsion polymerisation, as discussed below in Section 2.6.4. All polymerisation techniques relevant to this research are free-radical chain-growth polymerisations and, therefore, only these types of polymerisation are discussed below; other types of polymerisation such as step-growth and ionic polymerisations are omitted.

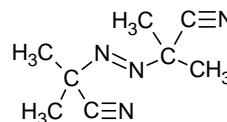
2.6.3 Polymerisation Mechanisms and Kinetics

Chain-Growth and Free-Radical Polymerisations

In chain-growth polymerisation reactions, the presence of an initiating molecule (known as an initiator), which begins the linking process by reacting with the monomer to form a reactive compound, is required. In free-radical chain-growth polymerisations, the initiator would be a compound that can be broken down into an unstable, highly reactive compound called a free-radical. Widely used free-radical initiators include organic compounds that contain a labile group, such as an azo (-N=N-), disulphide (-S-S-) or peroxide (-O-O-) compound. Examples of free-radical initiators include benzoyl peroxide and 2,2'-azobisisobutyronitrile (AIBN) and are shown in Figure 2.12 below.



Benzoyl peroxide



AIBN

Figure 2.12 Free-radical initiators. Organic compounds containing a labile group.

Chain-growth polymerisations take place in three distinct steps:

- 1) initiation of active monomer,
- 2) propagation or growth of the active free-radical chain, and
- 3) termination of the active chain.

These steps are introduced in general terms below and then applied to each specific polymerisation, as discussed in Section 2.6.5.

Initiation

In order for the polymerisation reaction to begin, the introduction of free radicals into the system is required. This can be achieved by the addition of a thermolabile initiator: an initiator containing bonds that can be broken by heat. The initiation step itself is comprised of two distinct steps: 1) thermal dissociation of the initiator to yield two radicals, followed by 2) the association step, which is the addition of a single monomer molecule to the initiator radical.

The kinetics of the dissociation of the initiator can be represented by the reaction equation (2.6.2) below:



where

I = initiator molecule

R• = initiator radical

k_d = dissociation rate constant

The dissociation rate constant, k_d , is dependent on temperature; its dependence is given by the Arrhenius equation, shown in equation (2.6.3) below:

$$k_d = Ae^{\frac{-E_a}{RT}} \quad (2.6.3)$$

where

A = pre-exponential factor [units vary and depend on the order of reaction]

E_a = activation energy for dissociation [kJ mol^{-1}]

R = universal gas constant = $8.314 \times 10^{-3} \text{ kJ K}^{-1} \text{ mol}^{-1}$

T = temperature [K]

Dissociation of the benzoyl peroxide initiator to form two initiator radicals can be represented by the chemical equation shown in Figure 2.13 below:

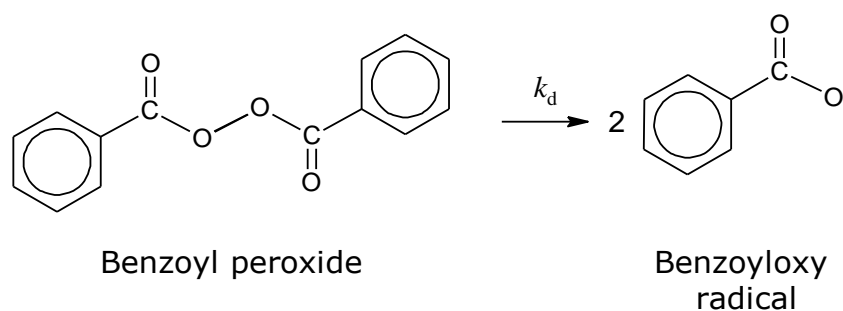


Figure 2.13 Thermal dissociation of benzoyl peroxide to form two benzoyloxy radicals

Similarly, the dissociation of AIBN can be represented by the chemical equation shown in Figure 2.14 below:

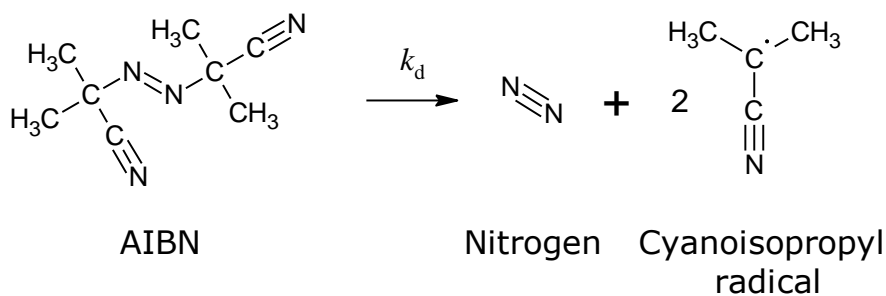


Figure 2.14 Thermal dissociation of AIBN to form two cyanoisopropyl radicals

The association step, in which a monomer molecule, M, is attached to the initiator radical, can be represented by the chemical equation (2.6.4) below:



where

$R\bullet$ = initiator radical

M = monomer

$RM\bullet$ = monomer-ended radical

k_a = rate constant for monomer association

Propagation

During the propagation step, additional monomer units are added to the initiated monomer species, and can be represented by the chemical equation (2.6.5) below:



where

k_p = propagation rate constant

Subsequently, additional monomers are added, in succession, onto the radical chain and can be represented by a general chemical equation, as shown in equation (2.6.6) below:



Termination

The sequence of monomer addition by propagation continues until the system undergoes a termination process. One means by which termination can occur is by the process called termination by combination, in which two propagating radical chains of x and y degree of polymerisation, respectively, come together at their free-radical ends to give a single terminated chain of $(x+y)$ degree of polymerisation. The combination occurs through the formation of a covalent bond, forming a paired electron bond

between the two merging radical chains, and can be represented by the reaction equation (2.6.7) below:

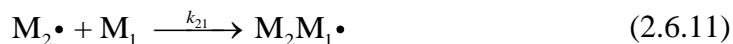


Alternatively, termination may occur by disproportionation, in which a hydrogen atom is transferred from one radical species to another to form two new terminated chain molecules. In this case, the hydrogen donor is left with an unsaturated carbon group whilst the other terminated end becomes fully saturated. Termination by disproportionation can be represented by the reaction equation (2.6.8) below:



Free-Radical Copolymerisation

Four different propagation routes are probable in free-radical copolymerisation of two different monomers and are illustrated by equations (2.6.9) to (2.6.12). Each propagation step has its own rate constant k_{ij} , for the addition of monomer M_j to radical M_i . Under the given reaction conditions, for homopolymerisation k_{ij} is the propagation rate constant k_p (recall equation (2.6.5)).



Assuming that the only significant changes in monomer concentrations result from propagation reactions, the rates of monomer disappearance according to the reaction steps denoted by equations (2.6.9) to (2.6.12) are, therefore, given as

$$-\frac{d[\text{M}_1]}{dt} = k_{11}[\text{M}_1\cdot][\text{M}_1] + k_{21}[\text{M}_2\cdot][\text{M}_1] \quad (2.6.13)$$

and

$$-\frac{d[M_2]}{dt} = k_{22}[M_2\cdot][M_2] + k_{12}[M_1\cdot][M_2] \quad (2.6.14)$$

Similarly, the time dependence of the concentration of radical $M_1\cdot$ is

$$-\frac{d[M_1\cdot]}{dt} = -k_{12}[M_1\cdot][M_2] + k_{21}[M_2\cdot][M_1] \quad (2.6.15)$$

Under steady-state conditions $[M_1\cdot]$ is sufficiently small that $\frac{d[M_1\cdot]}{dt}$ is negligible compared to the rates of change of concentrations of the reactants. Hence, if $\frac{d[M_1\cdot]}{dt} = 0$, then

$$k_{12}[M_1\cdot][M_2] = k_{21}[M_2\cdot][M_1] \quad (2.6.16)$$

and

$$\frac{[M_1\cdot]}{[M_2\cdot]} = \frac{k_{21}[M_1]}{k_{12}[M_2]} \quad (2.6.17)$$

During the copolymerisation process, the monomer is consumed and becomes incorporated into the copolymer structure; any relative change in the composition of the comonomer mixture, therefore, reflects the composition of the copolymer formed at that instance in time. Hence, how copolymer composition varies as a function of comonomer reactivity and concentration at any time can be predicted. The relative rates of incorporation of the two monomers into the copolymer at any instant is given by the instantaneous copolymerisation equation, which is obtained by dividing equation (2.6.13) by equation (2.6.14) to give

$$\frac{d[M_1]}{d[M_2]} = \frac{[M_1] k_{11}[M_1\cdot] + k_{21}[M_2\cdot]}{[M_2] k_{22}[M_2\cdot] + k_{12}[M_1\cdot]} \quad (2.6.18)$$

Equation (2.6.18) can be simplified by first defining a monomer reactivity ratio. The reactivity ratios for monomers 1 and 2 are defined, respectively, as

$$r_1 \equiv \frac{k_{11}}{k_{12}} \quad (2.6.19)$$

and

$$r_2 \equiv \frac{k_{22}}{k_{21}} \quad (2.6.20)$$

Equation (2.6.19) shows that the reactivity ratio r_1 for monomer 1 is the ratio of the propagation rate constants for the addition of M_1 (homopolymerisation) and of M_2 (copolymerisation) to a propagating radical-chain with monomer 1 at the radical end ($M_1\bullet$). Similarly, equation (2.6.20) shows that the reactivity ratio r_2 for monomer 2 is the ratio of propagation rate constants for the addition of M_2 (homopolymerisation) and M_1 (copolymerisation) to a propagating radical-chain with monomer 2 at the radical end ($M_2\bullet$).

Using the definitions of reactivity ratios and assuming a steady-state concentration of radicals for either $M_1\bullet$ or $M_2\bullet$ during the propagation, the instantaneous copolymerisation equation, also known as the Mayo-Lewis equation, becomes

$$\frac{d[M_1]}{d[M_2]} = \frac{[M_1] \left(r_1 [M_1] + [M_2] \right)}{[M_2] \left([M_1] + r_2 [M_2] \right)} \quad (2.6.21)$$

If the reactivity ratios are known, the Mayo-Lewis equation may be used to estimate the composition of copolymer, since the relative rate of monomer disappearance is equal to the relative rate of monomer incorporation. On the other hand, experimental values for the reactivity ratios can be obtained from known monomer concentration and determination of the copolymer composition. Copolymer composition can be determined by $^1\text{H-NMR}$ spectroscopy.

The reactivity ratios defined by equations (2.6.19) and (2.6.20) show that when both $r_1=1$ and $r_2=1$, then it follows that $k_{11} = k_{12}$ and $k_{22} = k_{21}$, indicating that there is no preferential monomer incorporation into the propagating chain, resulting in a completely random monomer sequence in the copolymer. If both reactivity ratios are zero, i.e. $k_{11} = k_{22} = 0$, the monomer sequence will be alternating. If both reactivity ratios are small but not exactly zero (tending to but not approaching zero), the comonomer will have a tendency to alternate, often with segments of alternating sequences, but will not be completely alternating. If both reactivity ratios are much greater than 1 (i.e. $k_{ii} \gg k_{ij}$), it means that the monomers are unlikely to react to each other, reacting only with themselves, resulting in a mixture of two homopolymers instead of copolymers.

It should be noted that choice of solvent may have an effect on radical copolymerisation and solvent effect on reactivity ratios can be significant, especially in copolymerisations involving monomers that are ionisable or form hydrogen bonds, but less so in copolymerisations involving only non-protic monomers (Moad and Solomon 2006). There have been attempts to rationalise solvent effects on copolymerisation by establishing correlations between radical reactivity and various solvent and monomer properties, but with little success (Moad and Solomon 2006).

2.6.4 Polymerisation Techniques and Processes

Polymer microspheres can be fabricated by free-radical chain transfer polymerisation by a number of different polymerisation techniques, each of which is discussed below.

Bulk Polymerisation

Bulk polymerisation is carried out in the absence of any medium, such as a solvent or dispersant, other than a catalyst or accelerator and is thus the simplest polymerisation technique, in terms of formulation. It yields highly pure polymers with minimal contamination, and usually requires just the monomer and a monomer-soluble initiator to proceed. It also results in high yield per reactor volume and easy polymer recovery because in the absence of solvent, no solvent removal is required. It is used for most step-growth polymers and some chain-growth polymers. However, due to the highly

exothermic nature of free-radical polymerisations (42 to 88 kJ mol⁻¹ (Fried 2003)) and the high activation energies involved, heat dissipation in bulk polymerisation is difficult and can be a problem if used for chain-growth polymerisations, and therefore requires careful temperature control such as by the installation of efficient cooling coils in the reaction vessel. Because of this exothermic nature, an increase in temperature results in an increase in polymerisation rate, thus resulting in further generation of heat that needs to be dissipated. The removal of heat becomes especially problematic towards the end of the polymerisation due to the rapidly increasing viscosity; because of high viscosities, there is also a need for complex and powerful stirring apparatus. In extreme cases, uncontrolled acceleration of the polymerisation rate can lead to disastrous “runaway” reactions (Odián 2004).

Solution Polymerisation

The difficulty of heat removal frequently associated with bulk polymerisations can be minimised by carrying out the polymerisation reactions in a solvent, and hence the process is termed solution polymerisation. In solution polymerisations, the polymerisation reaction takes place in a non-reactive organic solvent or in a medium with a high thermal conductivity, such as water. The heat generated and released by the reaction is absorbed by the medium, reducing the reaction rate. In addition to being a heat dispersion medium, the solvent also decreases the viscosity of the system, making stirring easier in solution polymerisations than in bulk polymerisations. However, it can be difficult to remove the solvent from the finished viscous polymer; hence, solution polymerisation is best used for polymers that are used in solution form, such as surface coatings and adhesives, otherwise a separate solvent-recovery step would be required.

Suspension Polymerisation

Heat transfer in polymerisation reactions may be improved by utilising the high thermal conductivity of water through the employment of suspension or emulsion polymerisation. Suspension polymerisations, also known as bead or pearl polymerisations, are in effect water-cooled bulk reactions, in which a water-insoluble monomer containing dissolved initiator is dispersed in water within a batch reactor

fitted with a mechanical stirrer. In suspension polymerisation, free-radical initiation is in the monomer phase, in which droplets of between 50 and 200 μm in diameter of monomer containing dissolved initiator are formed and function as miniature reactors for the polymerisation. As the polymerisation progresses, the droplets become sticky, viscous monomer-swollen particles. The reaction mixture needs to be continuously and vigorously agitated to prevent the coalescence of the sticky particles. Eventually, towards the end of the polymerisation reaction, the particles become rigid and can be recovered and cleaned by a variety of separation methods, as discussed in Section 2.6.7. Sizes of particles produced by suspension polymerisation typically fall within the range of around 50 and 500 μm , with the final reaction mixture containing around 25-50% polymer dispersed in water.

In general, the kinetics of suspension polymerisation follow the same reaction kinetics as described previously for free-radical polymerisation reactions. However, the importance of particle size and structure outweigh that of molecular weight for polymers produced by suspension polymerisation. Because of this, factors other than the chemistry of polymerisation affect the end product. Particle character in suspension polymerisation reactions is often related to the level of agitation, which depends on the diameter of the impeller as well as rotational speed. Low agitation levels tend to produce large monomer droplets and yield large polymer particles. Polymer particle sizes decrease as agitation levels increase to a level of agitation beyond which the particle sizes would become larger again due to an insufficiency of suspending agent beyond a certain point. Particle size distribution is important in suspension polymerisation and very large or very small particles would need to be avoided. This can be controlled and accomplished by careful selection of the suspending agent and other components as well as an optimised stirring protocol, achieved by trial and error.

Emulsion Polymerisation

Emulsion polymerisation is a heterogeneous reaction system, which consists of a discontinuous liquid phase (the monomer) dispersed throughout a different, continuous liquid phase (e.g. water) in the form of emulsions (i.e. colloidal dispersions). Emulsion polymerisation bears a superficial resemblance to suspension

polymerisation in its usage of water as a heat sink. However, its mechanism and reaction characteristics differ quite considerably from that of suspension polymerisation. In emulsion polymerisation, free-radical initiation occurs in the aqueous phase rather than in the monomer phase, which is characteristic of suspension polymerisation; the type of initiator used in emulsion polymerisation differs from that used in suspension polymerisation because of its solubility in water rather than in the monomer. Furthermore, emulsion polymerisations typically yield smaller sized particles (diameters range from about 0.1 to 1 μm) than those produced by suspension reactions (diameters from between 50 and 500 μm).

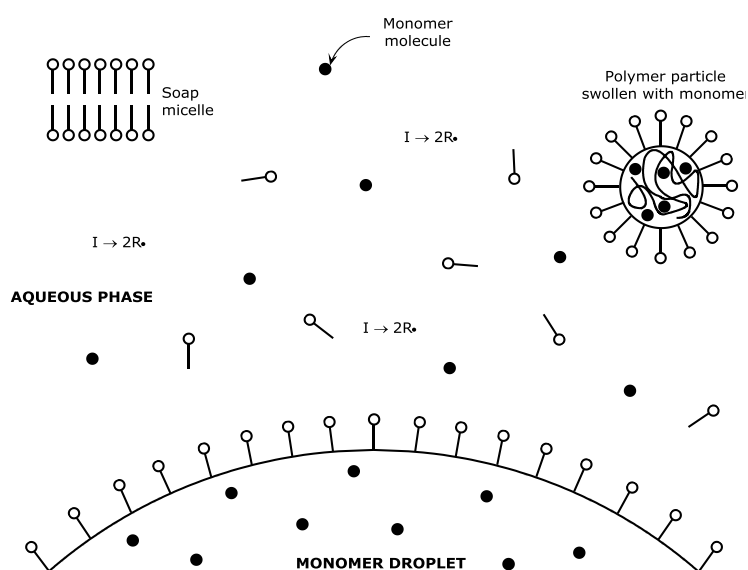


Figure 2.15 Representation of an emulsion polymerisation system

There are some evident advantages to emulsion polymerisation, including the ease of controlling the process. Thermal and viscosity difficulties apparent in bulk polymerisations are much less significant in emulsion polymerisations because stirring and heat removal due to the exothermic reactions are made easier through the use of water as a heat sink as well as a diluent.

Ingredients in an emulsion polymerisation consist of water, a water-insoluble monomer, an oil-in-water emulsifier and a free-radical initiator. Some emulsion polymerisation reactions may be conducted without the use of an emulsifier, which is discussed later on in this section. Most emulsifiers are either anionic or non-ionic

surfactants. Anionic surfactants include salts of fatty acids or alkane sulphonic acids; non-ionic surfactants are based upon polyether groupings or sugar derivatives. During the polymerisation process, the hydrophobic monomer molecules form droplets (of between 1 and 10 μm in diameter, depending on the polymerisation temperature and rate of agitation), which are stabilised by the surfactant molecules.

The emulsifiers are dissolved in the water at very low concentrations; at a certain surfactant concentration, known as the critical micelle concentration (cmc), the surfactant molecules start to aggregate to form micelles. At concentrations above the cmc, all residual surfactant molecules are micellar. Micelles can be rod-like or spherical in shape with their hydrophilic ends oriented outward, towards the aqueous medium, and their aliphatic tails pointing inward, towards the monomer droplet, as shown in Figure 2.15.

Surfactants and Surfactant-Free Polymerisation

Surfactants perform a number of functions in emulsion polymerisation. Essentially, their role is to ease emulsification and provide electrostatic and steric stability to the polymer particles. They are responsible for the stabilisation of monomer droplets, micelle formation, the number of particles, their size and control of their size and rate of particle growth and latex particle stability, during and after the polymerisation process. Electrostatic stabilisers are usually anionic surfactants, which provide colloidal stability by electrostatic repulsion of charges on the particle surface and their associated double layers.

The presence of surfactant can, however, be undesirable in cases where the polymer is used in applications such as instrument calibration and pore-size determination, since consistent and uniform particles would be needed in these cases. The amount of adsorbed surfactant varies with polymerisation and application conditions and therefore its presence may result in variable properties of the polymers. In addition, removal of the surfactant, either directly or by desorption, can cause coagulation or flocculation of the destabilised particles. In attempts to avoid these problems, the employment of surfactant-free emulsion polymerisation, in which no surfactant is

added to the reaction, is often considered to be a useful approach (Rudin 1999; Odian 2004).

In surfactant-free polymerisation, the initiator yields radicals that provide the polymer particles with surface-active properties. This can be achieved through the use of ionic initiators, such as the commonly used persulphate initiators, with the addition of copolymerisable surfactants, if needed. Latex particles prepared by this technique are stabilised by the chemically bound sulphate groups of the initiating $\text{SO}_4\cdot^-$ species derived from the persulphate ion ($\text{S}_2\text{O}_8^{2-}$). Since the surface-active groups are chemically bound, rather than physically adsorbed onto the particle surface, the latex particles can be cleaned and purified without loss of stability; the stability due to chemical binding also enables stability over a wider range of usage conditions, compared to that of latices produced using surfactants. However, particle number generated by surfactant-free polymerisation is generally lower by up to two orders of magnitude compared to those produced by conventional emulsion polymerisations containing added surfactants, typically 10^{12} versus 10^{14} particles per millilitre (Odian 2004).

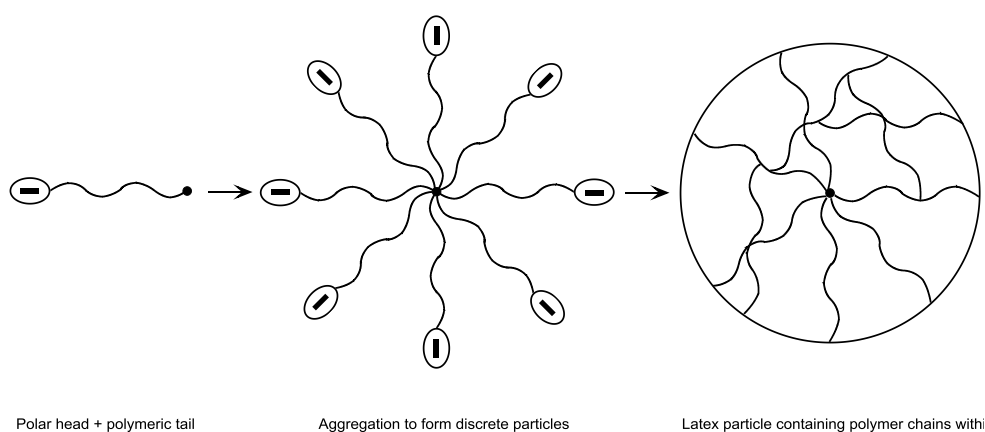


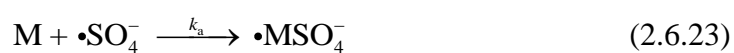
Figure 2.16 General mechanism of surfactant-free emulsion polymerisation

Kinetics of surfactant-free free-radical emulsion polymerisation is described and represented by equations (2.6.22) to (2.6.24) thus:

At the start, the persulphate ionic initiator ($S_2O_8^{2-}$) undergoes thermal decomposition to form two radicals, and initiates free-radical polymerisation, as shown in the following equation:



During the initiation step, each radical reacts with a monomer, to form a monomer-ended radical:



The monomer-ended radical propagates by further reacting with other monomers to form a polar head and a polymeric tail, as represented by equation (2.6.24) and Figure 2.16.



2.6.5 Polymer Microspheres in Bioconjugation and Protein Immobilisation

As previously mentioned, considerable work has been done and many developments have been made in the bioconjugation of microspheres, the immobilisation of proteins onto microsphere surfaces and the use of microspheres in immunoassays and biosensors (Olal 1990; Ortega-Vinuesa J. L. and Hidalgo-Alvarez 1993; Wong 1993; Hermanson 1996; Bangs Labs 1999a; Hall *et al* 1999; Siiman *et al* 2001; Baptista *et al* 2003; Jodar-Reyes *et al* 2005; López-León *et al* 2005). A large variety of polymer latex particles may be considered for these purposes; in this research, three types are considered: polystyrene (PS), polymethyl methacrylate (PMMA) and the copolymer poly(methyl methacrylate-co-2-hydroxyethyl methacrylate) (P(MMA-HEMA)).

Polystyrene (PS)

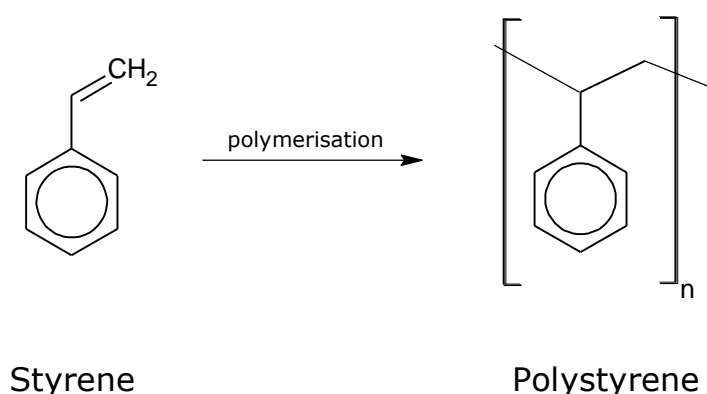


Figure 2.17 Polymerisation of styrene to form polystyrene

Polystyrene is a vinyl polymer and is made from the polymerisation of its monomer, styrene, as shown in Figure 2.17. Polystyrene latex particles have been widely used for bioconjugation in the biomedical fields and environmental sciences and much work has been done to understand their surface and colloidal chemistry and their interaction with biomolecules (Olal 1990; Ortega-Vinuesa J. L. and Hidalgo-Alvarez 1993; Seradyn 1999; Siiman *et al* 2001; Lubarsky *et al* 2004; Jodar-Reyes *et al* 2005; López-León *et al* 2005; Jodar-Reyes, Martín-Rodríguez *et al* 2006; Jodar-Reyes, Ortega-Vinuesa *et al* 2006). Studies of adsorption of the protein bovine serum

albumin (BSA) onto polystyrene surfaces showed that particles with highly hydrophobic surfaces adsorbed more BSA molecules than those with lower hydrophobicity, and were less likely to lose adsorbed BSA through desorption, following extensive buffer wash (Olal 1990). Whilst many studies have shown the ease of adsorption of proteins onto hydrophobic polystyrene surfaces, Okubo *et al* (1987) and Ortega-Vinuesa and Hidalgo-Alvarez (1993) report loss of colloidal stability when the polystyrene has been sensitised with IgG or other protein. Nevertheless, polystyrene has been widely used and has been a popular choice for use in latex agglutination tests (Gella *et al* 1991; Xu *et al* 2005) since it was first reported by Singer and Plotz (1956a).

Emulsion polymerisation of styrene initiated with benzoyl peroxide

Polystyrene latex particles can be produced by free-radical chain-growth polymerisation, via mechanisms introduced previously in Section 2.6.3 and as shown in Figure 2.18 to Figure 2.20 below:

Polymerisation of styrene initiated by benzoyl peroxide, the addition occurs as shown in Figure 2.18.

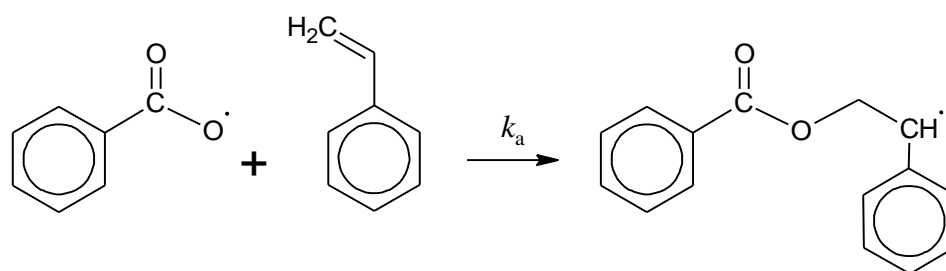


Figure 2.18 Polymerisation of styrene: initiation using benzoyl peroxide

During propagation, additional styrene units are added to the initiated species, as previously shown by the general equation (2.6.5); the first propagation step for styrene addition with benzoyl peroxide initiator is shown in Figure 2.19.

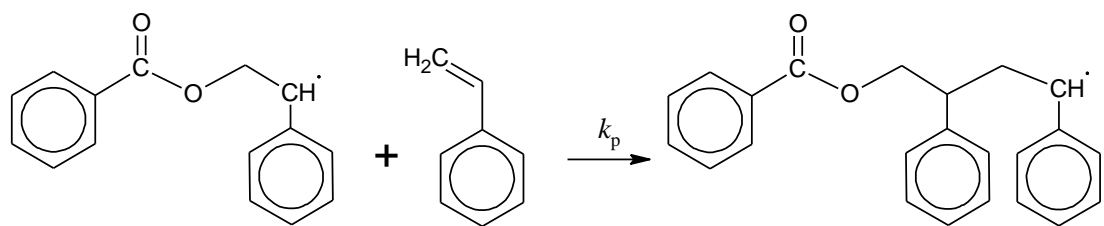


Figure 2.19 Polymerisation of styrene: propagation

In polymerisation of polystyrene, termination generally occurs by combination at temperatures greater than 60°C (Nicholson 1997), in which mutual annihilation of two radicals occurs by the combination of the radicals to form a paired electron bond, as shown by equation (2.6.7) and in Figure 2.20.

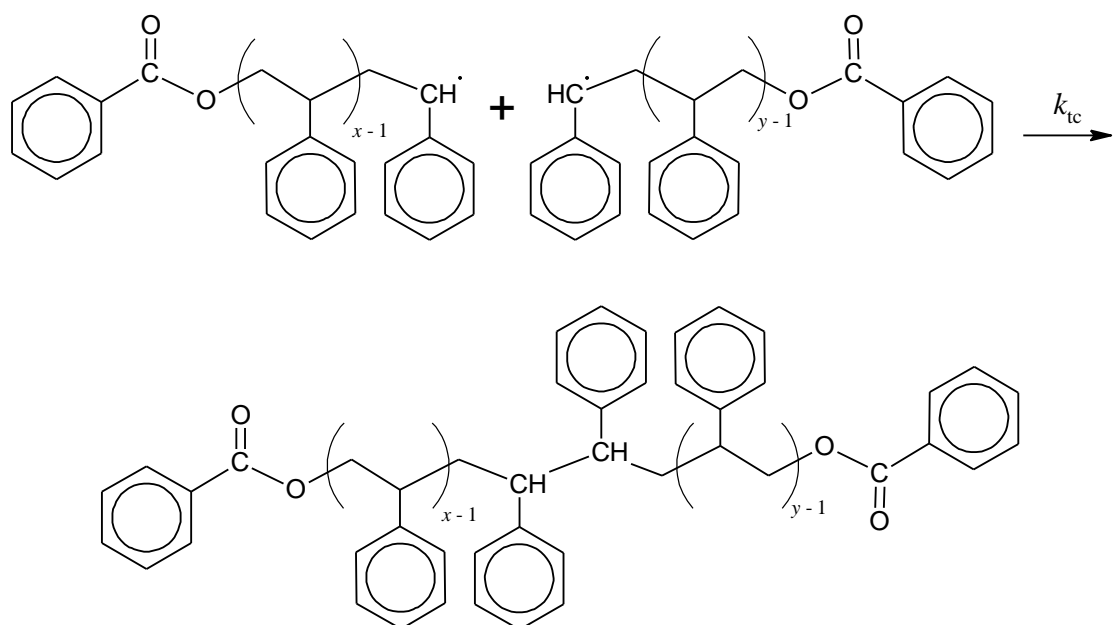


Figure 2.20 Polymerisation of styrene: termination by combination

Polymethyl methacrylate (PMMA)

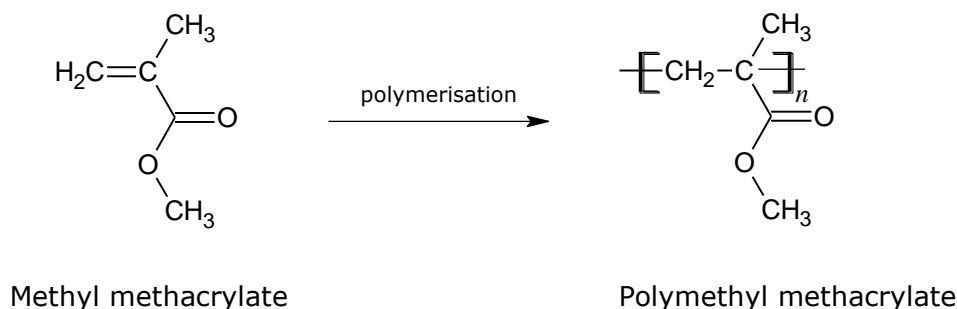


Figure 2.21 Polymerisation of methyl methacrylate to form polymethyl methacrylate

Polymethyl methacrylate (PMMA) is a methacrylic polymer and is made from the polymerisation of its monomer, methyl methacrylate (MMA), as shown in Figure 2.21. Like polystyrene, it can easily be produced by a variety of polymerisation methods; in addition, it is very versatile and widely used for many purposes. Although PMMA is probably most commonly known for its use as a substitute to glass, in the form of a sheet plastic, its uses in latex form are becoming more widely researched. Its excellent biocompatibility, good mechanical strength and outstanding optical quality have been reported by a number of studies and have therefore made it a popular choice of material for use in a wide range of applications from electronics, biomedical science and materials science (Araujo *et al* 1999; Müller *et al* 2000; Romanov *et al* 2001; Ahlin *et al* 2002; Ayhan 2002); its use in drug delivery is well documented (Borchard *et al* 1994; Araujo *et al* 1999; Ahlin *et al* 2002) and is becoming a major part of the biomedical sciences. For these reasons, it was considered to be a potentially ideal material for this research, to be used for antibody conjugation and microbial detection using fluorescence and an optical detection system.

Surfactant-free emulsion polymerisation of methyl methacrylate using a persulphate initiator

Similarly to polystyrene, PMMA microspheres can be produced by free-radical chain-growth polymerisation, via mechanisms discussed previously in Section 2.6.3. Although, like styrene, emulsion polymerisation of MMA containing a surfactant can

be initiated using benzoyl peroxide or AIBN, there are certain advantages to using surfactant-free polymerisation. As previously discussed in Section 2.6.4, the presence of surfactants in a polymerisation system may result in variable properties of the polymer and can cause the particles to coagulate.

Therefore, in order to minimise variation in polymer properties – to maximise monodispersity and ensure uniform particle sizes – and to avoid flocculation and coagulation, surfactant-free emulsion polymerisation of methyl methacrylate has been deemed to be the preferred method of PMMA microsphere production to be used for the immobilisation of antibodies for use in microbial detection using immunochromatographic assays. The mechanism of surfactant-free emulsion polymerisation of methyl methacrylate is shown in Figure 2.22 to Figure 2.24 and described as follows:

In initiation by a persulphate initiator such as potassium persulphate, also known as potassium peroxydisulphate, addition occurs as shown in Figure 2.22.

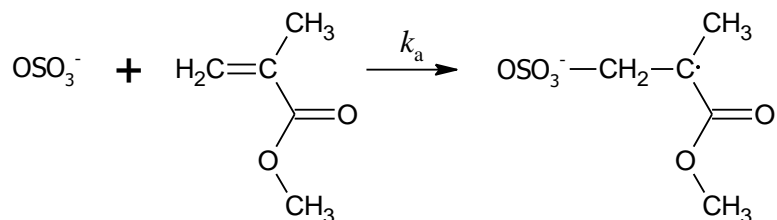


Figure 2.22 Surfactant-free emulsion polymerisation of methyl methacrylate: initiation using a persulphate initiator

During propagation, additional MMA units are added to the initiated species, as was shown by equation (2.6.24); the first propagation step for MMA addition with a persulphate initiator is shown in Figure 2.23.

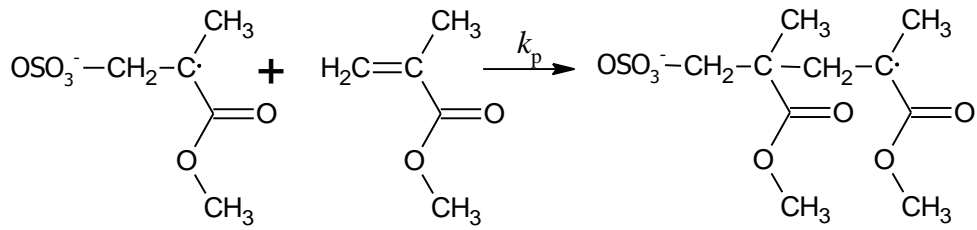


Figure 2.23 Surfactant-free emulsion polymerisation of methyl methacrylate: propagation

In the polymerisation of MMA, termination generally occurs by disproportionation at temperatures greater than 60°C (Nicholson 1997), in which a hydrogen atom is transferred from one radical species to form two new terminated chain molecules, as shown by equation (2.6.8) and in Figure 2.24. In the reaction shown, the hydrogen atom has been transferred from radical Y to radical X, yielding product Y' (unsaturated) with one fewer hydrogen atom than product X' (saturated).

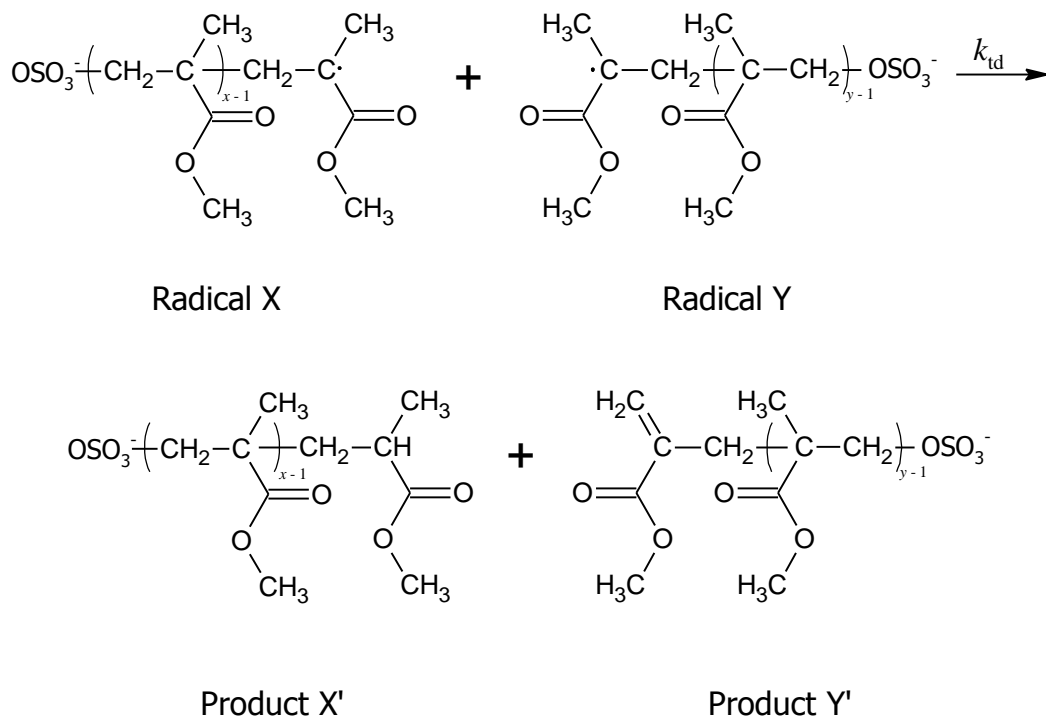


Figure 2.24 Surfactant-free emulsion polymerisation of methyl methacrylate: termination by disproportionation

During the polymerisation of methyl methacrylate, an organic solvent such as toluene may be added to the reaction system. It has been shown that toluene contributes to the control of the rate and heat of reaction, stabilising the particles as a result, in addition to controlling the particle size and maximising the monodispersity of the produced

surfactant-free microspheres (Wang *et al* 2004). Similarly, toluene is used during the polymerisation of methyl methacrylate reported by Müller *et al* (2000), who used surfactant-free emulsion polymerisation initiated by potassium peroxydisulphate to prepare monodisperse PMMA microspheres (with and without the incorporation of an internally labelled fluorescent dye) with diameters between 200 and 400 nm.

Poly(2-Hydroxyethyl methacrylate) (PHEMA)

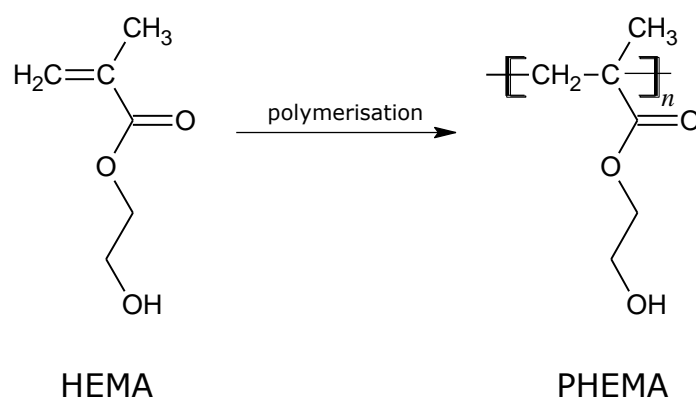


Figure 2.25 Polymerisation of 2-hydroxyethyl methacrylate to form poly(2-hydroxyethyl methacrylate)

Like polystyrene and MMA, poly(2-hydroxyethyl methacrylate) (PHEMA) latex particles and cross-linked PHEMA hydrogels have been used in many biomedical and pharmaceutical applications, including its use in soft-contact lenses, endovascular occlusion of blood vessels and drug delivery systems (Liu *et al* 2000; Tauer *et al* 2005). Due to HEMA's similarity in structure to MMA, with the additional hydroxyl functional group, it was taken into consideration as a possible copolymer for the purpose of providing a suitable surface functional group in the conjugation of antibodies to microsphere surfaces using covalent chemical coupling.

In its monomer form, HEMA is highly soluble in aqueous media; once polymerised, PHEMA is no longer completely soluble in water, but can be swollen in water and aqueous electrolyte solutions by about 40% by weight (Tauer *et al* 2005). PHEMA is hard and brittle when dried but soft and flexible in its swollen state. The hydrophilic nature of PHEMA and solubility of its monomer in water requires careful

consideration of its polymerisation process and the stabilisers and initiators used. Tauer *et al* (2005) report successful polymerisation in aqueous media of stable PHEMA latex particles with diameters below 500 nm through the usage of AIBN as an initiator. Furthermore, they state that the use of hydrophilic initiators such as potassium peroxodisulphate “leads to complete coagulum formation even in the presence of surfactants”.

Copolymers using HEMA

PHEMA on its own is not an ideal material to be used for bioconjugation for the purpose of applying it to immunochromatographic assays. This is because although it is hard and brittle when dried, it becomes soft and flexible when in contact with water and aqueous electrolyte solutions due to swelling. Applications in immunochromatographic assays require that the microspheres retain their structure and properties.

Although PHEMA cannot be used as a homopolymer for the required purpose, it has an attractive potential to be used as a copolymer because of its hydroxyl functional group. Since polystyrene and PMMA were investigated and discussed previously, it is only logical that their use with HEMA is explored.

Poly(styrene-co-2-hydroxyethyl methacrylate) (P(S-HEMA))

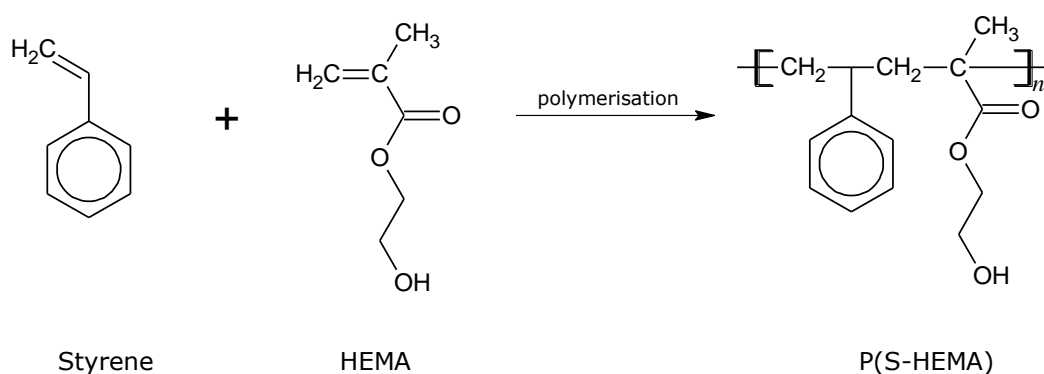


Figure 2.26 Copolymerisation of styrene and HEMA to form P(S-HEMA): one possible outcome in the form -ABAB-

A number of studies have been conducted on the copolymerisation of styrene with HEMA to form poly(styrene-HEMA) (P(S-HEMA)) with the purpose of improving the colloidal stability of polystyrene when sensitised with an antibody and of investigating its wider use in bioconjugation, and have reported increased colloidal stability of the microspheres as a result (Kamei *et al* 1986; Okubo *et al* 1987; Okubo *et al* 1989). More recently, surface characterisation of the copolymer has been carried out (Martín-Rodríguez *et al* 1996) and Ukun *et al* (2005) have reported successful production of uniform P(S-HEMA) microspheres of around 4 μm in diameter, which was used in the dye affinity adsorption of albumin.

Poly(methyl methacrylate-co-2-hydroxyethyl methacrylate) (P(MMA-HEMA))

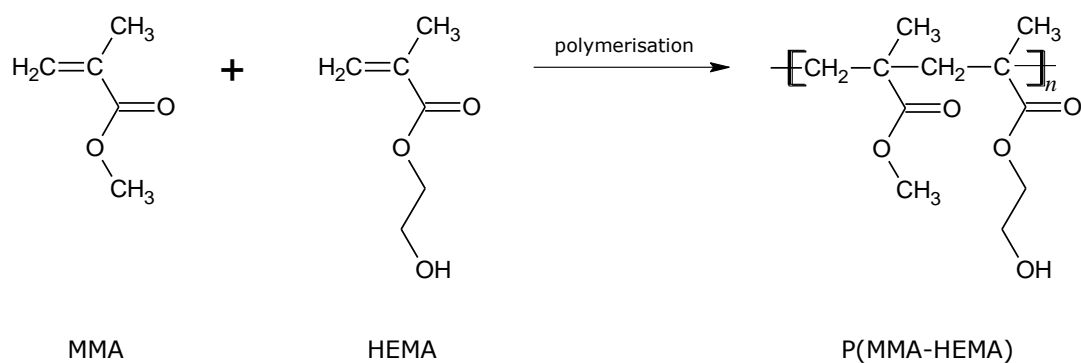


Figure 2.27 Copolymerisation of MMA and HEMA to form P(MMA-HEMA): one possible outcome in the form -ABAB-

Poly(methyl methacrylate-co-2-hydroxyethyl methacrylate) (P(MMA-HEMA)) is a synthetic heteropolymer that is synthesised from the monomers methyl methacrylate and HEMA. Its biocompatibility, combined with mechanical strength that is sufficient for biotechnological applications, has made it suitable for enzyme immobilisation (Arica *et al* 1997; Arica 2000; Denizli *et al* 2000; Yavuz *et al* 2002).

The similarity in chemical structure between HEMA and MMA should enable the resulting copolymer to retain most of the desirable chemical and optical properties of PMMA, whilst allowing the hydroxyl group provided by the HEMA constituent to endow the microsphere with a surface functional group required for the covalent

chemical coupling of the microsphere with the Fc region of an antibody, as further discussed in Section 2.8.3.

Yavuz *et al* (2002) report successful copolymerisation of MMA and HEMA, using suspension polymerisation, to yield stable P(MMA-HEMA) microspheres of around 4 μm in size. However, given the requirement in this research for microspheres with diameters below 500 nm, Yavuz and colleagues' (2002) method alone would not satisfy the conditions. Hence, it was deduced that the synthesis of monodisperse and stable P(MMA-HEMA) microspheres with diameters below 500 nm could be achieved through a combination of methods reported by Yavuz *et al* (2002), Tauer *et al* (2005) and Müller *et al* (2000) and incorporating selected techniques based on their findings, as discussed below. Optimisation and refining of the overall method would be accomplished through experimentation.

Suspension polymerisation generally yields particles of a larger size range than emulsion polymerisation, as previously discussed in Section 2.6.4. Therefore, emulsion polymerisation would be the logical alternative in order to create microspheres with diameters below 500 nm, as in the cases of Müller *et al* (2000) and Tauer *et al* (2005). Using a persulphate initiator in polymerisations involving HEMA has been found to result in particle aggregation (Tauer *et al* 2005); therefore, it was deduced that AIBN should be the initiator of choice, as per Yavuz and colleagues' (2002) method.

2.6.6 Microsphere Surface Chemistry and Surface Modification

Surface properties of microspheres play an important role in bioconjugation and immobilisation, and extensive work has been done to develop increasingly sophisticated methods for the characterisation and modification of microsphere surfaces (Ortega-Vinuesa Juan L. *et al* 1995; Martín-Rodríguez *et al* 1996; Chen *et al* 2002; Li *et al* 2004).

Analysis and characterisation of microsphere surfaces can be done using a variety of methods, including microscopy techniques such as scanning electron microscopy and atomic force microscopy (Jandt 2001), which are discussed later on in Section 2.6.8.

Other methods include Fourier transform infrared (FTIR) and nuclear magnetic resonance (NMR) spectroscopies.

It was previously discussed that microsphere surface chemistry can be modified by providing surface functional groups through the employment of copolymerisation techniques. This is a form of chemical modification carried out during the polymerisation stage. In addition to modifying the surface properties via chemical means, a variety of methods have been developed to enable direct modification of surface properties post-polymerisation. Such techniques include plasma and laser treatment of microsphere surfaces (Hegemann *et al* 2003) and even the use of the atomic force microscope to manipulate biomaterials and interfaces (Jandt 2001).

2.6.7 Cleaning and Separation of Microspheres

As previously discussed in Section 2.6.2, microspheres that are to be used in microbial detection are required to be of high quality. One of the factors that constitute the quality of the microspheres is the cleanliness of the solution as well as the microsphere surface. After the production of microspheres, unwanted chemical residue may be present in the solution and on the surface of the particles. It is therefore necessary to consider techniques to minimise contamination. Filtration methods, ranging from conventional normal flow filtration to the more sophisticated tangential flow filtration, are considered and discussed.

Types of Filtration

Filtration is a process used to separate solid particles in a liquid solution or suspension, based on their size and charge differences, by utilising a pressure differential. There are two distinct operational modes of filtration – normal flow filtration (NFF) and tangential flow filtration (TFF).

During normal flow filtration, the liquid containing the suspended particles is conveyed directly towards the filtration membrane under an applied pressure. In practice this is usually carried out using gravitational pressure or vacuum suction. In standard gravitational filtration, a cone-shaped filter paper is simply placed into the

upper part of a funnel, which is suspended above a flask; liquid transferred to the funnel is allowed to pass through the filtration membrane to the collection flask by gravitational pressure. In vacuum filtration, a Buchner or Hirsh filtration unit is connected either to a water tap equipped with an aspirator or a vacuum pump to force liquid through the filtration membrane by the application of reduced pressure – the creation of a vacuum.

As the solution passes through the membrane, particles that are smaller than the size of the pores are able to cross over to the downstream side, leaving those particles larger than the pore size on the upstream side. This process is also commonly referred to as through-flow filtration or dead end filtration. However, because the term normal flow is illustrative of the direction of fluid flow, i.e. normal to the membrane surface, it is the term of choice and shall henceforth be referred to as such. NFF is commonly used in the sterile filtration of clean streams, virus and protein separation, along with a wide variety of other applications.

During tangential flow filtration (TFF), the solution is pumped along the membrane surface and an applied pressure forces a portion of that solution to pass through the membrane onto the filtrate side. Similarly to NFF, particulates and macromolecules larger than the membrane pore size (as well as some smaller-sized particles) are retained on the upstream side as retentate. Unlike in NFF, in which the retained solids quickly form a filtration cake caused by the build-up of particles on the surface of the filtration membrane, particles in a TFF retentate stream simply get swept along by the tangential flow, making this filtration technique ideal for the separation of fine particles. Tangential flow filtration is also commonly referred to as cross-flow filtration; however, as with normal flow filtration, the term tangential flow is illustrative of the direction of fluid flow, in this case tangential to the filtration membrane, and is therefore the term of choice and shall henceforth be referred to as such.

Tangential Flow Filtration

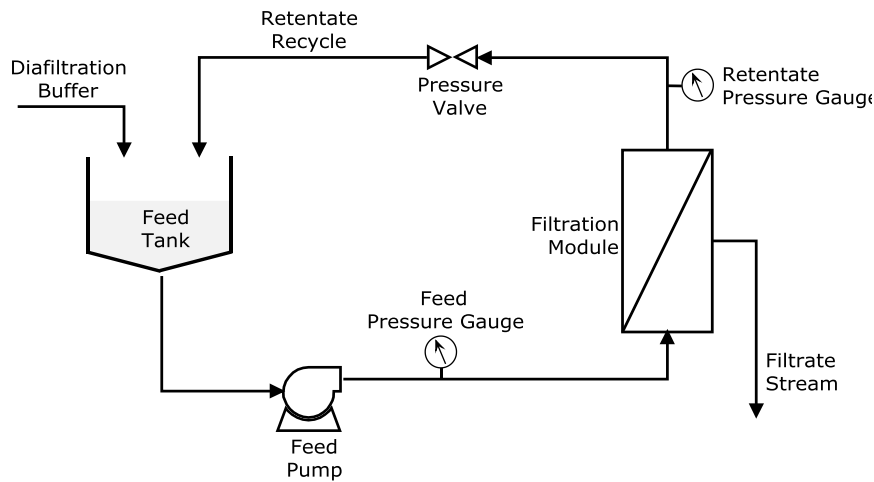


Figure 2.28 Schematic diagram of a tangential flow filtration system. Adapted from (Millipore 2003).

During a unit operation of a TFF system, the flow of the feed stream is generated by a feed pump, as shown in the schematic diagram of a typical TFF system in Figure 2.28. The feed stream is pumped through a channel, which is situated between two membrane surfaces within the filtration module. With each pass of fluid over the membrane surface, a portion of the fluid is forced through the membrane by the applied pressure and into the filtrate stream, resulting in a feedstock concentration gradient between the more concentrated wall conditions at the membrane surface and the less concentrated bulk conditions at the centre of the channel; the flows and forces in a TFF channel are illustrated in Figure 2.29. In addition, progressively more fluid is passed through the membrane on to the filtrate side, resulting in a concentration gradient along the length of the filtration channel, with a decrease in concentration from the feed at the inlet to the retentate at the outlet. This also explains the pressure drop from the feed to the retentate as a result of the flow of feedstock flow along the length of the membrane. However, the pressure along the length of the membrane on the filtrate side is more or less constant because the flow there is relatively low, and therefore there is little restriction. A pressure profile in TFF channel is shown in the graph in Figure 2.30.

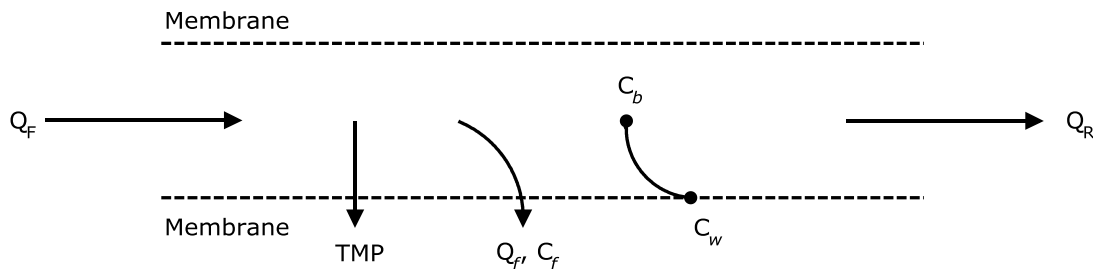


Figure 2.29 Flows and forces in a tangential flow filtration channel. Adapted from (Millipore 2003).

Parameters used in Figure 2.29 are defined as follows:

Q_F : feed flow rate [$l\ h^{-1}$]

Q_R : retentate flow rate [$l\ h^{-1}$]

Q_f : filtrate flow rate [$l\ h^{-1}$]

C_b : component concentration in the bulk solution [$g\ l^{-1}$]

C_w : component concentration at the membrane surface [$g\ l^{-1}$]

C_f : component concentration in the filtrate stream [$g\ l^{-1}$]

TMP: applied pressure across the membrane [bar]

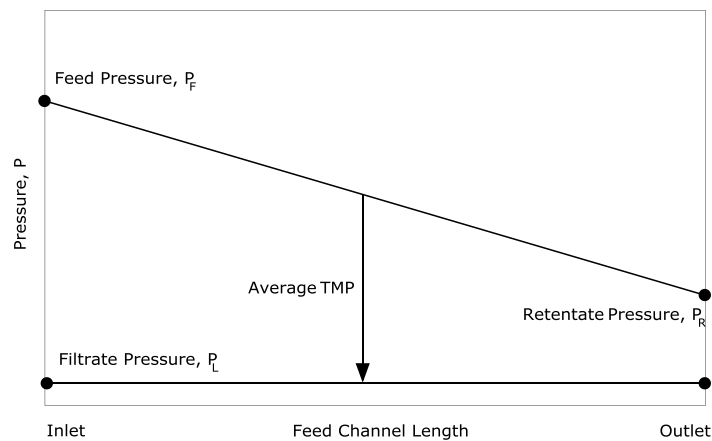


Figure 2.30 Pressure profile in a TFF channel. Adapted from (Millipore 2003).

Comparing Tangential Flow Filtration to Normal Flow Filtration

The difference between tangential flow filtration and normal flow filtration, shown in Figure 2.31, is quite pronounced and can be better understood once the mechanism of retention has been analysed. The ability of the membrane in TFF to perform effective

surface filtration is the basis of its efficiency; this is especially important where suspended or colloidal particles are involved. In TFF, high recirculation rates ensure higher tangential flow velocities across the membrane surface. This promotes turbulence, increasing the rate of re-dispersion of the retained solids in the bulk feed.

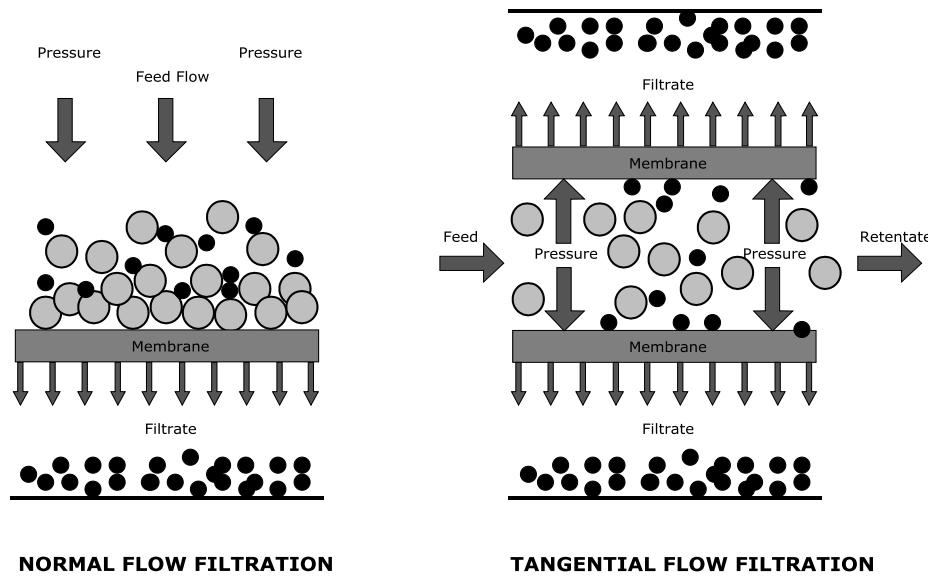


Figure 2.31 Comparison of Normal Flow Filtration and Tangential Flow Filtration separation mechanisms

In contrast to TFF, in NFF retention occurs as a result of particle build-up on the surface and within the pores of the filtration membrane. The applied pressure forces the entire feed through the membrane filter, producing a filtrate that contains fewer and fewer particles as the build-up on top of the membrane surface increases to form a filter cake. The feed and filtrate travel simultaneously along the length or surface area of the filter, generating one product stream for every feed. On the other hand, in TFF one feed generates two product streams: the retentate and the permeate (or filtrate), as shown in Figure 2.28. Per pass recovery in a TFF system is quite low compared to that in an NFF system because in an NFF system only the solids are removed. However, because TFF is a continuous process, the retentate containing the particles that did not pass through the membrane is re-circulated around the system as retentate recycle in order to increase the total recovery, but at the expense of increased energy usage.

As the filtration in an NFF system progresses, provided the transmembrane pressure is kept at a constant, the build-up of particles rapidly increases and the filter cake becomes increasingly thicker, resulting in a reduced filtration rate. When the membrane build-up reaches saturation and the flow or pressure approaches a limit, the filtration must be interrupted in order to clean or replace the membrane filter. This bulk mode of operation is a major disadvantage, especially when process streams containing a high solid content are involved. This disadvantage in an NFF system is overcome by the efficient fluid management in a TFF system. Thus, for feed streams with a high solid load (\geq approx. 1 wt%) TFF may be more suitable than NFF, which is more suitable for feed streams containing lower concentrations of solids (\leq approx. 0.5 wt%). However, if the retained solids constitute the recovered product or if the nature of the solids is the cause of increased fouling, then TFF would be the preferred method. In addition, when particle size or molecular weight distribution is an important consideration – separation of proteins, enzymes, colloidal particles and oily emulsions – TFF should be considered.

2.6.8 Microspheres Imaging

Microspheres that are to be used for the immobilisation of antibodies and in microbial detection need to have a narrow size and shape range. Imaging technology has made it possible to determine visually the size and shape distributions of the microspheres. There are numerous imaging techniques currently available; two are discussed here. Scanning electron microscopy (SEM), probably one of the most commonly used techniques for surface topography imaging, and atomic force microscopy (AFM), a much more recent and extremely sophisticated technique, are both powerful microscopy techniques for imaging microspheres. The technologies behind each of the microscopy methods are quite different and each has its advantages and disadvantages. Each of their technologies and a comparison of their uses in microsphere imaging are discussed below.

Scanning Electron Microscopy (SEM)

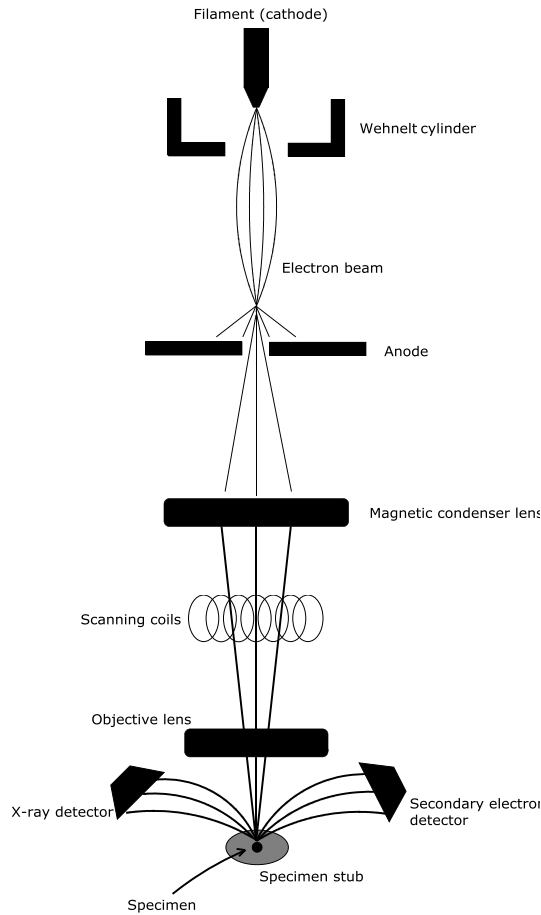


Figure 2.32 SEM column

A scanning electron microscope (SEM) is a type of electron microscope that creates images of the surface of a sample by using a high-energy beam of electrons to scan the sample surface in a raster scan pattern. Surface topography, composition and electrical conductivity information from the sample is obtained as a result of the signal produced by interaction of the electrons with the sample's atoms.

The high-energy beam of electrons, which follows a vertical path through the SEM, is produced by an electron gun, such as a thermionic electron gun or a field emission gun, which is located at the top of the microscope, as shown in Figure 2.32. The most common electron gun used is the thermionic electron gun, which consists of a

filament which functions as a cathode, an anode plate with an opening in the centre, and a Wehnelt cylinder. A positive electrical potential is applied to the anode, making it positive with respect to the filament and therefore creating attractive forces for electrons. A voltage is applied to the filament, causing it to heat up and produce electrons, which then accelerate toward the anode. Electrons are also emitted from the sides of the filament but are repelled toward the centre by the Wehnelt cylinder, which is supplied with a negative electrical potential. The electrons that were repelled towards the centre by the Wehnelt cylinder then pass through the opening in the anode plate and down the microscope's column; the beam of electrons is then condensed and focused by condenser lenses and an objective lens, respectively, and reaches the sample as a high intensity beam.

Upon hitting the sample, the interaction of the beam of electrons with the sample's atoms causes a number of things to be ejected from the sample: secondary electrons, produced by the interaction of the electrons from the electron beam with the loosely held outer electrons of the sample; backscattered electrons, caused by the deflection of the electrons from the electron beam by the nuclei of the atoms in the sample; transmitted electrons, which are the electrons from the electron beam that pass through the sample; and x-rays, light and heat. A number of detectors collect the ejected electrons, convert them into a voltage and amplify the signal, which is then sent to a display monitor.

Because of the extremely small size of electrons, they are easily deflected by gas molecules in the air. For this reason, the SEM column must operate within a vacuum in order to ensure the electrons reach the sample. Samples to be viewed using an SEM need to undergo specific preparations prior to being placed within the SEM's vacuum chamber. All liquids must be removed from the sample and the sample needs to be either electrically conductive or coated with a conductive layer to avoid charge build-up. Metals, which are naturally conductive, do not require further preparation. However, non-metals like polymer microspheres are not naturally conductive and need to be coated with a conductive layer, using a device called a sputter coater, again conducted within a vacuum.

Atomic Force Microscopy (AFM)

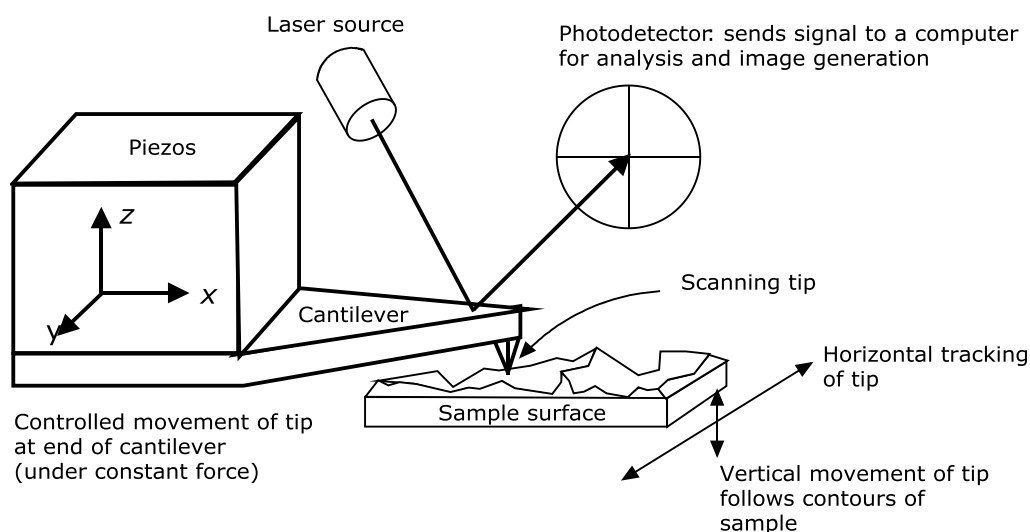


Figure 2.33 Schematic diagram of how an AFM operates. Adapted from Lehenkari *et al* (2000).

The atomic force microscope (AFM) differs from conventional microscopes, including the SEM, in that instead of relying on electromagnetic radiation, such as photons or electron beams, to create an image the AFM is a mechanical imaging device that uses the piezoelectric effect on a sharpened probe to measure three-dimensional topography and other physical properties of a surface. The probe, located on the end of a flexible cantilever, is positioned close enough to, but not touching, the surface of the sample and interacts with the surface's force field. It scans across the sample surface in a raster pattern while maintaining a small, constant force. The resulting image is created from the motion of the probe being scanned over the sample surface. Figure 2.33 shows a schematic diagram of how a typical AFM operates.

There are two main imaging modes associated with the AFM: contact mode and tapping mode. In contact mode, the probe is scanned in a raster pattern and the change in cantilever deflection is monitored with a split photodiode detector. The cantilever deflection is maintained at a constant value by a feedback loop, which vertically moves the scanner in order to maintain a constant photodetector difference signal and maintains a constant force during scanning. The topographic image of the sample surface is recreated from computer-stored data containing information on the vertical

distance that the scanner moves at each x, y data point. In this AFM imaging mode, the probe glides over the sample surface, as shown in Figure 2.34.

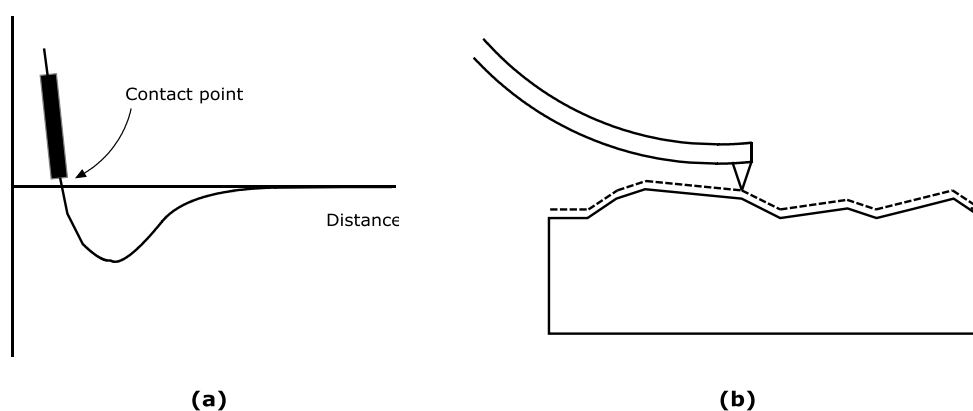


Figure 2.34 Contact mode AFM. Adapted from West (2007). (a) Potential diagram showing the region of the probe while scanning in contact mode. (b) In contact mode the probe glides over the surface.

There are certain disadvantages to using the contact mode, which limits its use on certain types of sample. Because of this ‘contact’ with the sample surface, contact mode AFM imaging is more suited to hard samples rather than soft samples like polymers and biological samples. The constant downward force on the tip can easily damage, and thus change the topography of, many soft surfaces. In addition, small particles like submicron-sized microspheres and biological samples like DNA and cells need to be placed on a substrate in order to be imaged. If using the AFM in contact mode, the force exerted on the sample often destroys it or pushes it out of the field of view by the tip as it moves back and forth in its raster pattern. These drawbacks associated with contact mode have been rectified by the development of the tapping mode, shown in Figure 2.35.

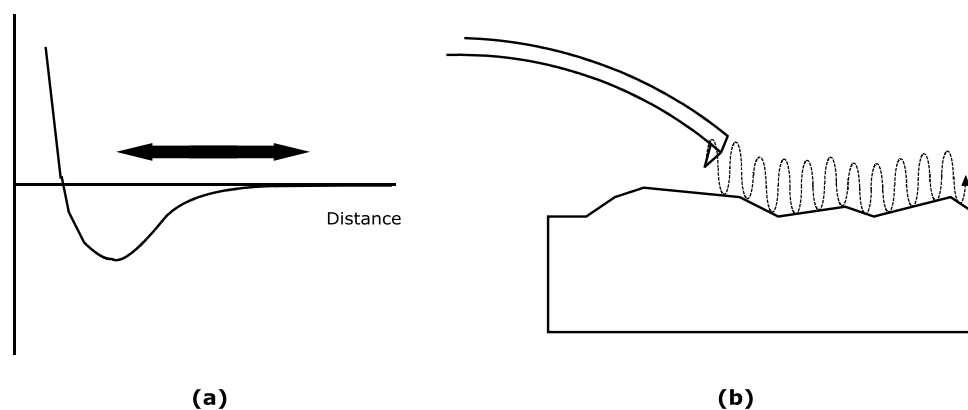


Figure 2.35 Tapping mode AFM. Adapted from West (2007). (a) Potential diagram showing the motion of the probe in tapping mode. (b) The probe vibrates as it scans across the surface.

In tapping mode, the cantilever oscillates at its resonance frequency, causing the tip to lightly tap the sample surface as it scans in the usual raster pattern across the surface. Laser deflection is used to detect the root-mean-square amplitude of the cantilever oscillation, and a topographical image is reconstructed from the recorded movement of the scanner, which is controlled by a feedback loop. The feedback loop maintains a constant oscillation amplitude by moving the scanner vertically at every x , y data point. This oscillation of the scanner over the sample surface eliminates the lateral, shear forces present in contact mode, thus giving the tapping mode a marked advantage over contact mode and enabling it to image soft, fragile and adhesive surfaces without damaging their surfaces. Tapping mode AFM is therefore the preferred method for imaging polymer microspheres.

Comparison of the AFM to the SEM

As previously mentioned, the AFM and the SEM are both powerful imaging techniques and have certain advantages and disadvantages. One major advantage of the AFM over the SEM is that the environment in which the sample is analysed does not need to be in a vacuum. The AFM can image samples in vacuum, air or even liquid, which makes it an especially attractive imaging technique for use in polymer science, biology and nanotechnology. In addition, because the AFM does not require a vacuum environment or the sample to be electrically conductive, sample preparation required for AFM imaging is minimal compared to that required for SEM imaging. Samples viewed by an AFM do not require special treatments such as the conductive

layer coating, which could irreversibly change or damage the sample. Another advantage the AFM has over the SEM is that it takes measurements in three dimensions – x , y and z (vertical measurement) – whereas the SEM only provides a two-dimensional topographical image. With respect to topographic imaging, the AFM is superior to the SEM and can image much smaller particles (approx. 1nm) than the SEM (approx. 100 nm). However, both the SEM and the AFM can be used for other analyses in addition to topographic imaging.

The greatest advantage that the SEM has over the AFM is that it provides elemental analysis of the sample, which the AFM does not do. Because of the interactions of the electrons in the electron beam with molecules within the sample in an SEM, the various emissions resulting from these interactions can be detected and analysed by the SEM. Although the AFM does not provide elemental analysis, it uses physical properties such as electrostatic and magnetic properties, elasticity and conductivity to differentiate between materials. Thus, the use of electrons in SEM technology has made it superior in measuring chemical composition and the mechanical nature of the AFM has made it superior in measuring physical properties of surfaces (West 2007).

Table 2.1 A summary of the comparison of the AFM to the SEM (West 2007).

	SEM	AFM
Samples	Must be conductive	Insulating/ conductive
Magnification	2 dimensional	3 dimensional
Environment	Vacuum	Vacuum/ air/ liquid
Time for image	0.1 - 1 minute	1 - 5 minutes
Horizontal resolution	100 nm	0.2 nm
Vertical resolution	n/a	0.5 nm
Field of view	1 mm	100 μ m
Depth of field	Good	Poor
Contrast on flat samples	Poor	Good

2.7 Adhesion Mechanisms and Theories

In order to understand the available methods of attaching a ligand such as an antibody or other protein to the surface of microspheres, be it metallic microspheres such as colloidal gold or polymer microspheres such as PMMA, some appreciation of the mechanisms of adhesion is necessary. It should be noted, however, that there is no single, unifying theory that describes or explains all adhesive bonds in a general and comprehensive manner. In this section, different adhesion theories are discussed in varying degrees of detail, with more emphasis placed on the types of adhesion that are more relevant to this research, such as adsorption and chemisorption.

Because there is no unifying theory that describes all adhesive bonds in a comprehensive manner, the categorisation of adhesion mechanisms often overlaps. For instance, some similarities exist between adsorption and chemisorption, and in some classifications, they are classed into the wider theory of adsorption (Kinloch 1987). Schultz and Nardin (2003), on the other hand, treat them as distinct and separate. In order to avoid confusion when referring to adsorption, this research takes Schultz and Nardin's (2003) approach, and does not class chemical bonds and chemisorption as part of the adsorption theory. This is also because adsorption and chemical bonding are considered two different options for bioconjugation and immobilisation. Therefore, when adsorption is referred to, it will not include chemical bonding.

2.7.1 Mechanical Interlocking

The mechanical interlocking theory suggests that adhesion occurs primarily as a result of the anchoring of the adhesive with the substrate by interlocking into the irregularities of the substrate surface. In mechanical interlocking, the adhesive must not only wet the substrate, but also have rheological properties that would enable it to penetrate pores and openings in a reasonable time. This theory of adhesion was demonstrated by E M Borroff and W C Wake in the 1940s by measuring the adhesion between rubber and textile fabrics and showing that, in that case, penetration of the protruding fibre ends into the rubber was the most important parameter in such

adhesive joints (Schultz and Nardin 2003). However, adhesion does not occur only between rough surfaces, and the fact that effective adhesion between smooth surfaces is achievable makes it clear that the mechanical interlocking theory only applies to a limited number of adhesion types and cannot, therefore, be considered to be universal. Other factors such as surface charge or chemical composition and functionality must come into consideration and are discussed below.

2.7.2 Electrostatic or Electronic Adhesion

The electrostatic or electronic adhesion theory, a controversial theory proposed by B V Deryaguin and co-workers in 1948, suggests that a significant contribution to intrinsic adhesion is due to electrostatic forces that arise when materials of different electronegativities or electronic band structures come into contact (Kinloch 1987). According to this theory, adhesive force arises due to the interaction of positive and negative charges through the transfer of electrons across an interface, which creates an electrical double layer at the interface.

The controversy of this theory is attributed to Deryaguin's statement that electrostatic forces are an important cause, rather than just a result, of high joint strength. Deryaguin *et al* analysed the adhesive-substrate junction as a capacitor which is charged due to the contact of the two different materials, whereby separation of the two plates of the capacitor during interfacial failure of this system leading to an increase in potential difference until a discharge occurs (Schultz and Nardin 2003). This theory makes the presumption that adhesion is due to the attractive electrostatic forces across the electric double layer. An example of electrostatic adhesion is the bringing of a polymer into contact with a metal: electrons are transferred from the metal to the polymer and results in the creation of an electrical double layer at the polymer-metal interface.

Further studies by C L Weidner on Deryaguin's methods could not affirm Deryaguin's methods, since the electrical double layer could not be identified without separating the adhesive bond. It was also argued that the adhesive bond strength was an exaggeration and therefore, like the mechanical interlocking theory, the electronic theory is now generally not considered to contribute significantly to intrinsic adhesion

(Kinloch 1987; Schultz and Nardin 2003). Details of the studies on the discrediting the validity of Deryaguin's methods and of this theory is beyond the scope of this research and is therefore not discussed in detail.

2.7.3 Diffusive Adhesion

The diffusion theory of adhesion is principally concerned with the adhesion of polymers to themselves, known as autohesion, or to other polymers. Primarily advocated by S S Voyutskii in the early 1960s, the theory stipulates that the adhesion strength of polymers is due to the entanglement of long-chain macromolecules across the interface after the materials have experienced mutual diffusion, or inter-diffusion (Kinloch 1987). It implies, however, that the polymer chains or chain segments are sufficiently mobile and are mutually compatible and miscible, and with similar polarities, conditions which are usually satisfied in the autohesion of elastomers and in the solvent welding of compatible, amorphous plastics (Kinloch 1987). However, the overwhelming majority of adhesive and substrate polymers are not compatible; this may be because the polymers are not mutually soluble or because one polymer is highly cross-linked, is crystalline or is above its glass transition temperature. Therefore, the diffusion theory has found limited application and does not contribute significantly to the intrinsic adhesion.

2.7.4 Adsorption or Dispersive Adhesion

The adsorption theory of adhesion is the most widely applicable theory of adhesion and especially important in bioconjugation. It states that adhesion between two materials will occur given that sufficiently intimate molecular contact is achieved at the interface, owing to the resulting interatomic and intermolecular forces that are generated on the surface of the adhesive and substrate. Of these forces, van der Waals forces, referred to as secondary bonds, are the most common (Kinloch 1987). Other forces, relative to this research, that can contribute to adsorption and that are classified as secondary bonds include hydrogen bonds.

Secondary bonds are thus termed as an arbitrary measurement of the relative strengths of the adhesive bonds, with secondary bonds constituting weaker bonds and primary bonds, to which chemical bonding is referred, constituting stronger bonds.

Van der Waals forces are defined as “the attractive or repulsive forces between molecular entities (or between groups within the same molecular entity) other than those due to bond formation or to the electrostatic interaction of ions or of ionic groups with one another or with neutral molecules” (IUPAC 1997), and are comprised of three types of intermolecular forces: dipole-dipole interactions, dipole-induced dipole interactions and London dispersion forces.

An electric dipole consists of two electric charges, positive and negative, which are separated by a small distance. When a molecule contains two atoms of substantially different electronegativities bonded together, a permanent electric dipole moment occurs due to the existence of partial charges on its atoms, and the molecule is said to be polar. If a molecule is unpolarised but comes sufficiently close to a dipole, the unpolarised molecule may experience an induced dipole.

Dipole-dipole interaction, also known as Keesom interactions after Willem Hendrik Keesom, occurs between two polar molecules. If the two molecules are orientated so that their opposite partial charges are closer together than their like charges, a net attraction between them occurs.

Dipole-induced dipole interaction requires one of the two participating molecules to be polar. The second need not be polar; if it is, then this interaction supplements the dipole-dipole interaction previously described. In dipole-induced dipole interaction, the presence of the partial charges of the polar molecule causes a polarisation or distortion of the electron distribution of the other molecule. Regions of the partial positive and negative charge are created on the second molecule as a result, rendering the molecule polar. The partial charges developed in this way behave like those of a permanently polar molecule; therefore a net attraction occurs between the permanently polar molecule and the induced polar molecule as it would in a dipole-dipole interaction.

London dispersion interaction, named after Fritz London who first described it, is essentially an induced dipole-induced dipole interaction, and occurs between all types of molecule, whether they are polar or not. This interaction arises from the instantaneous transient dipoles possessed by all molecules due to fluctuations in the instantaneous positions of electrons. Considering two nonpolar molecules in close proximity to each other, because of the endless fluctuations of the electron density, the regions of equal and opposite partial charge would arise in one of the molecules, giving rise to a transient dipole, even though there were originally no permanent partial charges on either molecule. The induced transient dipole can in turn induce a dipole in the adjacent molecule, causing it to interact with the original transient dipole.

A hydrogen bond is an attractive interaction between two molecules, each of which contains a highly electronegative atom such as nitrogen, oxygen or fluorine, and where one of the molecules contains a hydrogen atom covalently bonded to that atom's highly electronegative atom. These bonds can occur intermolecularly (between molecules) or intramolecularly (within the same molecule) and is stronger than van der Waals interactions but weaker than chemical bonds such as covalent or ionic bonds. They are considered to be secondary bonds.

2.7.5 Chemisorption or Chemical Adhesion

Chemisorption, which comes from the terms chemical (ad)sorption, is a form of adsorption that requires two adhering materials to form a chemical bond: covalent, ionic or metallic. Although, as previously mentioned, it can be considered in the general classification of adsorption, it is in this research regarded as a different form of adhesion and not to be the same as adsorption. Chemical bonds are referred to as primary bonds and are the strongest form of adhesion. Bonds of materials adhered through chemical bonding are unlikely to be broken by changes in physical conditions such as slight changes in temperature or pH and would usually only undergo bond breakage via chemical reactions.

Surface and interfacial chemistry play an important role in chemical bonding adhesion. For chemical binding to occur, the adhering species require chemically

compatible functional groups to be available and accessible, in addition to favourable bonding conditions such as optimum temperature, pH and, in the case of solutions, adequate but not excessive agitation. Surface chemistry is especially important in bioconjugation and immobilisation when chemically binding a protein onto a microsphere surface. For this reason, extensive work has been done to characterise microsphere surfaces as well as to modify them so they are suitable for specific bindings (Martín-Rodríguez *et al* 1996; Jandt 2001; Chen *et al* 2002; Li *et al* 2004).

2.8 Conjugation of Monoclonal Antibodies to Polymer Microspheres

There are a number of methods by which antibodies may be attached, or conjugated, to a microsphere solid support. In the case of colloidal gold, conjugation is achieved by adsorption. However, polymeric microspheres differ due to their surface chemistry.

Physical methods of attachment such as adsorption methods are often adequate for conjugation (Bangs Labs 1999a). However, adsorption is reversible and under certain conditions such as pH or temperature changes, the proteins may be desorbed from the microsphere surface. A more permanent solution is covalent chemical coupling of the antibody onto the microsphere. Choosing the appropriate method for the application is important, as this will affect the binding capacity and activity of the antibodies to antigens.

2.8.1 Simple or Passive Adsorption

The mechanism for adsorption is primarily based on hydrophobic London Van der Waals attractions between the hydrophobic domains of the ligands and the polymeric surface of the microspheres. It is the simplest and most straightforward method of attaching ligands to particle surfaces. However, attachment may occur via both ionic interactions and hydrophobic interactions, usually in the case of less hydrophobic ligands or more hydrophilic microspheres. Where attachment is due in part to ionic interactions, the stability of the adsorption is affected by environmental conditions in the suspension: pH changes are likely to result in desorption of the ligands. It has been shown and is therefore generally recommended (Bangs Labs 1999a; Duke Scientific Corp 2004) that the pH of the binding buffer at which binding efficiency is greatest is at or near the protein's isoelectric point (pI) – the pH at which the protein is at electrical neutrality or at which it is at its minimum ionisation (Hale *et al* 1995).

Simple adsorption of a protein to a microsphere solid support follows a few preparation guidelines. Firstly, a diluted solution of protein and a diluted suspension of microspheres are prepared, in turn, in the reaction buffer. The protein solution is then added to the microsphere suspension at a ratio of one volume of protein solution

to ten volumes of microsphere suspension; the mixture is incubated. After incubation, unbound proteins are removed and the microsphere conjugate can then be stored in an appropriate storage buffer in a refrigerator. However, at no point should the microsphere suspension or conjugated microsphere suspension be frozen: freezing the microspheres may result in leaching of the dyes from within the spheres and lowering the optical quality of the spheres.

When preparing the reaction buffer, it should be noted that the composition of the reaction buffer depends on the type of protein being adsorbed and, more importantly, the biological activity of the final conjugate. As previously mentioned, the binding efficiency of proteins is usually greatest at their isoelectric point: the molecules' hydrophobic sites are usually more exposed and, in the case of antibodies, the molecules are more compact, allowing increased molecule per unit surface area for binding. In order to determine the appropriate buffer composition, a series of optimisation experiments is required where the different parameters – different concentrations of protein and reaction buffers at different pHs – are modified. Also, different buffers should be tested to find the most appropriate one; some common buffers used commercially are acetate buffer, phosphate buffered saline (PBS), borate buffer, citrate-phosphate buffer, carbonate-bicarbonate buffer and 2-(N-morpholino)ethanesulphonic acid (MES).

When adding the protein solution to the microsphere suspension, this must be done rapidly with efficient vigorous mixing. A vortex mixer is sufficient when working with small volumes. However, larger volumes require vigorous stirring using a magnetic stirrer in a flask while the protein is rapidly added to the centre of the vortex; care must be taken to ensure that foaming does not occur. Excessive vigorous mixing should also be avoided as this may detach the adsorbed antibody from the microsphere surface. Gentle mixing during adsorption is beneficial to overcome slow diffusion and assist in adsorption of the antibodies. Again, optimisation experiments should be performed in order to determine the optimal mixing force as well as the incubation temperature and period.

Unbound material can be removed by several methods. Large particles (diameter > 0.2 μm) can be cleaned by centrifugation and then re-suspended between washes by

vortex mixing, followed by gentle ultrasonication using a bath sonicator. However, care must be taken to avoid the use of excessive centrifugation forces to prevent the particles from being difficult to re-suspend. The disadvantages of centrifugation are that the process is time-consuming and a large loss of material may occur.

Other methods for purifying the conjugate are tangential flow filtration, which was discussed in Section 2.6.7, and dialysis. When using filtration methods, it is necessary to ensure that the pore size of the filter or dialysis material is large enough to allow the dissolved protein molecules to pass through efficiently. It is also important that the buffer used for cleaning is the same as the buffer used for storage as change in buffer pH or composition after washing could result in desorption of the bound protein. The addition of detergents or other surface active agents after the coating and washing of the microspheres may also cause desorption and should therefore be avoided.

2.8.2 Complex Adsorption

Complex adsorption is similar to simple adsorption but, as the term implies, requires additional steps in order to increase the attachment strength of the protein adsorption. This may involve the addition of a number of steps as well as a combination of steps.

A common complex adsorption method is to attach the protein by simple adsorption followed by crosslinking with glutaraldehyde. Glutaraldehyde acts like a “glue”, reinforcing the binding strength between the protein and the microsphere. Another complex adsorption method is by initially adsorbing a ligand, such as Protein A or Protein G, onto the microsphere and then using it to capture the intended antibody. It has been claimed (Bangs Labs 2002) that this is a superior method, enabling the maximisation of the correct orientation of the antibody: Protein A and Protein G bind specifically to the Fc region of antibodies so the Fab portions of the antibody should point away from the surface to allow for efficient capture of target antigen. Although this could be a highly effective method of ensuring the attachment strength and correct orientation of the antibody to the microsphere surface, the overall size of this complex should then be taken into account when testing for diffusion of the conjugate on a nitrocellulose strip. The more linkers and substances added to the conjugation complex, the larger will be the size of the conjugate, therefore adversely affecting the

detection speed. Thus, this must be taken into account when deciding which adsorption method to use.

2.8.3 Covalent Chemical Coupling

There are many benefits of covalently attaching antibodies onto microspheres. However, these methods may not be necessary if the correct adsorption method is used and the conjugate is tested and found to be stable. Covalent methods may be unnecessarily complicated compared to the simpler and more straightforward methods of adsorption; thus, care must be taken in choosing the appropriate method. There are, however, some obvious advantages to covalent coupling.

Perhaps the most significant advantage of chemical covalent coupling is that it is irreversible: the proteins are permanently bound and will not leach over time. The addition of detergents for washing and surfactants for eliminating non-specific binding do not cause the proteins to be detached from the surface: adding detergents and surfactants to adsorbed proteins could displace the proteins. Covalently bound antibodies tend to be less affected by changes in physical conditions such as changes in temperature or pH. Vigorous mixing of the protein-microsphere conjugate will not cause the protein to become endangered from detachment. There is also evidence that covalent binding also increases the surface coverage of proteins by about 10-40% (Bangs Labs 2002), compared to adsorption. Another very important advantage of covalent binding over adsorption is that the ligands can be more favourably orientated on the microsphere surface by binding the correct functional group on the microsphere surface to the carboxy terminal of the Fc region of the IgG molecule. This would then enable the availability of the Fab regions for interaction with target antigens.

Covalent coupling of antibodies to microspheres usually requires that the microspheres have the specific surface chemistry that will enable the chemically bonding of the two. Steps are usually undertaken to ensure that this is the case by chemically modifying the surface chemistry of the microspheres by copolymerisation so that the required functional groups are available for covalent binding. There are

several coupling protocols and each need to be considered depending on the required end result and functionality of the conjugate (Wong 1993; Hermanson 1996).

2.9 Principles of Fluorescence

Fluorescence is a three-stage process by which light of a particular wavelength is absorbed by some atoms and molecules and then, after a brief interval known as the fluorescence lifetime, is re-emitted at a longer wavelength. This phenomenon can be depicted by an electronic-state diagram, known as the Jabłoński diagram, shown in Figure 2.36. It is described in more detail below.

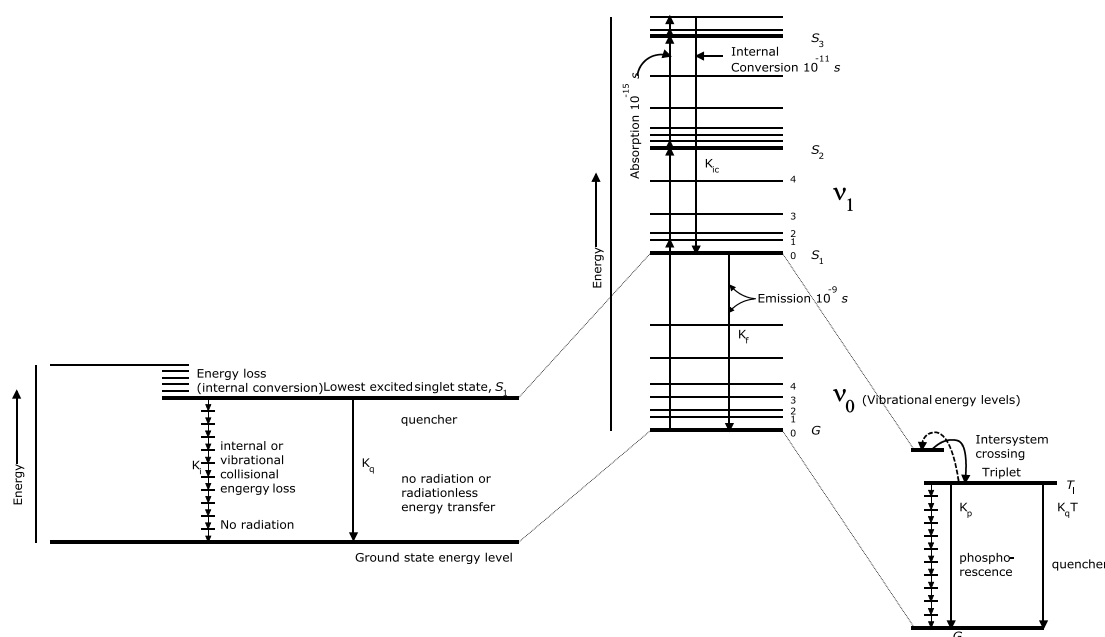


Figure 2.36 Jabłoński diagram

The Jabłoński diagram shown in Figure 2.36 illustrates the singlet ground state, denoted by G, as well as the first (S₁), second (S₂) and third (S₃) excited singlet states. The thick and thin horizontal lines represent electron energy levels and vibrational energy states, respectively. In this depiction of the Jabłoński diagram, the rotational energy states are ignored.

2.9.1 The Three Stages of the Fluorescence Process

$$E = h\nu_A = h \frac{c}{\lambda_A} \quad (2.9.1)$$

where

E = energy of incoming photon [J]

h = Planck's constant [J s]

ν_A = frequency of the incoming photon at the excitation (absorption) wavelength [Hz]

c = speed of light [m s^{-1}]

λ_A = excitation wavelength [m]

The three stages of the fluorescence process are excitation, the excited-state lifetime and emission.

At the first stage, the excitation stage, a photon of energy E, described by equation (2.9.1) above, is supplied by an external monochromatic light source such as a light emitting diode (LED), an incandescent lamp or a laser. Planck's Law states that "energy associated with electromagnetic radiation is emitted or absorbed in discrete amounts which are proportional to the frequency of radiation" (Licker *et al* 2003). Given that $\nu_A = c/\lambda_A$, meaning that frequency is inversely proportional to wavelength, it shows that the energy of the photon is also inversely proportional to the wavelength. This means that shorter incident wavelengths have a greater quantum of energy. The incoming light is absorbed by the molecule and creates an excited electronic singlet state. This process distinctly differs from chemiluminescence, in which the excited state is created and populated by a chemical reaction.

The functional group within a molecule that allows the particle to display fluorescence is known as a fluorophore. It is also sometimes referred to as a chromophore, and these two words can be used interchangeably.

Absorption of a photon of energy by a fluorophore is an all or nothing process. That is to say that either the photon is absorbed in its entirety, or it is not absorbed at all. Also, it should be noted that any particular fluorescent molecule can only absorb light at certain, specific, wavelengths. These wavelengths are known as absorption bands. The absorption of light at these wavelengths, and the subsequent emission at a longer wavelength, causes the electron cloud of the fluorescent molecule to move between a number of different vibrational and rotational orbital states. These different states correspond to different molecular energy levels, and can be best illustrated by means of the Jabłoński diagram shown in Figure 2.36 above.

The movement of the fluorophore between different excitation states takes place very quickly, so quickly in fact that the whole process (all three steps outlined above) takes place in only a small fraction of a second. The absorption of the incident photon takes approximately 10^{-15} seconds, and this corresponds to the time taken for the excitation of the fluorophore from ground state (G_0) to one of the excited states (S_1 , S_2 , etc). The particle then relaxes into the lowest excited singlet (S_1) (assuming that it is not in this state already), through a process known as internal conversion. Internal conversion, or loss of energy in the absence of emitted light, refers to the transfer of kinetic energy from the excited particle to other particles in the solvent solution through collision. This process takes approximately 10^{-11} seconds. Finally, the fluorophore will lose energy again, relaxing from the lowest excited singlet state (S_1) back into its ground state (G_0). During this final relaxation stage, the excess energy is released in the form of a photon and it is during this stage where fluorescence of the particle occurs. It takes approximately 10^{-9} seconds for the fluorophore to move between states S_1 and G .

Repeated excitation and relaxation of a fluorophore will eventually lead to the molecule becoming bleached, or photobleached. This refers to the permanent cessation of the particle's ability to fluoresce due to photon-induced chemical damage. Different fluorophores can withstand a large number of state transitions before this occurs. For example, the fluorescent dye fluorescein isothiocyanate (FITC) can be excited approximately 30,000 times before bleaching begins to take effect.

The area on the right of the Jabłoński diagram in Figure 2.36 shows an additional process that can occur when the fluorophore is raised to the excited singlet state S_1 . Sometimes, rather than returning directly to the ground state G and emitting a photon as previously discussed, the molecule may move into a transition state (T_1) through intersystem crossing. From here, the particle can release its energy as light in the much slower process of phosphorescence, and by doing so return to the ground state. Alternatively, the particle may move back into the single state S_1 and simply emit a photon in the form of fluorescence albeit following a slight delay to allow for the movements between T_1 and S_1 . Movement into the transition state is a relatively rare occurrence, and hence phosphorescence is a relatively rare phenomenon compared to fluorescence.

2.9.2 Absorption and Emission Spectra

The likelihood of an electron moving between excitation states depends on the degree of similarity between the vibrational and rotational energy states it exists in when at its ground state, G_0 , and when in the excitation state, S_1 . Therefore, a transition even becomes more probable in particles where there is a maximum overlap between potential electron positions in states G_0 and S_1 . The area of overlap can be considered to indicate what level of excitation energy is most likely to be absorbed.

Although the most likely state for an electron at room temperature is G_0 , within this state exists a number of different vibrational energy states ($\nu_0 = 0, 1, 2 \dots$) that may be occupied. Each of these vibrational states will require a different amount of absorption energy from the incident photon in order to make it jump into the next excited state. The different absorption energies required give rise to an absorption spectrum containing multiple peaks, as shown in Figure 2.37. It should be noted that the relative heights of the peaks indicate what proportion of the fluorescent particles are in each level of the ground state at any given time.

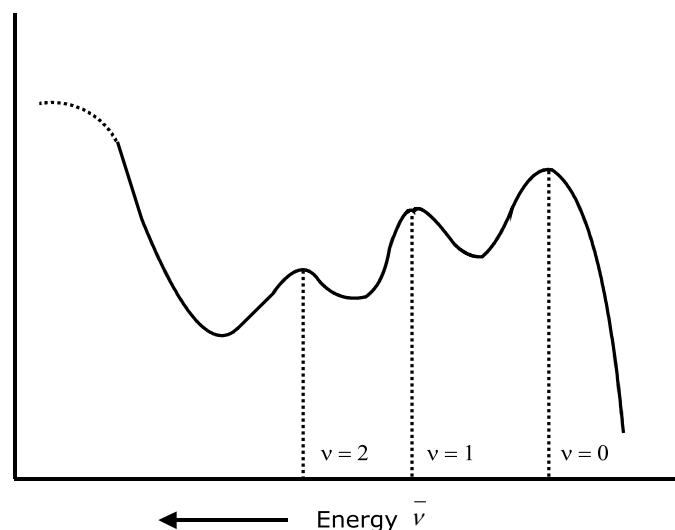


Figure 2.37 Multippeak absorption spectrum

Just as with absorption energy in the ground state, the chance of an excited electron returning to a particular ground state vibrational energy level is also dictated by the degree of overlap of the vibrational and rotational energy levels of the ground and excited state energy levels. If other competing energy loss processes were to be ignored, then the fluorescence emission spectrum is the mirror image of the absorption spectrum, which is known as the Mirror Image Rule and shown in Figure 2.38.

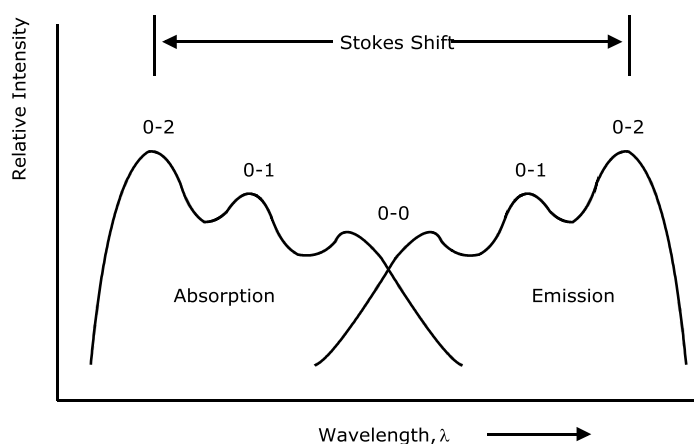


Figure 2.38 Absorption and emission spectra depicting Mirror Image Rule and Stokes Shift

If the absorption and emission spectra are overlaid on to one another, then the difference between the two peaks is proportional to the change in wavelength between

the incident and the emitted light. This phenomenon is known as Stokes Shift and is shown in Figure 2.38 and Figure 2.39.

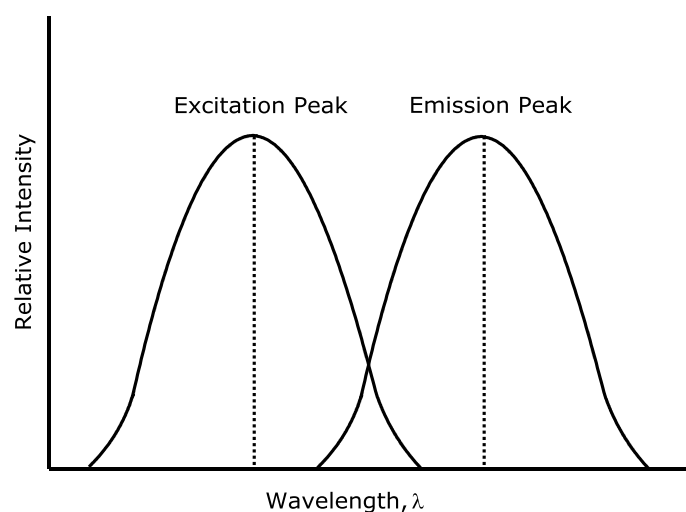


Figure 2.39 Excitation and emission spectrum of a fluorophore

Stokes shift refers to the fact that emission is generally shifted to longer wavelengths than the absorption because emission occurs from lower energy singlet states. The existence of the Stokes shift is critical to making fluorescence such a sensitive technique. Stokes shift allows a low number of emitted photons to be detected against a low background separated from the large number of excitation photons.

2.9.3 Quantum Yield

The quantum yield, Q , which can range from 0 to 1, is the ratio of the number of photons emitted to the number of photons absorbed by the fluorophore. It is, in effect, a measure of the fluorophore's efficiency, and can be determined by the following equation:

$$Q = \frac{\text{photons emitted}}{\text{photons absorbed}} \quad (2.9.2)$$

Fluorescence, F , is expressed as a function of the quantum yield of the fluorophore and the amount of light absorbed by the photon. It is calculated via the formula below:

$$F = I_0 \varepsilon c x Q \quad (2.9.3)$$

where

I_0 = the intensity of the light beam falling on the solution

ε = the molar absorptivity coefficient of the fluorophore [$\text{l mol}^{-1} \text{cm}^{-1}$]

c = the concentration of the fluorophore [mol l^{-1}]

x = the pathlength of the beam through the solution [cm]

The molar absorptivity coefficient, also referred to as the molar extinction coefficient, is wavelength dependent and is different for different materials, but for a given compound at a particular wavelength, the value is constant. It is a measure of how strongly a light absorbing particle, or fluorophore, absorbs light at that selected wavelength. Q relates to the total photon emission throughout the fluorophore's entire fluorescence spectrum. The equation (2.9.3) above shows that fluorescence is proportional to the quantum yield, Q , multiplied by the quantity of light absorbed, $I_0 \varepsilon c x$, which is derived from the Beer-Lambert Law.

The Beer-Lambert Law, also known simply as Beer's Law, states that the absorbance, A , of a sample (or fluorophore) is directly proportional to its concentration – i.e. the relationship is linear. It also relates the reduction in the intensity of light passing through a material to the pathlength of the beam through that material. It can be expressed as follows:

$$A = -\log \frac{I}{I_0} = \varepsilon c x \quad (2.9.4)$$

where

A = the absorbance of the fluorophore

I = the intensity of light after passing through a sample of length x

I_0 = the incident light intensity

ε = the molar absorptivity coefficient [$\text{l mol}^{-1} \text{cm}^{-1}$]

c = the fluorophore concentration [mol l^{-1}]

x = the pathlength of the beam through the solution [cm]

2.9.4 Fluorescence Lifetime

The fluorescence lifetime, τ , of a particle, or more accurately the mean fluorescence lifetime, is the average time during which the particle remains in an excited state, following the excitation by a monochromatic light but prior to returning to the ground state. Whilst in this state, it is possible for the fluorophore to undergo conformational changes and interact with its immediate environment.

Upon excitation of the fluorophore, the fluorescence intensity will instantly jump to its maximum and then decrease exponentially over time. Thus, τ can be determined by observing the rate of decay of the emitted light intensity as a function of time, t , as per the following equation:

$$I(t) = I_0 e^{-\frac{t}{\tau}} \quad (2.9.5)$$

where

$I(t)$ = the fluorescence intensity measured at time t

I_0 = the initial intensity immediately after the excitation pulse, at time $t = 0$

t = time [s]

τ = the fluorescence lifetime [s]

At time $t = \tau$,

$$I(\tau) = I_0 e^{-\frac{\tau}{\tau}} = I_0 e^{-1} \quad (2.9.6)$$

This means that the fluorescence intensity at time τ has decayed to $1/e$ (approximately 37%) of the initial intensity, I_0 . Note that it is assumed that at time $t = 0$, the light pulse is infinitesimally small as to be instantaneous. Given that fluorescence is proportional to the number of excited particles, in order to measure the fluorescence lifetime it is necessary to investigate the speed with which the fluorescence decays after an excitation pulse.

Since the amount of fluorescence is proportional to the excited state population of singlets, to measure the fluorescent lifetime, it is necessary to enquire as to how fast fluorescence decays after a pulse of excitation. The decay of a fluorescent molecule in a uniform solvent is usually monoexponential. In cells, where multiple environments exist, the decay of the fluorescent lifetime of a fluorophore is often multiexponential. A number of other deactivation or energy depleting processes can compete with fluorescence for return of the excited state electrons to the ground state. These include: internal conversion (k_i), phosphorescence (k_p) and quenching (k_q). Other than fluorescence and phosphorescence, the processes for return of the excited state electrons to the ground state represent non-fluorescent mechanisms.

The benefit of using fluorescence is that the light to be detected by the photodetector would not be lost to absorption or scattering. If the signal is small, it can be enhanced by increasing the intensity of the excitation light source, since the emitted light is directly proportional to the intensity of the incident light. Therefore, incorporating fluorescent molecules into the design of the detection device will enable the device to become more sensitive and to be able to detect much lower concentrations of antigen in samples.

2.10 Detection and Signal Recovery

The terms “visual” and “optical” detection need to be clarified for the purpose of this project. In these works, visual detection refers to the identification or observation of a result by using the naked eye. Optical detection refers to the identification or analysis of a result by an electronic component or device, such as a photodetector or a spectrophotometer. Results shown or displayed using an optical detection method usually take a numerical form, which can be plotted on a graph. Results obtained via the visual detection method are more subjective since the human eye cannot accurately place a numerical value to the degree in which something is observed. For example, in chromatography it is possible to see the colouration of a sample by the naked eye – visual detection – and it may even be possible to subjectively judge the intensity of the colouration by describing the colouration as faded or intense. However, an optical detection device would assign a numerical value to the intensity of the colouration detected by the photodetector. If the colouration of the chromatography sample covers a range of intensity from the very faded through to the very intense, then by using the optical detection method, the range of numerical value can be assigned to the varying intensities and then plotted on a graph.

One of the aspects of detection that is attempted in this study is the improvement of signal-to-noise ratio at different illumination conditions by determining a suitable method or methods for differentiating between background levels of detection and actual reading, and identifying relevant data. One method that is to be considered for this purpose is the lock-in amplification method.

2.10.1 Signal Measurements and Noise

While optical fluorescence detection is superior to visual detection, there is the problem of “noise” that needs to be overcome. Inevitably, when increasing the input energy for the magnification of the output signal, some of the incident light will get through to the output signal, causing noise. In order to minimise the noise from the light source in the output, a filter that absorbs light at the wavelength of the input light source needs to be introduced. This helps to reduce some of the unwanted light and

reduce this noise. However, despite filtering out some unwanted light signal, there are other factors that affect the signal recovery and constitute as noise, such as electrical interference from the power system, external light leaking into the instrument and background fluorescence.

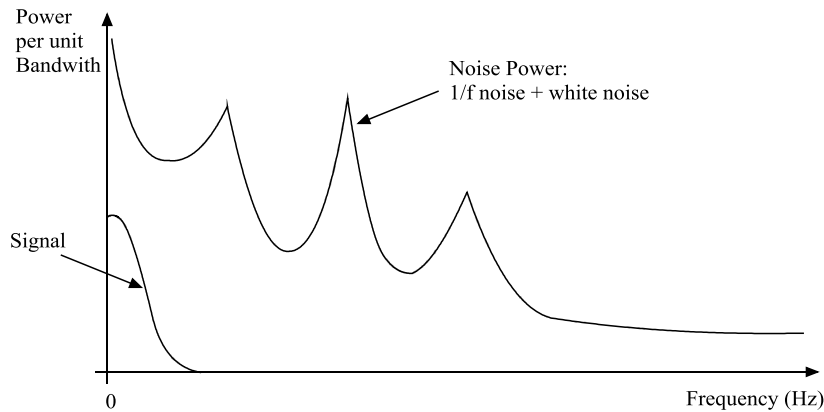


Figure 2.40 Signal buried in noise

For very small amounts of particles, noise may become significantly large in comparison and the signal of interest may become buried within the noise, as shown in Figure 2.40. This is a common problem in signal measurements. A solution needs to be found in order to single out and magnify the signal of interest while discarding the noise. Therefore, a more sophisticated method needs to be used. This can be achieved by introducing a combination of techniques. Before introducing the noise-reduction techniques, however, a few words should be said about the different types of noise.

Shot noise, or Schottky noise, refers to the random emission and velocity of electrons from a cathode. The strength of this noise increases for increasing magnitudes of the average current flowing through the conductor. Johnson noise, also known as thermal noise, is the noise generated by thermal agitation of electrons in a conductor. This may be held to apply to charge carriers in any type of conducting medium. Johnson and shot noise are intrinsic phenomena of all electrical circuits and are referred to collectively as white noise. Another type of noise that is found in many devices such as transistors, light sources and lasers is known as $1/f$ noise. The noise that is seen in

signal measurement amplification outputs is made up of these various types of noise; the total noise is the sum of the white and 1/f noise.

At lower frequencies, the total noise power is greatest: this is where 1/f noise is high. However, at higher frequencies, 1/f noise is insignificant compared to white noise. The total noise is reduced and levels off at these higher frequencies. This factor becomes important when considering the lock-in amplifier.

2.10.2 Phase Sensitive Detection and the Lock-In Amplifier

To reiterate, a solution needs to be found in order to single out and magnify the signal of interest while discarding the noise. This could be achieved using a combination of methods:

Firstly, a low pass filter can be introduced, the effect of which is shown in Figure 2.41, in order to reject noise at higher frequencies. However, this could only result in a small improvement in signal-to-noise ratio because although higher frequency components that do not contain any signal information are rejected, the information relating to the transmission of the sample is near zero hertz: the region where the noise is highest. Therefore, in order to measure high optical density, the signal information would need to be moved away from the high-noise zero or near zero-hertz region. There are two ways in which this could be done.

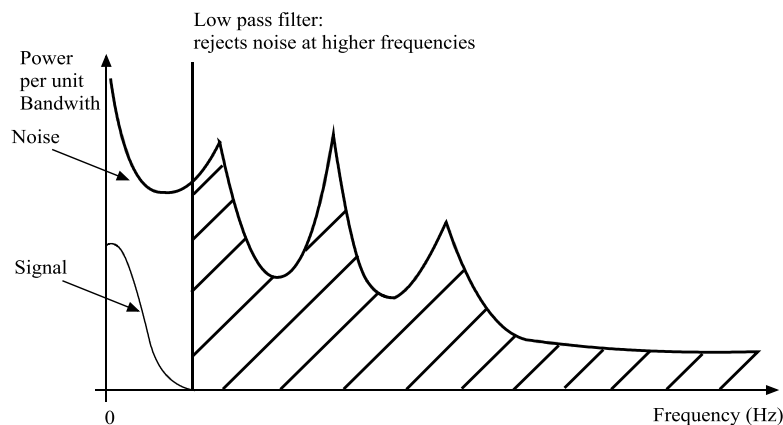


Figure 2.41 Introduction of low pass filter

One is by placing an optical chopper, running at a predetermined reference frequency, between the light source and the detector to periodically interrupt the light. The other option, which achieves a similar effect, is by pulsing the light source itself, again at a predetermined reference frequency. This chopping or pulsing of the incoming light is controlled by the use of a lock-in amplifier.

Lock-in amplifiers measure the amplitude and phase of signals buried in noise by acting as a narrow bandpass filter, which removes a large proportion of unwanted noise while allowing through the signal of interest. In other words, they measure the magnitude of a signal in a very narrow frequency band while rejecting all components of the signal that are outside that very narrow frequency band. Whether analogue or digital, all lock-in amplifiers are based on the concept of phase sensitive detection to single out the component of the signal at a specific reference phase and frequency. Noise signals at frequencies other than the reference frequency are rejected.

The reference frequency at which the optical chopper or pulse generator operates is pre-determined. In order to allow the lock-in amplifier to function most effectively, this reference frequency needs to be where the interference from noise is already at its minimum. At higher frequencies the spectrum flattens out, as shown in Figure 2.40 and Figure 2.41, resulting in fairly constant shot noise and negligible $1/f$ noise. Therefore, it is at the higher frequencies, around the region where the spectrum has flattened out, that the chopper or pulse generator would operate most effectively. In order to achieve this, the signal of interest is modulated – i.e. converted to AC – to the same frequency as the reference frequency and therefore shifted away from the zero or near-zero Hertz region (where the background noise is high) to be amplified at the higher frequency region (where the background noise is low).

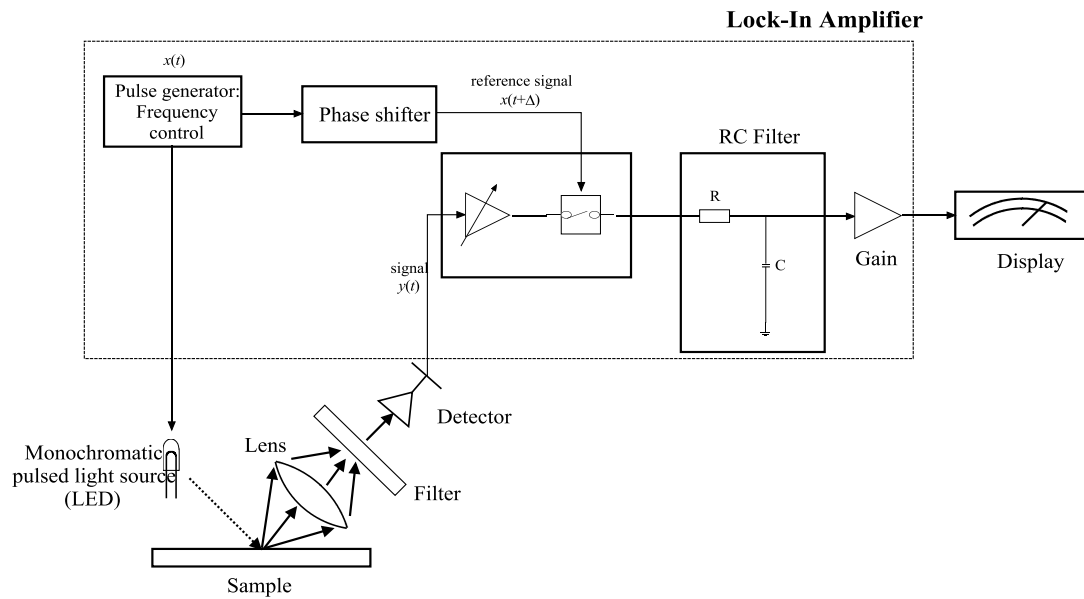


Figure 2.42 Schematic diagram of an experimental set-up using a lock-in amplifier

Figure 2.42 shows a schematic diagram used in a typical set-up of a microbial detection system which utilises a lock-in amplifier. In this arrangement the pulse generator controls the frequency, ω , at which the incident light $x(t)$ is pulsed, or if an optical chopper is used the frequency at which the chopper operates. The weak light output signal $y(t)$ emitted from the sample, running at the same reference frequency ω is stimulated by the periodic signal $x(t)$ from the chopper or pulsed light. Because the experimental signal $y(t)$ and the chopper controlled signal $x(t)$ occur at the same frequency ω , they are “locked” at the same pulsing frequency before being input into the phase sensitive detector (PSD).

Relative travelling times of the experimental signal and reference voltages around the system may differ and could therefore cause $y(t)$ and $x(t)$ to arrive at the PSD out of phase. As a result, it is necessary to adjust one of the signals in order to restore phase alignment. This can be achieved by passing the reference signal $x(t)$ through a phase-shifter to delay or advance it by an amount Δ so that the resulting signal $x(t+\Delta)$ corresponds to $y(t)$, thus restoring phase alignment of the signals prior to their arrival at the PSD. Once inside the PSD, the synchronised experimental signal $y(t)$ and phase-adjusted reference signal $x(t+\Delta)$ are multiplied together. This, in effect,

cancels out the majority of the noise originally present on the experimental signal $y(t)$. This is because the multiplied signal, combining the reference and experimental signals, become significantly large as to render the noise negligible in comparison. The output signal from the PSD is then sent through a low-pass RC filter with a time constant that is longer than one period of the reference frequency, which averages the output of the PSD. With everything else filtered out the remaining frequency is then amplified with an operational DC amplifier. The original weak signal $y(t)$ is then displayed as a magnified output signal z , with a significantly reduced noise.

The main advantage of the system shown in Figure 2.42 is that all the components are available in very small sizes; therefore, the entire assembly can be constructed into a compact hand-held device. To all intents and purposes, the entirety of the electronics can be built into an effective area of around $10 \times 10 \text{ cm}^2$. In addition, the electrical power consumption of the proposed electro-optical sensing system would be considerably low, which enables the power of this portable device to be supplied by a battery.

Chapter 3 Experimental Methods

3.1 Preliminary Studies

3.1.1 Preliminary Experiment

A preliminary study was carried out in order to obtain the maximum peak wavelength of reflected light from colloidal gold and colloidal gold-antibody conjugate samples supplied by Alchemy Laboratories, Dundee. The samples studied were 40 nm colloidal gold and 40 nm colloidal gold-antibody conjugate. The light source used was a 60W light bulb from a desk lamp; the samples were, in turn, illuminated. Reflectance measurements were performed on the colloidal gold suspension and the colloidal gold-antibody conjugate suspension in two separate cylindrical vials. These measurements were obtained using a Bentham spectrophotometer.

3.1.2 Design of cubic sample holder to house cylindrical vial

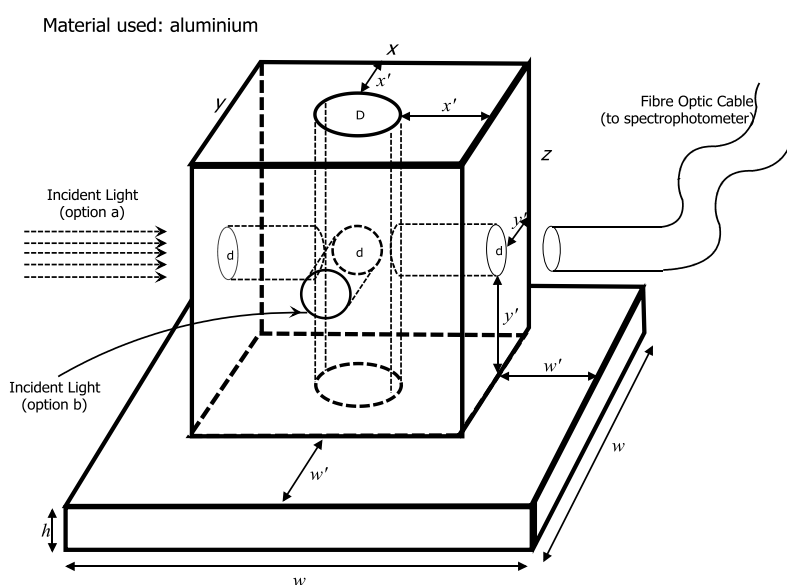


Figure 3.1 Aluminium sample holder to house cylindrical vial containing sample

As part of the light experiments set-up and in order to refine the method used in the preliminary experiment described in Section 3.1.1, an aluminium sample holder was designed and manufactured, a schematic diagram of which is shown in Figure 3.1 and the dimensions used shown in Table 3.1. This sample holder was used in the experiments described in sections 3.1.3 and 3.1.4.

Table 3.1 Dimensions for aluminium sample holder used to house cylindrical vial

Dimension	Value (cm)
x	2.7
y	2.7
z	2.7
x'	0.7
y'	0.9
w	6.7
w'	2.0
h	0.5
D	1.3
d	0.9

3.1.3 White Light Experiment on Colloidal Gold and Colloidal Gold Conjugate



Figure 3.2 Fibre-optic white light (cold) source

The reflectance spectra of different dilutions of colloidal gold and conjugate solutions were obtained. The illumination source was white light delivered through a fibre-optic cable, as shown in Figure 3.2. The dilutions were made using a series dilution method, with each dilution being a 1 in 10 dilution of its forerunner.

3.1.4 Fluorescence Experiments

The fluorescent dye Lumogen Red F was chosen as a potential candidate for use in microsphere preparations. Two experiments were set up in order to determine the emission wavelength and detection limit for Lumogen Red.

In the first fluorescence experiment, a solution of Lumogen Red in methyl methacrylate was prepared in a sample cuvette. A green LED light source, driven by a current of 51 mA, was used to illuminate the sample and the emitted light was transmitted by a fibre optic cable to a monochromator and detector. The intensity versus wavelength curves were then displayed on a computer screen.

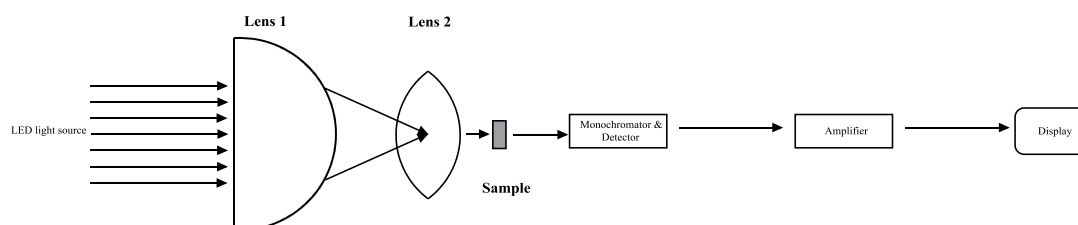


Figure 3.3 Set up of first fluorescence experiment. Illumination source and detector are aligned in a straight line.

In the first set-up, the emitted light was detected at 180° to the incident light, as shown in Figure 3.3. No filter was applied to the light source.

In an attempt to prevent any green light from the LED passing through and being detected by the photodetector, the experiment was repeated with the application of a filter at the point directly after the sample (before the detector). The excess green light should then be absorbed by the filter and the remaining light can then pass onto the sample to illuminate the sample.

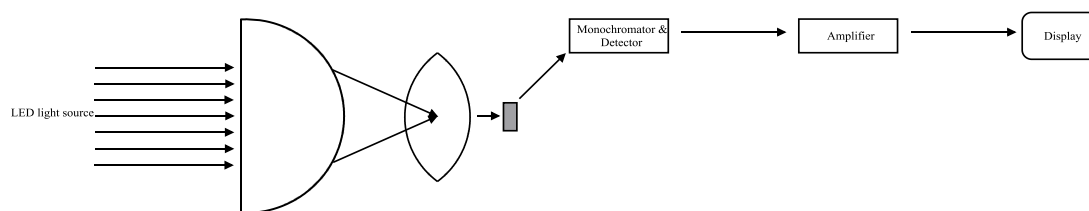


Figure 3.4 Set up of second fluorescence experiment. Detection unit is at a right angle to the illumination source.

A second fluorescence experiment was conducted on dilutions of the Lumogen Red solutions by modifying the set-up from the first fluorescence experiment. In this set-up, the emitted light was detected at right angles to the incident light in the attempt to eliminate the detection of the light source that travels through the sample (Figure 3.4). This experiment was carried out without the use of any filter.

3.2 PMMA Synthesis

3.2.1 Preparation of Microspheres

PMMA microspheres and PMMA microspheres containing internally labelled fluorescent dyes were produced by emulsion polymerisation. The method used to produce PMMA is based on the method described by Müller *et al* (2000). The monomer methyl methacrylate is a colourless, volatile, flammable liquid and is carcinogenic, and must be handled with extreme care; its vapour can cause irritation to the eyes, nose and throat. All procedures involving methyl methacrylate, including polymerisation, were carried out in a fume cupboard.

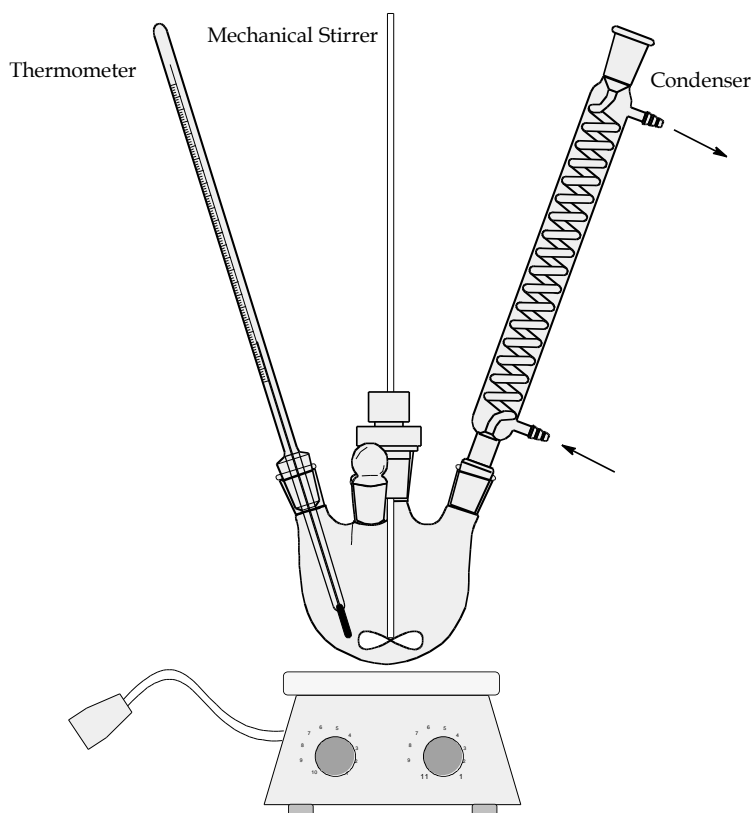


Figure 3.5 Set-up of equipment for PMMA synthesis

A series of PMMA suspensions was produced under varying reaction conditions. The procedures were executed as described below, using sample values from reaction 23; conditions varied according to the values shown in Table 3.2.

In a 1000 ml reaction vessel, 280 ml distilled water was stirred for 45 min under a moderate flow of nitrogen. In the case where fluorescent PMMA microspheres were prepared, 0.5 mg of Rhodamine B was added to the distilled water at the initial stage; in the case where unlabelled PMMA microspheres were prepared, no dye was added. Figure 3.5 shows the set-up for the polymerisation process. After the addition of 30 ml methyl methacrylate and 30 ml toluene, the flow of nitrogen was stopped and the mixture was heated to and kept at 90°C for 60 min.

Meanwhile, 1000 mg potassium peroxodisulphate (also called potassium persulphate) was added to 10 ml distilled water. To ensure the complete dissolving of the powder and to prevent oxygen from entering the system, the solution was vigorously shaken and gently heated in an ultrasonic bath under a moderate flow of nitrogen for 15 min.

The solution was then added to the reaction vessel as an initiator. The polymerisation was carried out in a nitrogen atmosphere at a stirring speed of 600 rpm for 45 min. The polymerisation was terminated by stopping the flow of nitrogen and allowing the toluene to evaporate whilst the temperature was maintained at 90°C. The start of a rise in temperature indicated the complete evaporation of toluene. At this point, the heat was removed and the contents of the vessel were allowed to cool to room temperature.

The largest particles were then separated by means of conventional normal flow vacuum filtration, using a Buchner filtration unit; the filtration membrane used was Whatman GF/A filter paper. The filtrate was then transferred to falcon centrifuge tubes for further separation by centrifugation, using an Eppendorf ultracentrifuge at 9500 rpm for 10 min. The sediment was resuspended in distilled water by vortex mixing and the centrifugation was repeated twice. The supernatants from the ultracentrifugation were discarded. The microspheres were resuspended by vortex mixing and stored in distilled water in brown glass bottles away from light to prevent photobleaching. Probes of the sample were taken for image analysis by scanning electron microscopy (SEM) and atomic force microscopy (AFM).

Table 3.2 PMMA Synthesis Reaction Conditions

Reaction	Amt H ₂ O in Reaction	Amt MMA, V _M	Amt Toluene, V _T	Reaction Temp, R _T	Stirring Speed, v _s	Reaction Time, R _t	Notes
	(ml)	(ml)	(ml)	(°C)	(rpm)	(min)	
1	280	30	30	88	1200	35	No dye
2	280	30	30	88	600	35	No dye
3	280	30	30	88	600	45	No dye
4	280	30	30	88	600	20	No dye
5	280	30	30	88	300	45	No dye
6	280	30	30	88	300	35	No dye
7	280	30	30	88	300	20	No dye
8	280	15	30	88	1200	35	No dye
9	280	15	30	88	600	45	No dye
10	280	15	30	88	600	35	No dye
11	280	15	30	88	600	20	No dye
12	280	15	30	88	300	45	No dye
13	280	15	30	88	300	35	No dye
14	280	15	30	88	300	20	No dye
15	280	30	30	88	600	45	0.5 mg Nile Red
16	280	30	30	88	600	45	1.9 mg Rhodamine B
17	280	30	30	88	600	45	0.9 mg Rosso Sitraxol 5B Fluor
18	280	30	30	88	600	45	1.2 mg Alexa Fluor 430

Reaction	Amt H ₂ O in Reaction	Amt MMA, V _M	Amt Toluene, V _T	Reaction Temp, R _T	Stirring Speed, v _S	Reaction Time, R _t	Notes
	(ml)	(ml)	(ml)	(°C)	(rpm)	(min)	
19	280	30	30	90	600	45	2.7 mg Rhodamine B
20	280	30	30	90	600	45	1.5 mg Rhodamine B
21	280	30	30	90	600	45	1.7 mg Rhodamine B temp started to rise before end of reaction time
22	280	30	30	90	600	45	1 mg Rhodamine B
23	280	30	30	90	600	45	0.5 mg Rhodamine B
24	280	30	30	90	600	45	No dye
25	280	30	30	90	600	45	No dye
26	280	30	30	90	600	45	0.5 mg Alexa Fluor 430

3.3 Copolymerisation of P(MMA-HEMA)

The method used to produce P(MMA-HEMA) is a combination of a modified version of the method used to produce PMMA and the method described by Yavuz *et al* (2002). The preparation of P(MMA-HEMA) was carried out in a fume cupboard.

In a three-neck 250 ml reaction vessel, 4.0 g of polyvinylpyrrolidone (PVP)(molecular mass 30,000) was added to 50.0 ml distilled water and 50.0 ml ethanol and stirred under in a moderate-flow nitrogen atmosphere for 45 min. Figure 3.6 shows the set-up for the polymerisation process. Meanwhile, a water bath was preheated to 65°C.

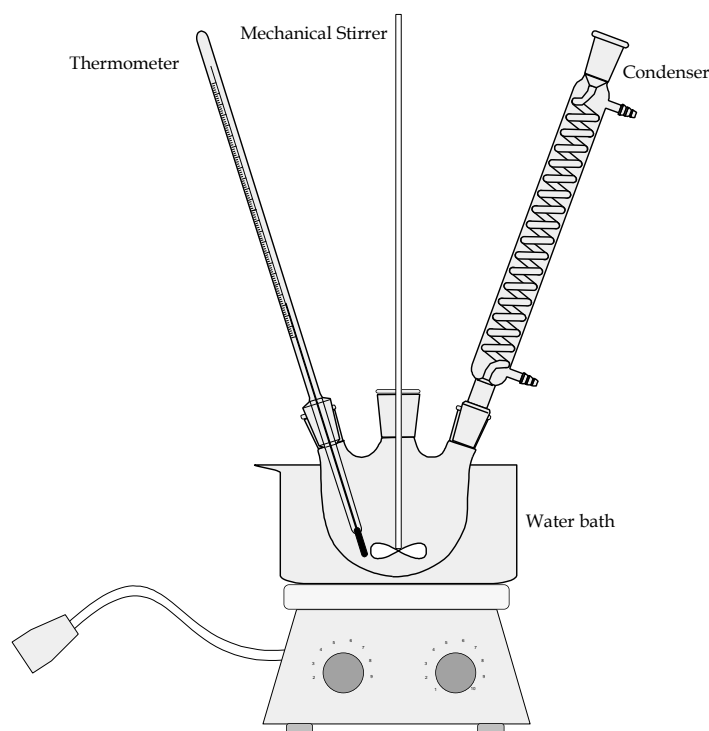


Figure 3.6 Set-up of equipment for P(MMA-HEMA) synthesis

After the 45 min was up, 4.0 ml of MMA and 2.0 ml of HEMA were added to the reaction vessel and the flow of N₂ stopped. The reaction vessel was immersed in the preheated water bath and the temperature maintained at 65°C for 1 h, after which 80 mg of AIBN was added to the reaction vessel and the flow of N₂ resumed.

The polymerisation was carried out in a nitrogen atmosphere at a stirring speed of 400 rpm for 24 h. During the reaction, the water bath surrounding the reaction vessel was covered with aluminium foil in order to minimise evaporation; the water bath temperature was maintained at 65°C.

After 24 h, the polymerisation was terminated by stopping the flow of nitrogen, and allowing the ethanol to evaporate, whilst the temperature was maintained at the polymerisation temperature. When all the ethanol had evaporated, the heat was removed and the particles were separated by means of conventional normal flow vacuum filtration method, using a Buchner filtration unit; the filtration membrane used was Whatman GF/A filter paper.

The filtrate was then transferred to falcon centrifuge tubes for further separation by centrifugation, using an Eppendorf ultracentrifuge at 9500 rpm for 10 min. The sediment was resuspended in distilled water by vortex mixing and the centrifugation was repeated twice. The supernatants from the ultracentrifugation processes were discarded. The microspheres were resuspended by vortex mixing and stored in distilled water in brown glass bottles in the dark.

Probes of the sample were then taken for size determination and imaging by scanning electron microscopy (SEM).

3.4 Preparation of Monoclonal Antibody

Anti-Phycoerythrin monoclonal antibody in ascites fluid was prepared and provided by Dr Keith Guy: School of Life Sciences, Napier University.

3.4.1 Purification of IgG

Anti-Phycoerythrin monoclonal antibody was purified using affinity chromatography, using an MAbTrapTM Kit (Amersham Biosciences). During the purification process, only high quality sterile water was used.

In preparation for the chromatography, the MAbTrapTM Kit was removed from the refrigerator and allowed to warm to room temperature. Meanwhile, the ascites fluid containing the anti-phycoerythrin monoclonal antibody to be purified was checked for cloudiness: a cloudy sample indicates aggregation of proteins and lipids, and cannot be passed through the chromatography column. To eliminate the cloudiness, the sample was centrifuged at 2500 rpm for 5 minutes and then passed through a 0.22 μm sterile filter (0.45 μm for very cloudy sample).

Once the kit had warmed to room temperature, the buffers were prepared by making 10 times dilutions of the binding buffer (2.5 ml binding buffer + 22.5 ml high quality sterile water to make a total volume of 25 ml) and the elution buffer (0.5 ml elution buffer + 4.5 ml high quality sterile water to make a total volume of 5.0 ml). The clear ascites fluid sample was then diluted at a 1:1 ratio with the prepared binding buffer. Additional buffer dilutions may be performed in the same way, if needed.

The application syringe was filled with the sterile water and connected to the chromatography column through a luer adaptor (provided with the kit). Care was taken to avoid introducing air into the column by making the connection “drop-to-drop”. The affinity chromatography column was set up as shown in Figure 3.7.

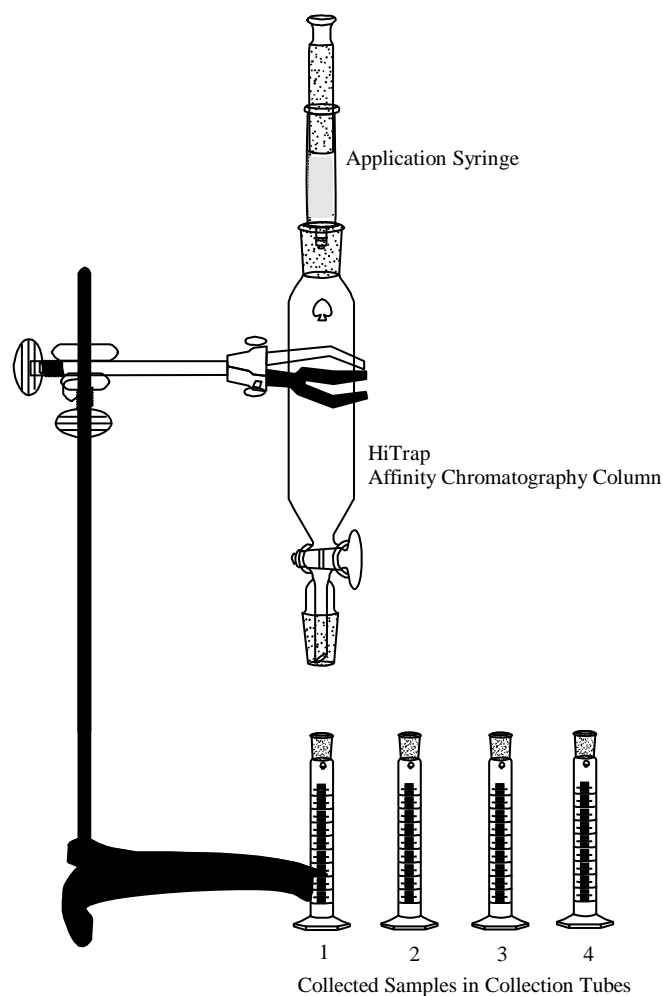


Figure 3.7 Purification of MAb by affinity chromatography

The ethanol preservative in the column was washed out with 5 ml distilled water at about 1 drop per second. Care was taken not to force the water through lest the gel inside the column become compressed. Once the column was washed out, it was equilibrated in excess of 3 ml of binding buffer. The sample, previously diluted 1:1 with binding buffer, was then applied using the syringe and then washed with 5-10 ml of binding buffer (or until no material appeared in the effluent): this was checked using a spectrophotometer. Again, great care was taken not to force the liquid through the column. 1 ml samples were collected in labelled collection tubes and then the absorbance at 280 nm was taken using a Beckman spectrophotometer to ensure that all unwanted material had been washed out of the column. The syringe was then rinsed out with distilled water and about 100 μ l of neutralising buffer per ml of sample were added to a set of labelled, clean collection tubes to allow for the immediate renaturing of the purified IgG to preserve the activity of the labile IgGs.

The elution buffer was applied to the column and 1 ml samples were collected in each of the tubes containing the neutralising buffers. Absorbance at 280 nm of the eluted samples was obtained and the samples containing the high concentrations of purified proteins were reserved; the remaining samples were discarded. The affinity column was then reconditioned with 5 ml of binding buffer and the MAb kit stored in a refrigerator for future use.

Desalting of the purified antibody is necessary for the removal of glycine HCl salts. A desalting column was used for this purpose. First, the desalting column was calibrated by adding 1% PBS NaN_3 to the column and then running the disc at the top of the column dry. 2 ml nuclear fast red dye was added to the column as indicator; 1 ml fractions of the sample were collected. When the disc was again dry, 1 ml BSA was added to wash off the dye. When the column ran dry, it was filled up to the top with BSA and then kept topped up. 1 ml samples were collected and then run through the spectrophotometer: the absorbance at 280 nm was obtained and the samples that contained high concentrations of dye were noted.

The desalting process was then carried out in the same way as the calibration, substituting the dye with the purified IgG. Absorbance at 280 nm was recorded and the tubes containing the purified antibody were retained and stored in PBS NaN_3 and then frozen for later use.

3.5 Conjugation of Antibody to PMMA Microspheres

Conjugation of antibodies to PMMA microspheres was carried out by passive adsorption. Maximum adsorption occurs at or near the isoelectric point (pI) of an antibody, which is at around pH 8.0 for IgG (Bangs Labs 1999a).

3.5.1 Preparation of Microspheres in Adsorption Buffer: Phosphate Buffer pH 8.0

5.3 ml of 0.1 M sodium phosphate monobasic; 13.8 g l⁻¹ (monohydrate, MW 138.0) was mixed with 94.7 ml of 0.1 M sodium phosphate dibasic; 26.8 g l⁻¹ (heptahydrate, MW 268.0) and the final volume adjusted to 200 ml with deionised water. The final pH was then adjusted to pH 8.0 using a sensitive pH meter. The microsphere suspension was diluted to 1% (w/v) solids (10 mg ml⁻¹) in the phosphate buffer.

3.5.2 Passive Adsorption

The amount of protein required to achieve surface saturation was calculated using the following equation:

$$S = \frac{6}{\rho D} C \quad (3.5.1)$$

where

S = amount of antibody required to achieve surface saturation (mg antibody/g of microspheres)

C = capacity of microsphere surface for given protein, which varies depending on the size and molecular weight of the protein to be coupled (mg protein / m² of polymer surface); for bovine IgG, C = 2.5 mg m⁻²

6/ρD = surface area/mass (m²/g) for microspheres of a given diameter

ρ = density of microspheres; ρ_{PMMA} = 1.19 g cm⁻³

D = diameter of microspheres [μm]

The microspheres were added to the antibodies and mixed gently for 1-2 hours. The suspension was then incubated overnight, with constant gentle mixing, at 4°C. The suspension was then washed by centrifugation 3 times. Probes of the sample were taken for image analysis using a cold field emission SEM.

3.5.3 Determination of Bound/Unbound Proteins

The supernatant of the centrifuged suspension was retained in order to determine the amount of unbound proteins, from which the amount of adsorbed protein can be indirectly quantified. Absorbance at 280 nm (A_{280}) of the supernatant was taken.

3.6 Microsphere Analyses using Imaging Technology

Several imaging techniques were used to analyse the microspheres and conjugates produced using methods described in sections 3.2, 3.3 and 3.5. However, not all samples were able to be analysed by all of the imaging techniques described in this section due to equipment access limitations.

3.6.1 Scanning Electron Microscopy

Initial analyses of the synthesised PMMA microspheres were carried out using a Cambridge Instruments StereoScan Mk II SEM.

Later analyses of microspheres, including those described in sections 3.3 and 3.5, were carried out on an upgraded and more sophisticated cold field emission SEM.

3.6.2 Atomic Force Microscopy

The atomic force microscope (AFM) used was a Picoscan SPM, courtesy of Dr Vasileios Koutsos of Edinburgh University.

Sample preparation

The vessel containing the required microsphere suspension sample was inverted several times to ensure that the microspheres were evenly dispersed. Using a dropping pipette, a small volume of sample was extracted and a drop was transferred onto a clean, dry microscope slide. The slide containing the microsphere sample was then allowed to dry in a dust-free environment.

Once dried, the sample was viewed under an AFM, using tapping mode, for image analyses.

3.6.3 Confocal Microscopy

Some attempts were made to introduce a third imaging option by trials on a Carl Zeiss AG, LSM 510 META confocal microscope but was not a major consideration.

3.7 Diffusion of Microspheres

After the production of a range of PMMA beads, one set that was incorporated with Rhodamine B dye was put to the test on nitrocellulose strips supplied by Alchemy Labs. The test was to show whether the beads would travel along the strip as expected. The PMMA beads were suspended in water and a small drop of the sample was placed on the conjugate release pad at one end of the nitrocellulose strip and timed as it diffused along the strip.

3.8 Detection Experiments

Dilutions of a stock solution of PMMA suspended in distilled water were prepared and then subjected to excitation and fluorescence detection in order to determine the detection limit of fluorescent dye-containing PMMA microspheres.

3.8.1 Preparation of 1% w/v PMMA Solution

A 100 ml stock solution of 1% w/v PMMA suspensions (0.01 g ml^{-1}) was prepared by the following method.

In order to prepare a solution of known concentration from a solution of unknown concentration – the PMMA sample produced from synthesis using the method described in Section 3.2 – the concentration of the solution must first be determined.

The solution of unknown concentration was inverted a few times to ensure mixing and the even distribution of microspheres throughout the solution. An empty and dry 10 ml beaker was weighed and noted. A small volume of around 1-5 ml of the PMMA solution – an exact volume is not necessary since it is the weight that is to be measured – was then transferred to the beaker. The beaker containing the small volume of solution was then weighed and then placed in an incubator over night to dry.

The beaker and dry contents were then removed from the incubator and placed in a desiccator (to prevent moisture) to cool before being weighed again. The concentration of the PMMA sample of unknown concentration was then calculated; a sample of the calculations used to determine the concentration of the PMMA solution is shown in Appendix I-A. Once the concentration of the synthesised PMMA sample was determined, the solution of 1% w/v PMMA suspensions was prepared, using the calculations shown in Appendix I-B.

3.8.2 Preparation of Dilutions of PMMA from a Common Stock

Dilutions of 10^{-1} down to 10^{-6} of the stock solution, with each dilution using the common stock solution, were prepared by the following method.

The stock solution was shaken to ensure thorough mixing of the microsphere particles and even distribution before each dilution. For the first sample, in which no dilution was made, the stock solution was simply transferred into a 10 ml volumetric flask. For each subsequent sample, in which the required dilution was made, a specific volume from the stock solution was transferred, in turn, to a volumetric flask of suitable size and then topped up to the mark with distilled water, the requirements of which are shown in Table 3.3.

Table 3.3 Volume of stock solution required to make up each dilution

Sample Number	Stock Volume (ml)	Total Sample Volume (size of vessel) (ml)	Dilution Level
0	10	10	none
1	1	10	10^{-1}
2	0.1	10	10^{-2}
3	0.01	10	10^{-3}
4	0.01	100	10^{-4}
5	0.01	1,000	10^{-5}
6	0.002	2,000	10^{-6}

3.8.3 Design and set-up of Detection Experiments

Material used: aluminium

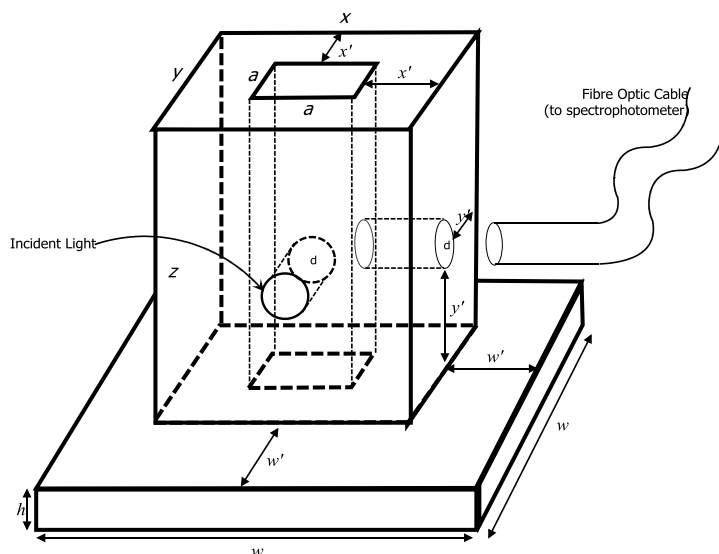


Figure 3.8 Aluminium sample holder to house a 1 cm pathlength cuvette

Similar to the cylindrical vial holder described in Section 3.1.2 and shown in Figure 3.1, a second aluminium sample holder was designed and manufactured for the purpose of housing a 1 cm pathlength cuvette. Its design and dimensions are shown in Figure 3.8 and Table 3.4 respectively.

Table 3.4 Dimensions used for aluminium sample holder used to house a 1 cm pathlength cuvette

Dimension	Value (cm)
x	2.7
y	2.7
z	3.5
x'	0.7
y'	0.9
w	6.7
w'	2.0
h	0.5
a	1.3
d	0.9

3.8.4 Detection Limit

Each of the dilutions, in turn, was inverted several times to ensure mixing and even distribution of the PMMA microspheres, and then transferred to a UV-grade precision macro silica cuvette, which, prior to the sample being transferred, was rinsed several times with distilled water and inverted to prevent cross-sample contamination.

The cuvette was then placed in a sample holder. The detection limit of the dilutions of fluorescent-dye containing PMMA microspheres was then tested by applying a blue LED light to each of the samples and the emitted fluorescent light detected by a spectrophotometer at right angles to the incident light, using the set-up shown in Figure 3.4. Each sample was subjected to varying intensities of light. In addition to the diluted samples, as a control, a “blank” containing only distilled water was also subjected to the light source at the varying intensities.

Chapter 4 Results

4.1 Preliminary Studies

4.1.1 Preliminary Experiment

Figure 4.1 shows the reflectance spectra for each of the samples, colloidal gold and colloidal gold-antibody conjugate, used in the preliminary experiment.

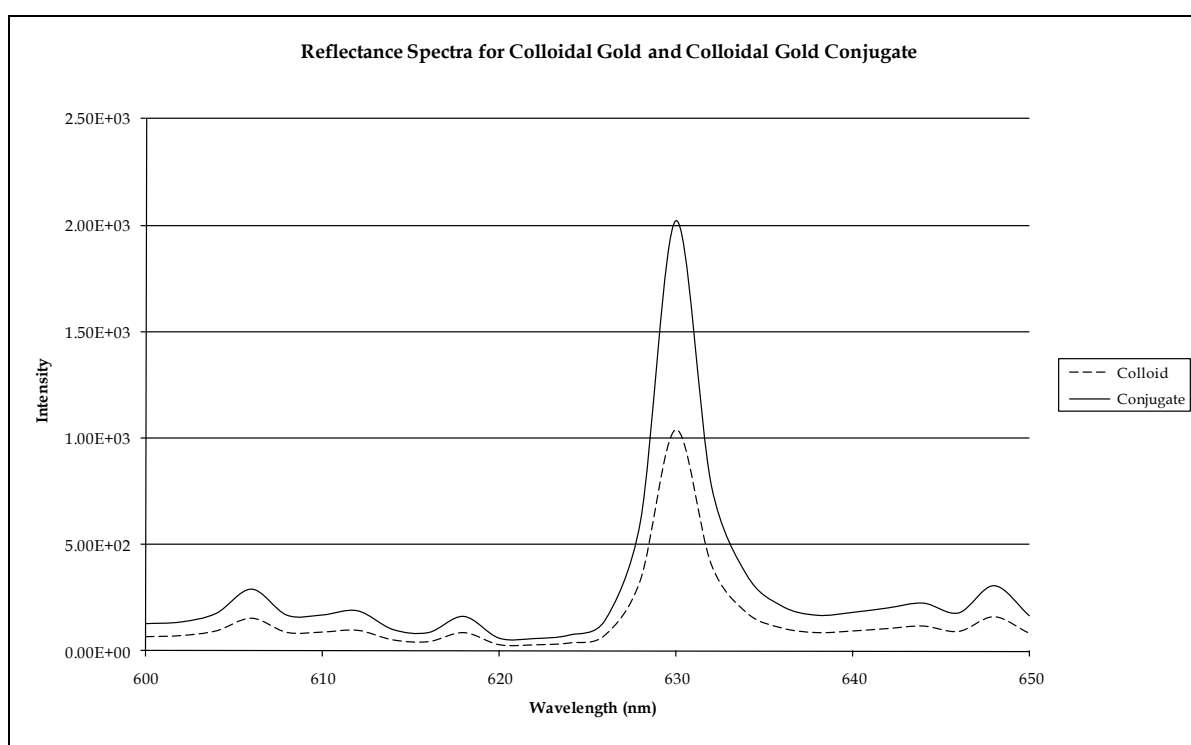


Figure 4.1 Result of preliminary experiment. Reflectance spectra of colloidal gold and colloidal gold-antibody conjugate using a 60 W desk lamp as a light source.

Both samples show reflectance peaks at 630 nm. However, the intensity of the reflectance spectrum for the conjugate sample is greater than that of the colloidal gold sample. This is discussed in Section 5.1.

4.1.2 White Light Experiment on Colloidal Gold and Colloidal Gold Conjugate

Figure 4.2 shows a graph of the reflectance spectra for the different dilutions of the colloidal gold and colloidal gold-conjugate samples. It shows that at higher colloidal gold concentrations, the overall measured light intensity is decreased and a red shift in the spectrum is introduced. Possible reasons for this are discussed in Section 5.1.

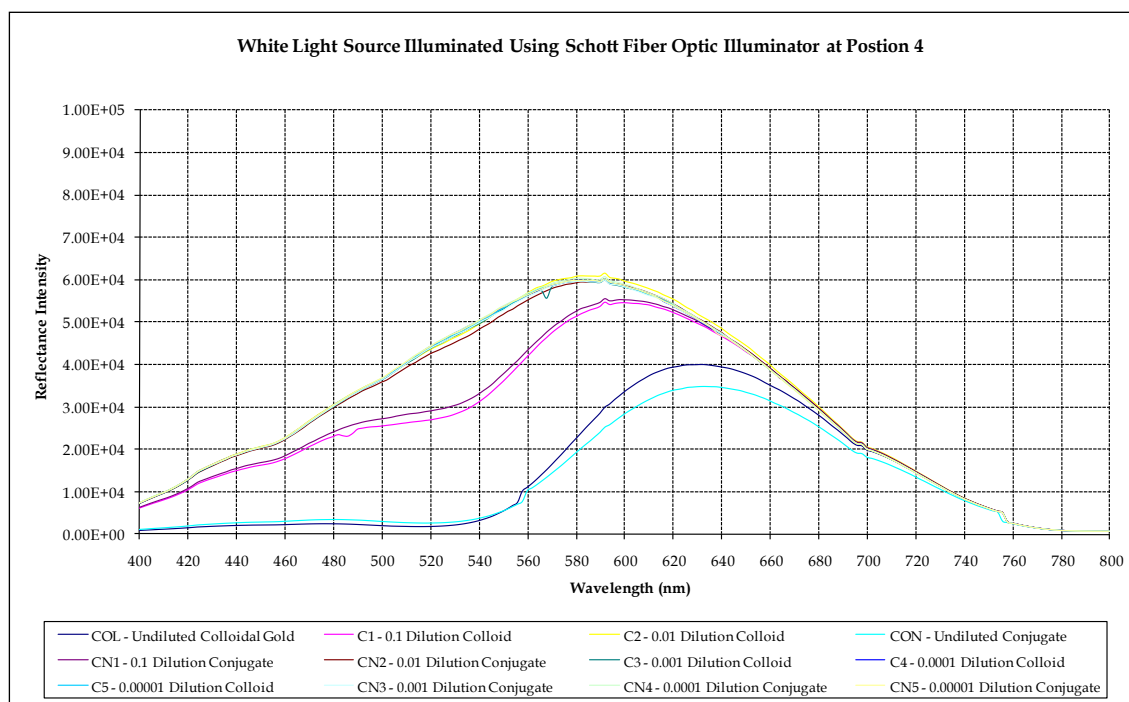


Figure 4.2 Result of white light experiment on dilutions of colloidal gold and colloidal gold-antibody conjugate

4.1.3 Fluorescence Experiment

Figure 4.3 and Figure 4.4 show the emission spectra for Lumogen Red in the first fluorescence experiment, where the emitted light was detected at 180° to the incident light, without and with the application of a filter, respectively. The graph in Figure 4.3 shows that the emission wavelength is about 605 nm.

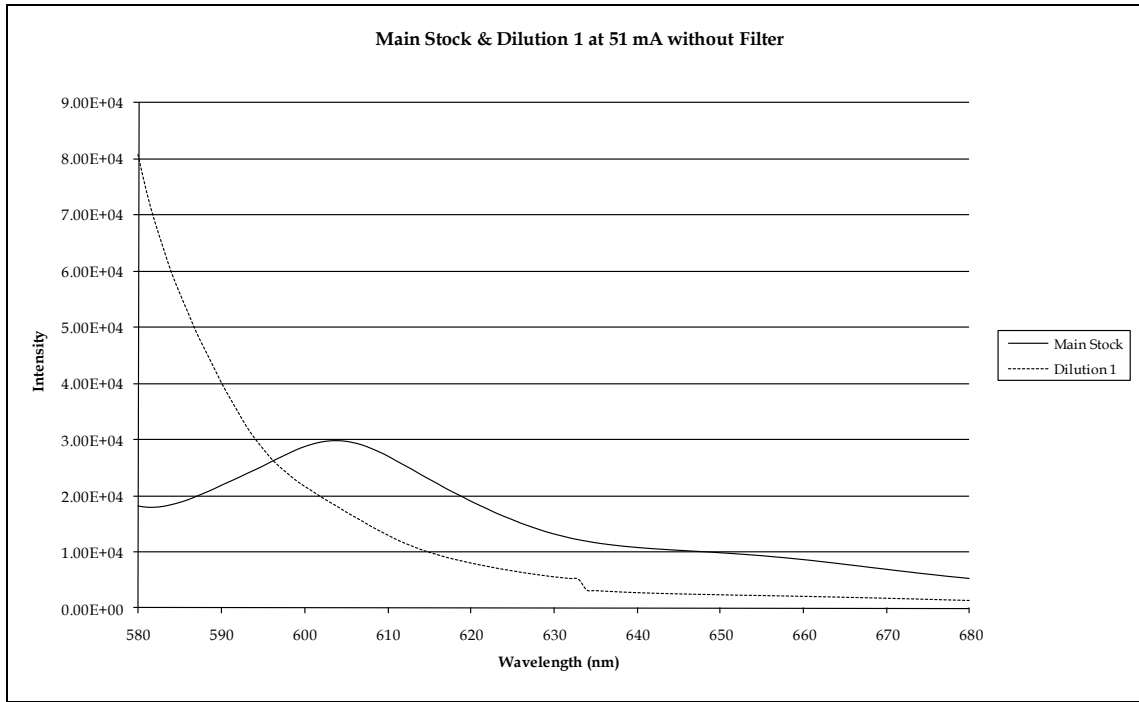


Figure 4.3 Result of the first fluorescence experiment without the use of a filter

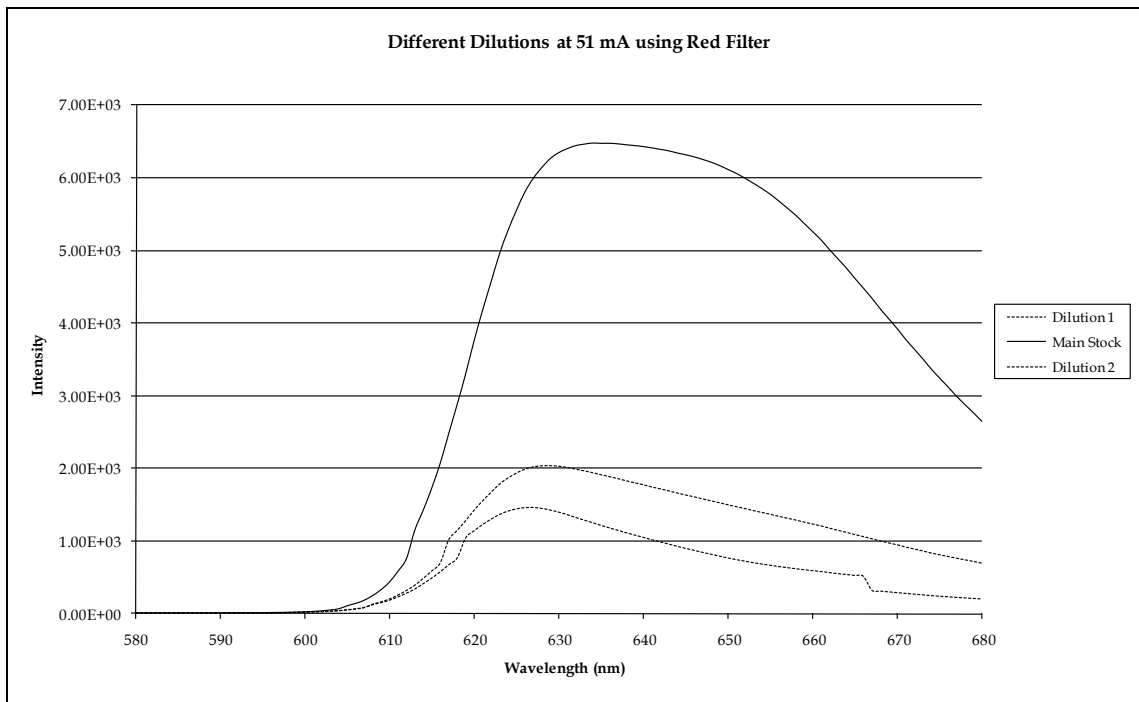


Figure 4.4 Result of the first fluorescence experiment, using a red filter

It can be seen from the graph in Figure 4.4 that after having applied the red filter, the green part of the spectra had been cancelled out, showing the maximum emission peak to be at 630 nm, corresponding to the reflectance spectrum of colloidal gold.

Figure 4.5 shows the results for the second fluorescence experiment, in which the emitted light was detected at right angles to the incident light. It shows the emission spectra for Lumogen Red and its dilutions at various intensities of illumination.

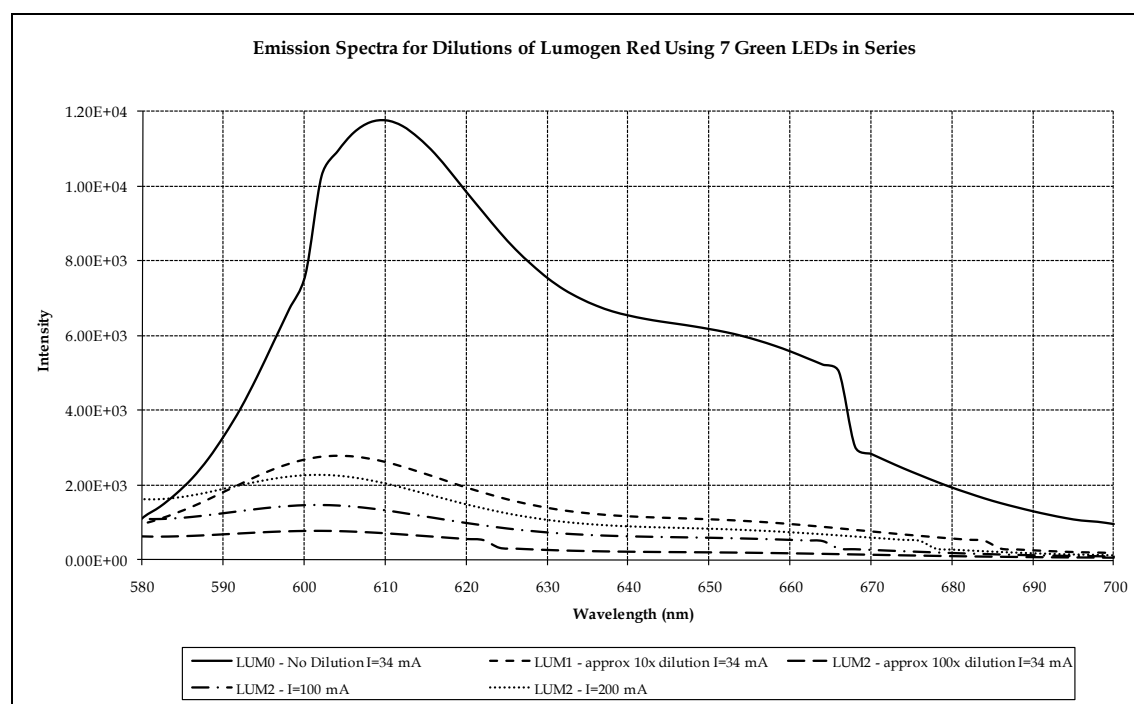


Figure 4.5 Result of second fluorescence experiment. Spectra of dilutions of Lumogen Red illuminated by varying intensities of green LED source.

The graph shows that for the undiluted solution of Lumogen Red, the emission wavelength is about 610 nm. After diluting the samples, the peak appears to have shifted a few nanometers towards the blue. The most diluted solution was a concentration of the order of 10^{-7} g l^{-1} . At this concentration, with a source illumination current of 34 mA, the light output detected was of the order of 10^3 .

4.2 PMMA Synthesis

4.2.1 AFM Imaging of PMMA Microspheres

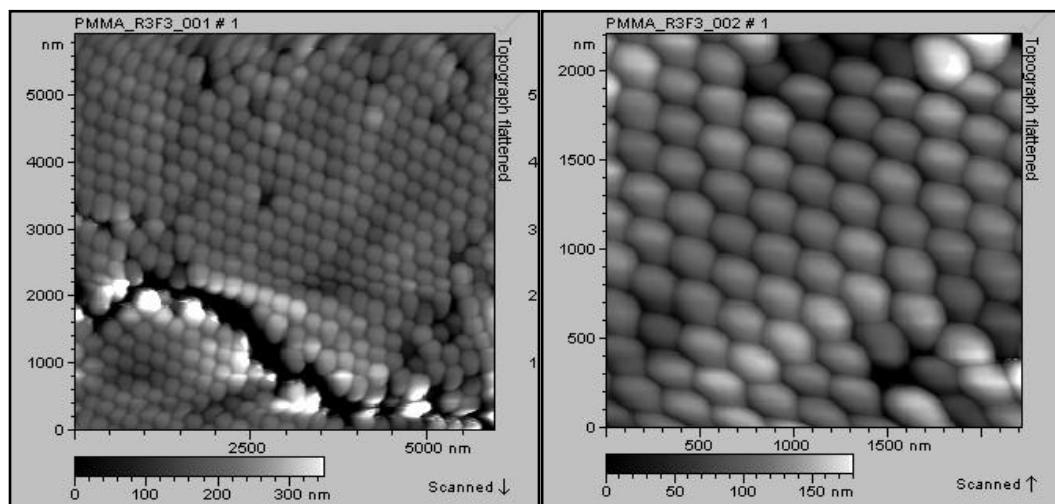


Figure 4.6 AFM Images of unlabelled PMMA microspheres: reaction 3

Figure 4.6 shows the size distribution of a sample of PMMA microspheres without the addition of any fluorescent dye. These microspheres are the result of conditions used in reaction 3, shown in Table 3.2. The images show a hexagonal distribution pattern and a uniform size of about 200 nm.

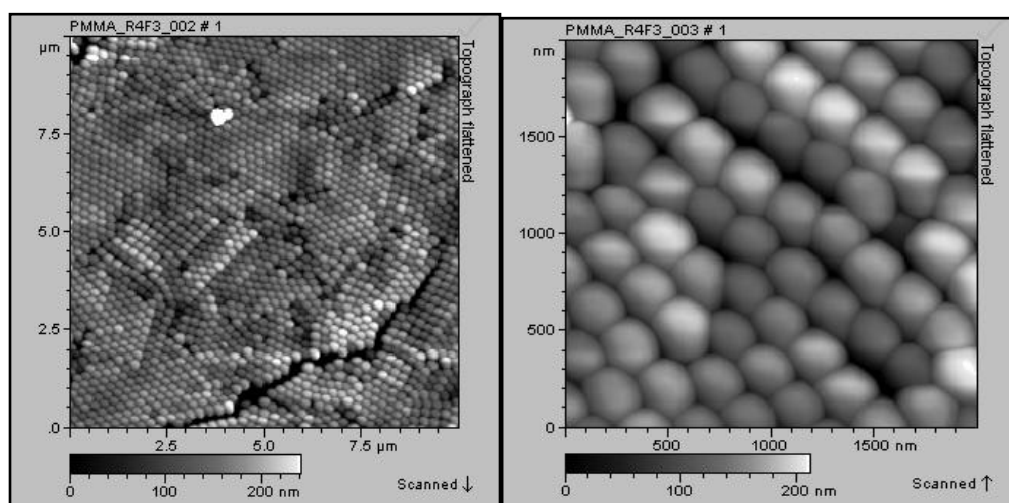


Figure 4.7 AFM images of unlabelled PMMA microspheres: reaction 4

Figure 4.7 shows AFM images obtained for reaction 4, in which the stirring speed of 600 rpm was consistent with the stirring speed used in reaction 3 but with a reduced reaction time of 20 min, as opposed to a reaction time of 45 min used in reaction 3. Microspheres produced in reaction 4 are around 200-300 nm in size.

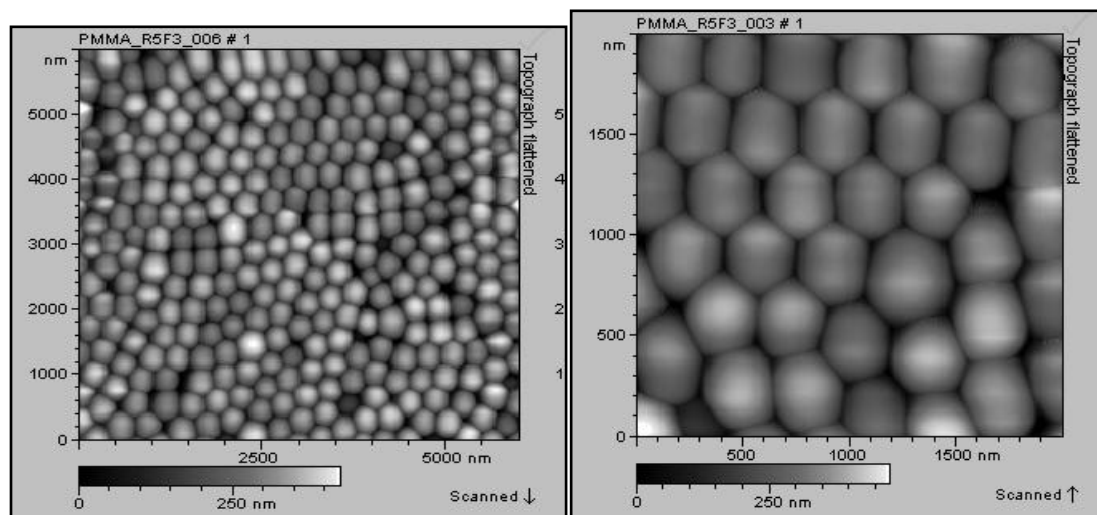


Figure 4.8 AFM images of unlabelled PMMA microspheres: reaction 5

Figure 4.8 shows AFM images obtained for reaction 5, in which the stirring speed was reduced to 300 rpm and the reaction was carried out over 45 min. Microspheres produced under these conditions are around 400-500 nm in size.

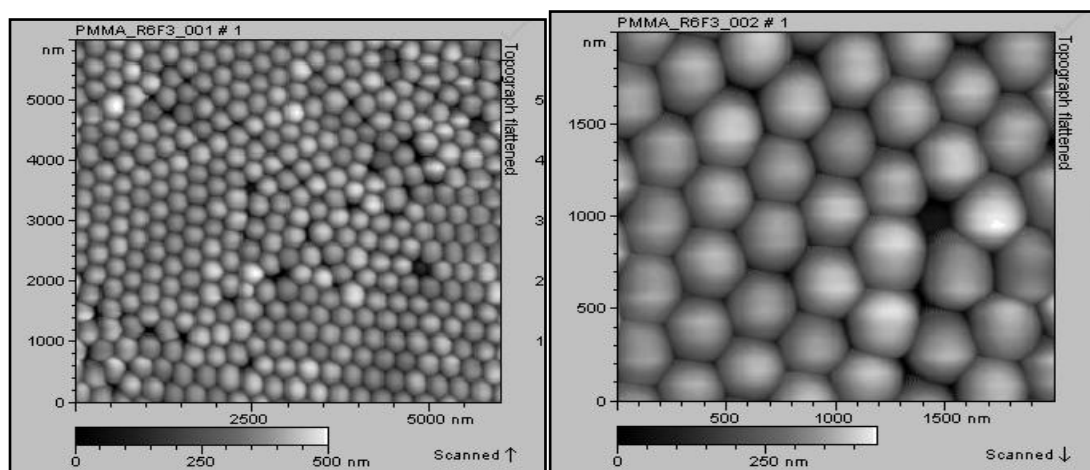


Figure 4.9 AFM images of unlabelled PMMA microspheres: reaction 6

Figure 4.9 shows AFM images obtained for reaction 6, in which the stirring speed was 300 rpm and the reaction was carried out over 35 min. Microspheres produced under these conditions are between 400-500 nm in size.

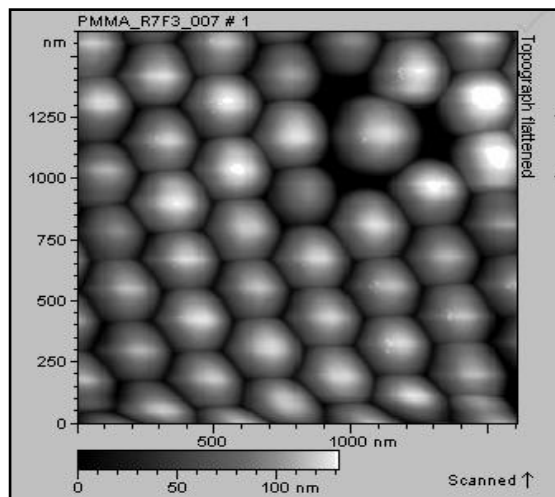


Figure 4.10 AFM image of unlabelled PMMA microspheres: reaction 7

Figure 4.10 shows AFM images obtained for reaction 7, in which the stirring speed was 300 rpm and the reaction was carried out over 20 min. Microspheres produced under these conditions are between 200-300 nm in size.

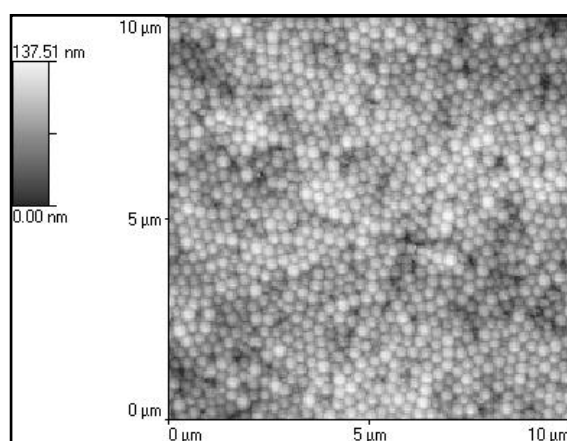


Figure 4.11 AFM image of PMMA microspheres, internally labelled with the fluorescent dye Rhodamine B

Figure 4.11 and Figure 4.12 are image analyses – using an Explorer II AFM, courtesy of Veeco Instruments – of a set of PMMA microspheres internally labelled with the

fluorescent dye Rhodamine B. The topography image (Figure 4.11) confirms that the sample is of soft polymer beads. Then line scans (Figure 4.12) of the image show that they are about 300 nm in diameter. This is larger than the PMMA beads that did not contain any fluorescent dye.

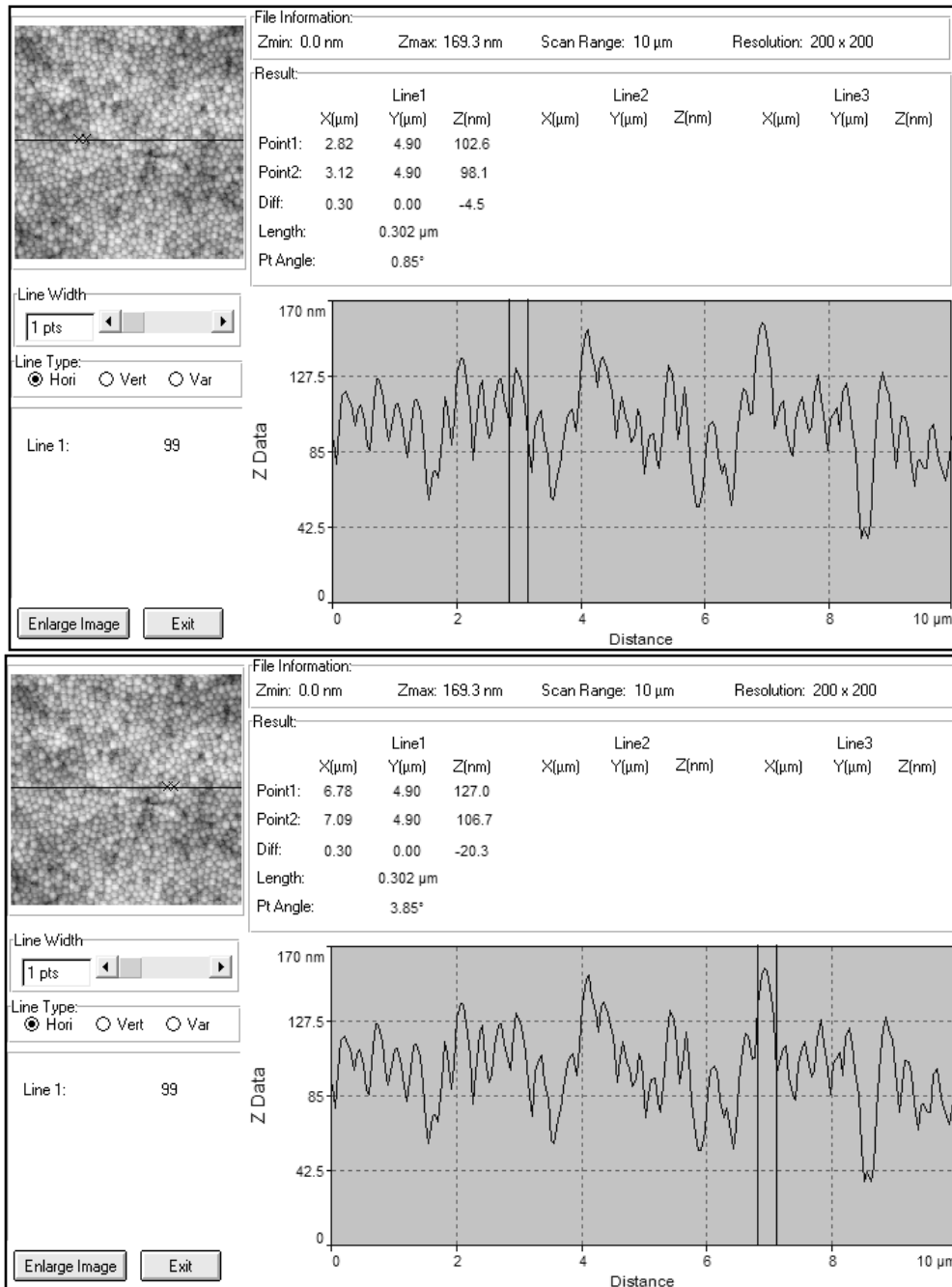


Figure 4.12 Cross-sectional line analyses of PMMA image shown in Figure 4.11

4.2.2 SEM Imaging of PMMA Microspheres

Figure 4.13 and Figure 4.14 show PMMA images obtained using a Cambridge Instruments StereoScan Mk II SEM.

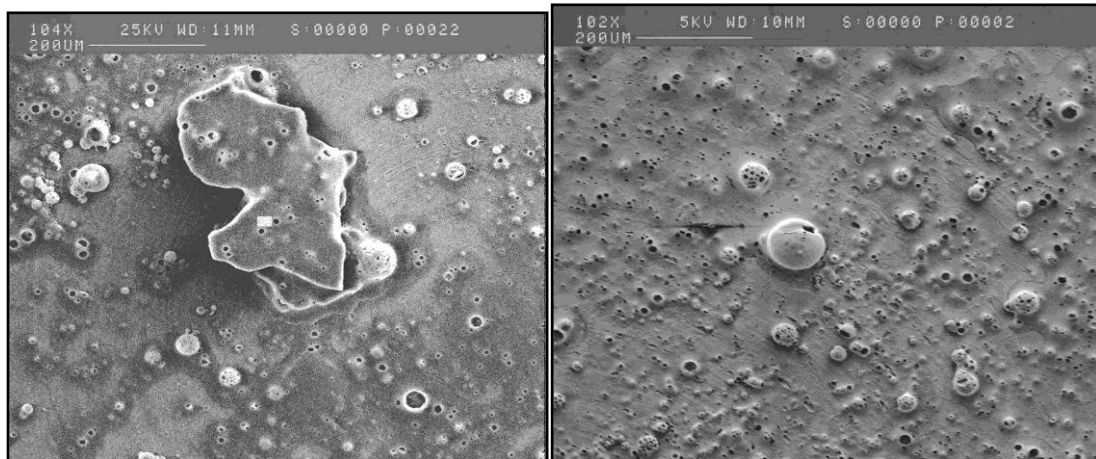


Figure 4.13 SEM image of unlabelled PMMA microspheres: images obtained using a Cambridge Instruments StereoScan Mk II SEM

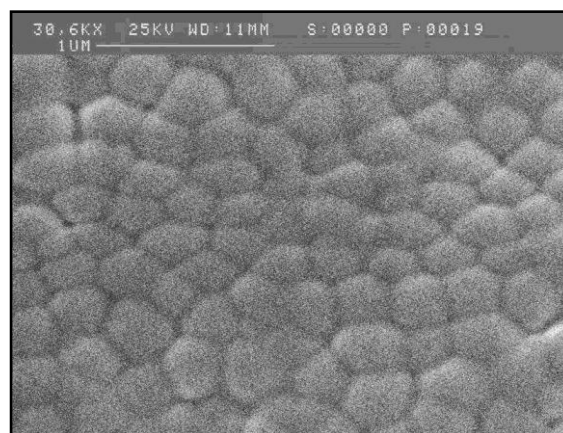


Figure 4.14 Zoomed in image taken from an area of the sample shown in Figure 4.13

4.2.3 Confocal Microscope Imaging of PMMA Microspheres

Figure 4.15 and Figure 4.16 show images of PMMA microspheres using a Carl Zeiss AG, LSM 510 META confocal microscope.

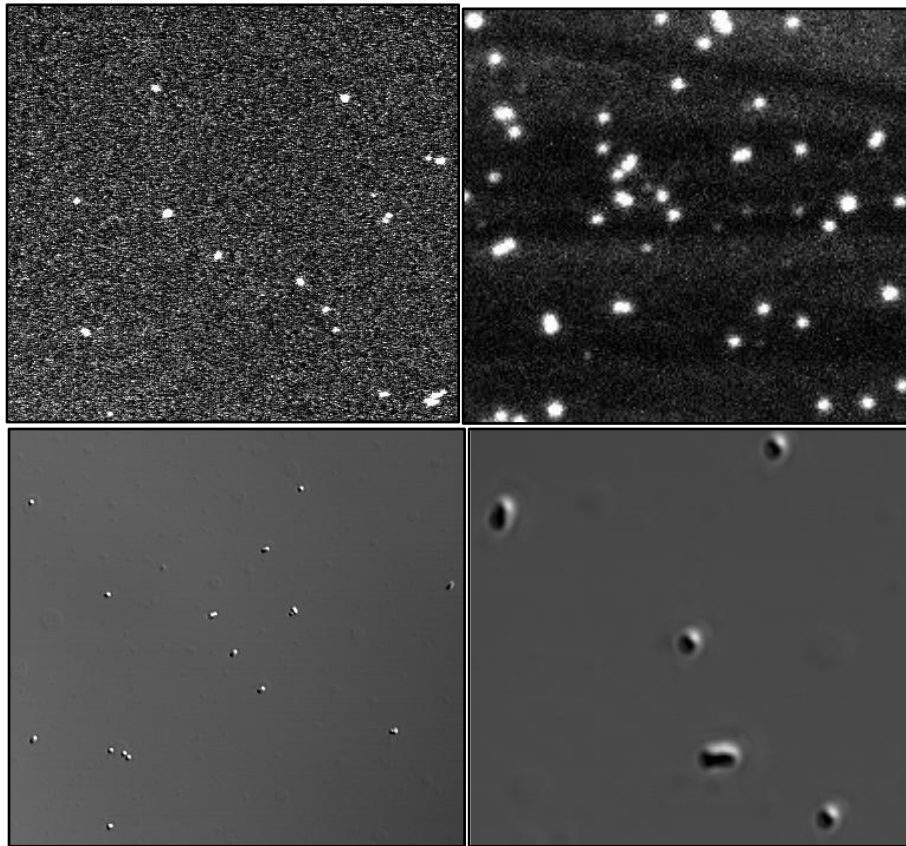


Figure 4.15 Images of PMMA microspheres obtained using a Carl Zeiss AG, LSM 510 META confocal microscope

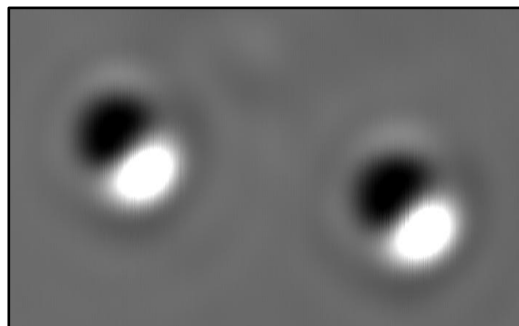


Figure 4.16 Zoomed image of PMMA microspheres obtained on a confocal microscope

4.3 Copolymerisation of P(MMA-HEMA)

4.3.1 SEM Imaging of P(MMA-HEMA)

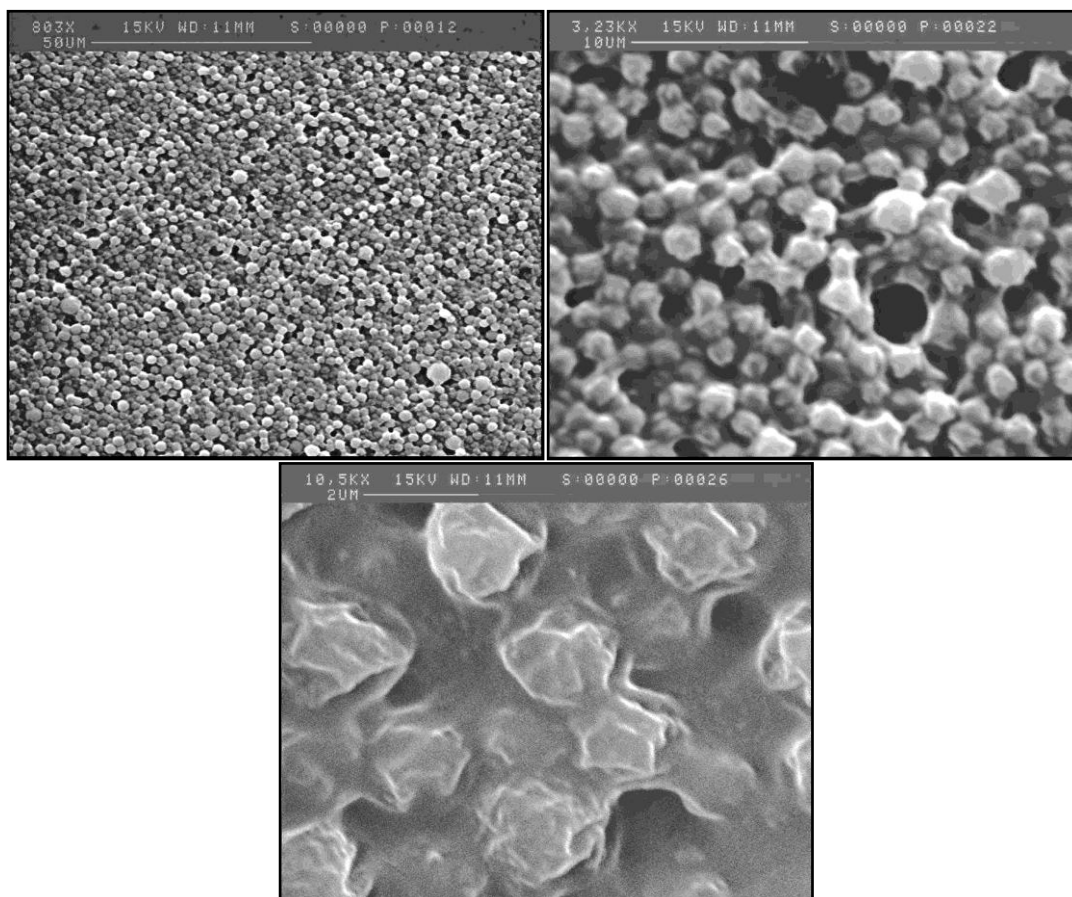


Figure 4.17 SEM images of P(MMA-HEMA) using a cold field emission SEM

It is apparent from the SEM Images in Figure 4.17 that the copolymerisation did not create uniform, monodisperse spherical microspheres. It can be seen from the images that the microspheres have become agglutinated. The ‘spheres’ appear flattened and somewhat stretched. These results are discussed in Section 5.2.

4.4 Preparation of Monoclonal Antibody

4.4.1 Purification of IgG

Figure 4.18 shows the absorbance spectrum for the purification of anti-phycoerythrin monoclonal antibody as carried out in the laboratory. This can be compared to the theoretical graph, shown in Figure 2.8. Although the shape of the curve from points 1 to 25 in Figure 4.18 do not match the theoretical curve exactly, points E1 to E5 show a clear peak at E2. It can be seen from the graph that the elution of protein occurred at points E2 and E3.

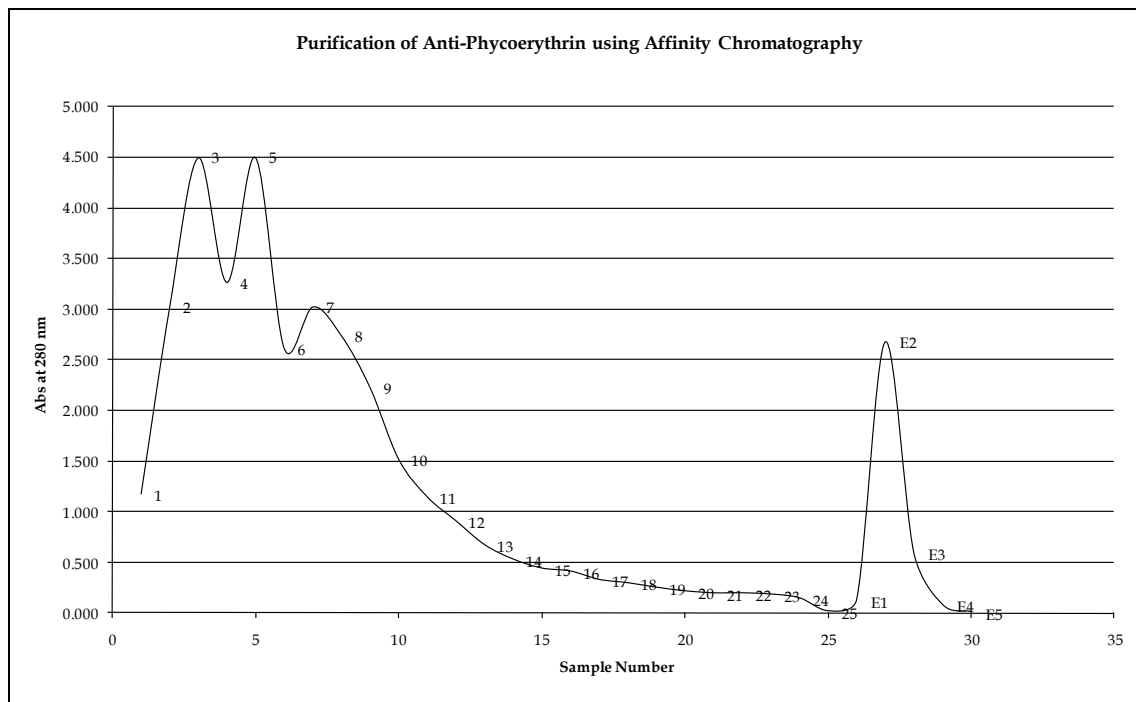


Figure 4.18 Absorbance spectrum for purification of anti-Phycoerythrin

4.5 Conjugation of Antibody to Microspheres

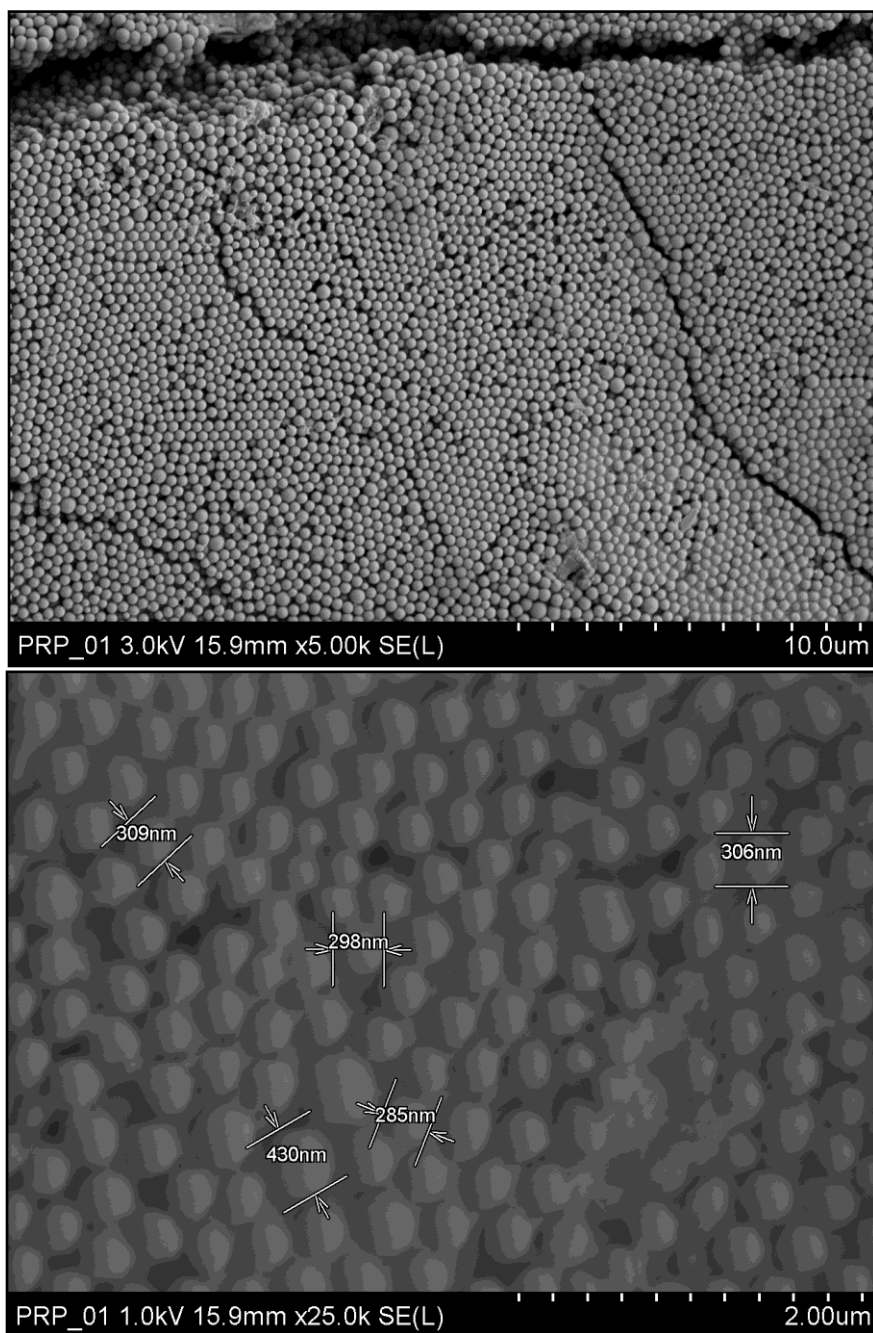


Figure 4.19 SEM images of PMMA in phosphate buffer, pH 8.0

SEM Images of PMMA microspheres (Figure 4.19) in phosphate buffer show the microspheres to be uniform in size at around 300 nm. On the other hand, the SEM images in Figure 4.20 show that after conjugation of mouse IgG to the PMMA

microspheres, the particles appear to no longer be uniform in size and have also aggregated. Possible reasons for this are discussed in Section 5.3.

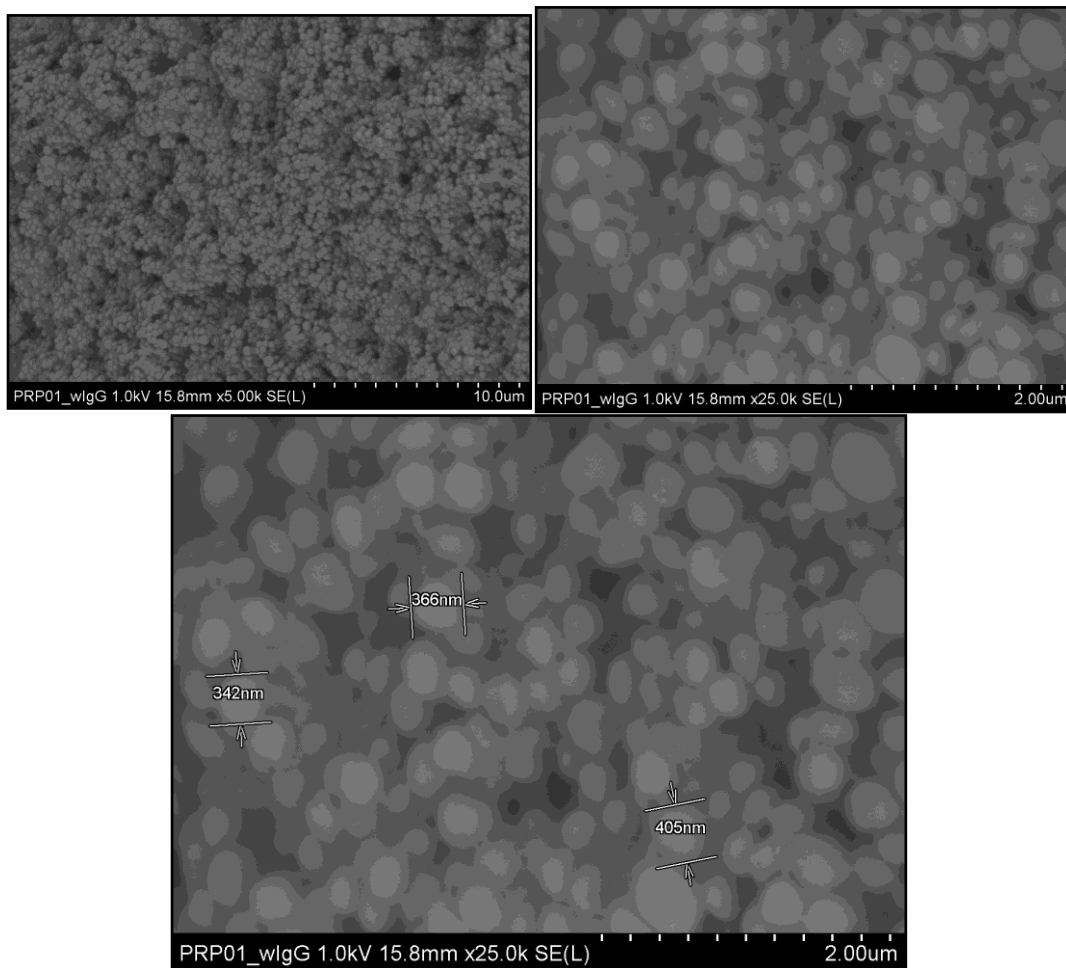


Figure 4.20 SEM images of PMMA-IgG conjugate in phosphate buffer

4.6 Diffusion of Microspheres

Figure 4.21 shows the average rate of diffusion of Rhodamine B-incorporated PMMA along nitrocellulose strips, compared to the rates of diffusion of colloidal gold and colloidal gold conjugate. The rate of diffusion of the colloidal gold was the greatest and that of the PMMA the least. The diffusion rate of Rhodamine B-labelled PMMA was 57.65% of the diffusion rate of colloidal gold.

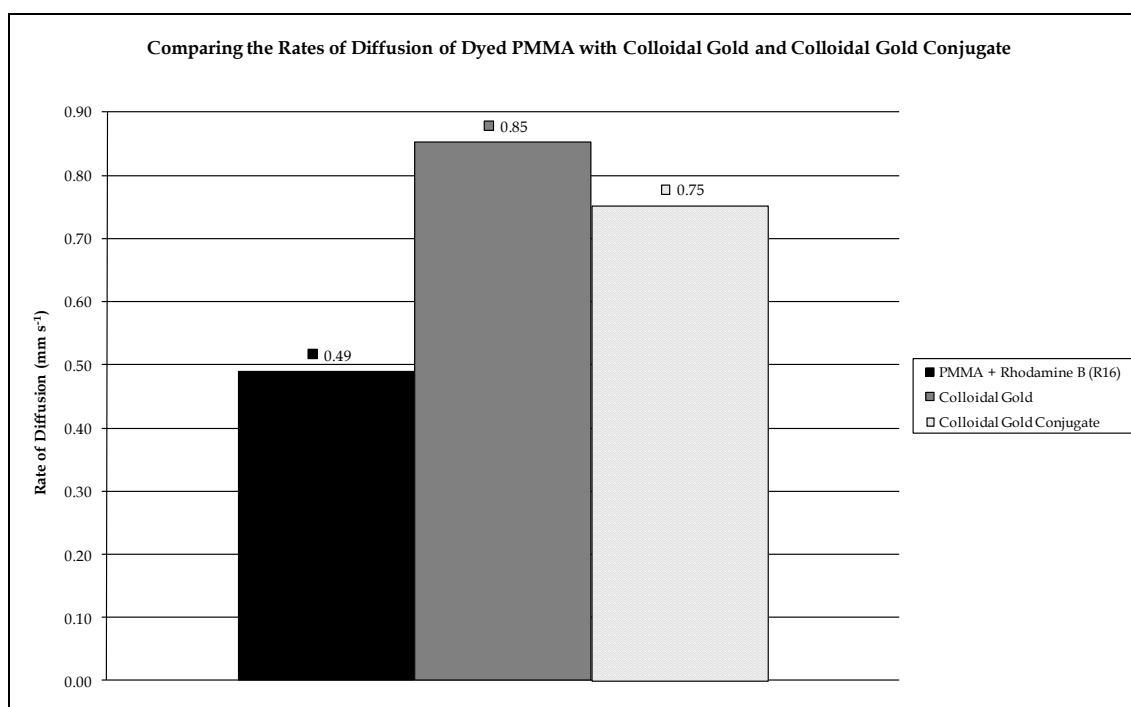


Figure 4.21 Rate of diffusion of PMMA along nitrocellulose strips as compared to colloidal gold and its conjugate

4.7 Detection Experiments

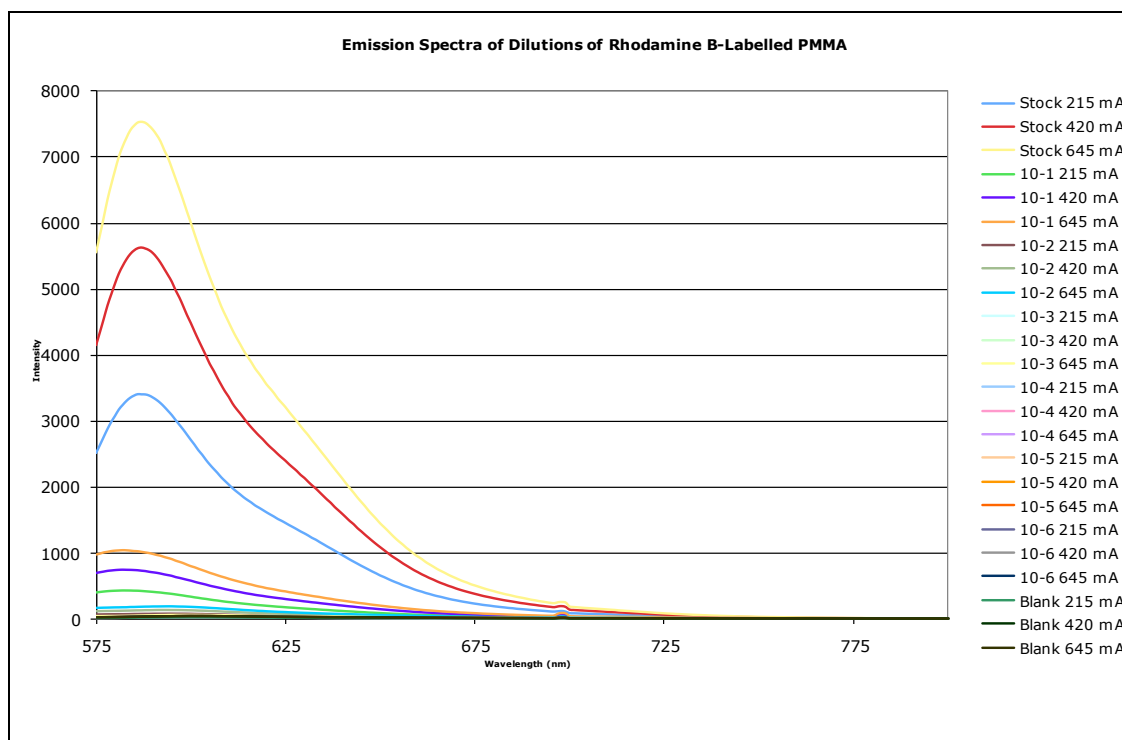


Figure 4.22 Emission spectra of dilutions of Rhodamine B-labelled PMMA

Figure 4.22 shows the emission spectra for dilutions of Rhodamine B-labelled PMMA suspended in distilled water. From this graph, it is unclear where the detection limit lies due to the large difference in emission intensity between the stock solution and the most diluted solution. Therefore, further graphs showing individual or only some of the dilutions were produced, as shown in Figure 4.23 to Figure 4.29, in order to better see the comparison between individual dilutions and the blank (containing only distilled water), and thus be able to determine the detection limit.

The graph in Figure 4.23 shows that for each LED intensity, the intensity of the emitted light from the sample solution (dilution 10^{-3}) is greater than the blank's intensity. However, the graphs for the remaining diluted samples (shown in Figure 4.24 to Figure 4.26) show that the emitted light intensity for samples 10^{-4} to 10^{-6} cannot clearly be distinguished from the intensity for the blank, which is reflected in

the graphs comparing only the peak intensity values of the dilutions, as shown in Figure 4.30 to Figure 4.33.

For the respective dilutions, the emission intensities are greatest when the light source intensity is greatest and least when the light source intensity is least, which can be seen in the graphs in Figure 4.23 to Figure 4.26 and is as predicted. The peak intensities show a linear relationship, which is also as predicted.

The peak value graphs (Figure 4.30 to Figure 4.33) show that the relationship between the peak emission intensities for each of the samples and the source intensities is linear, which is as expected.

However, when investigating the graph comparing the intensity versus concentration for all the dilutions, it seems that after dilution 10^{-3} (Figure 4.30) the emission intensities are no longer distinguishable from the blank, which contained just water. This is more clearly shown in the graphs in Figure 4.31 to Figure 4.33.

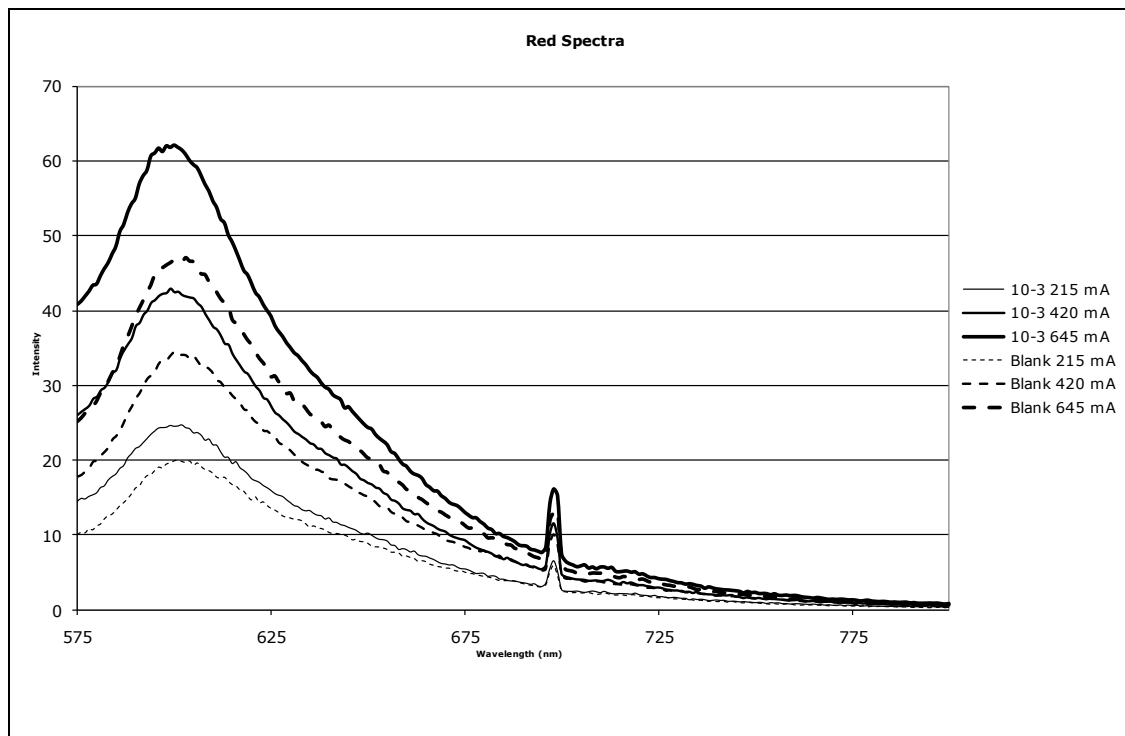


Figure 4.23 Emission spectra for 10^{-3} dilution subjected to varying LED intensities, compared to the Blank

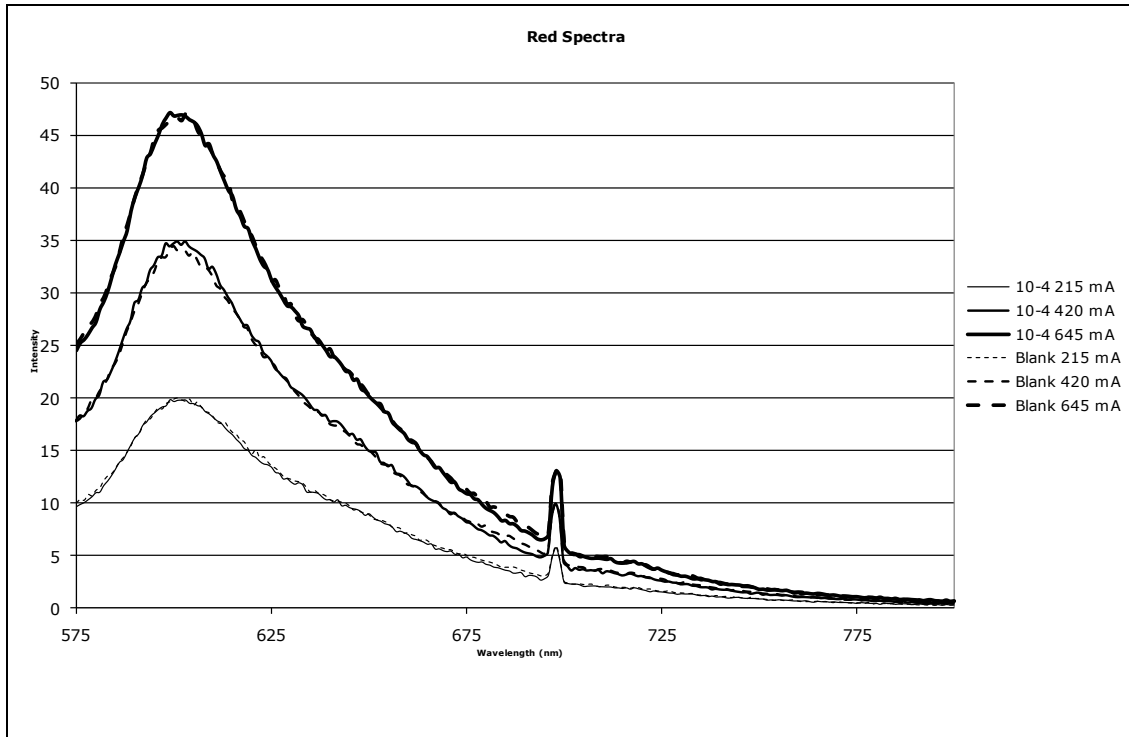


Figure 4.24 Emission spectra for 10^{-4} dilution subjected to varying LED intensities, compared to the Blank

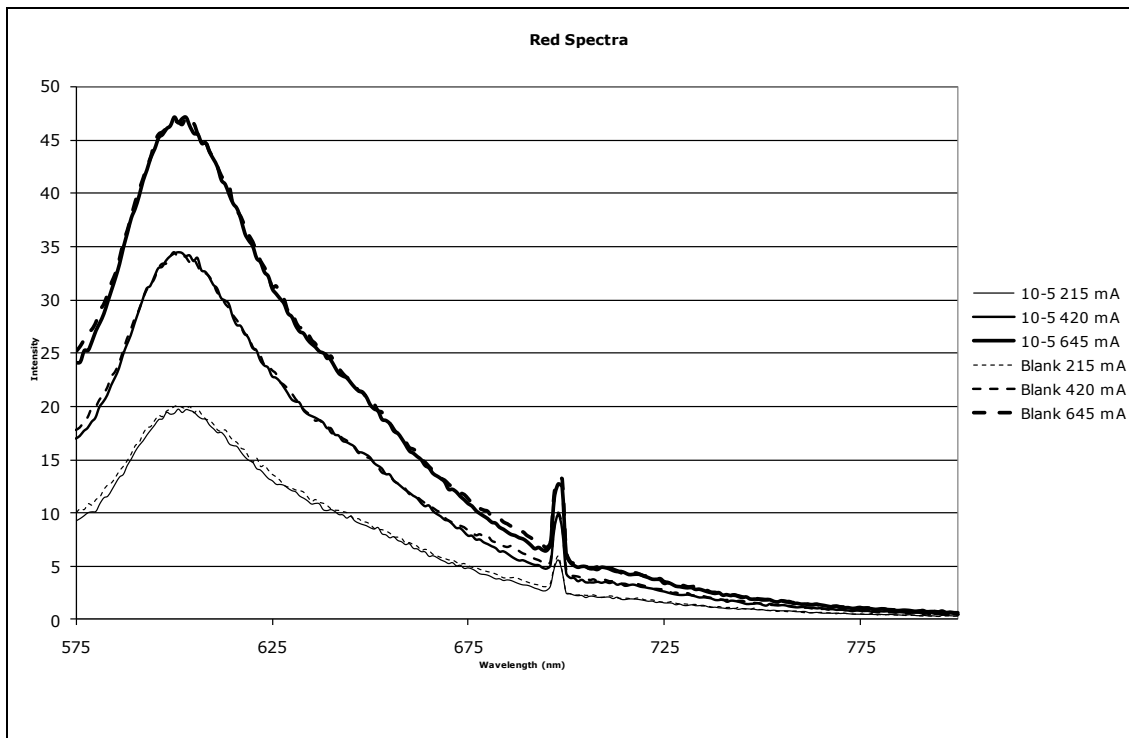


Figure 4.25 Emission spectra for 10^{-5} dilution subjected to varying LED intensities, compared to the Blank

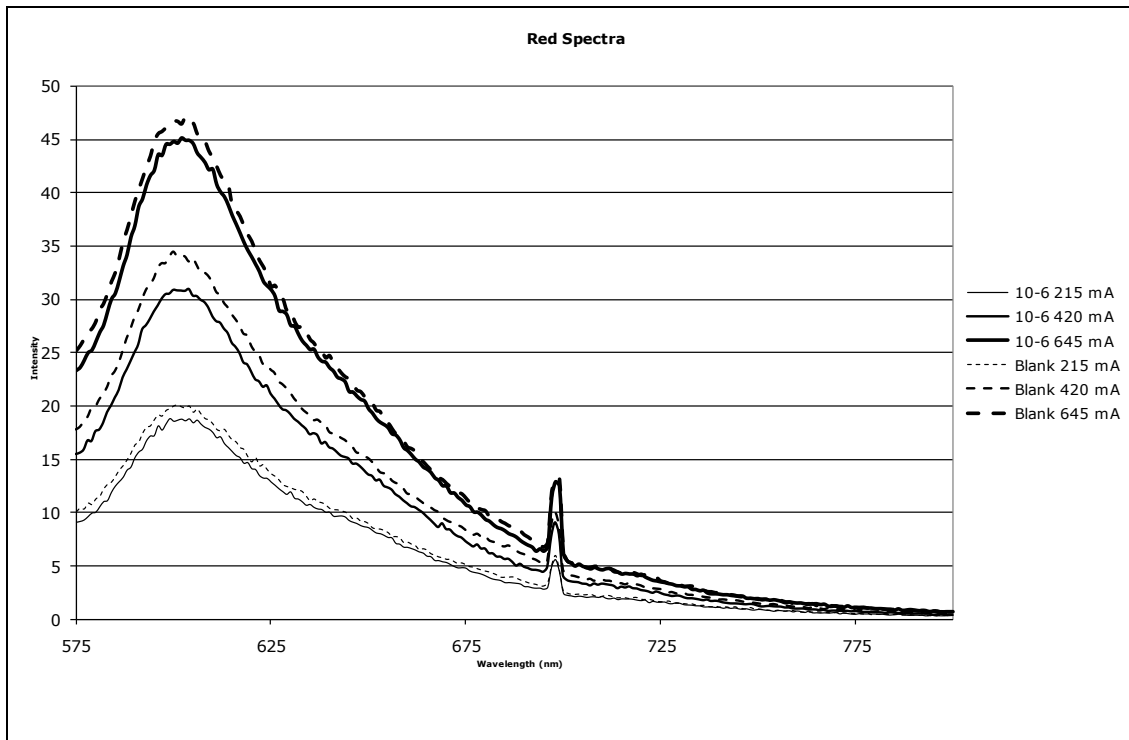


Figure 4.26 Emission spectra for 10^{-6} dilution subjected to varying LED intensities, compared to the Blank

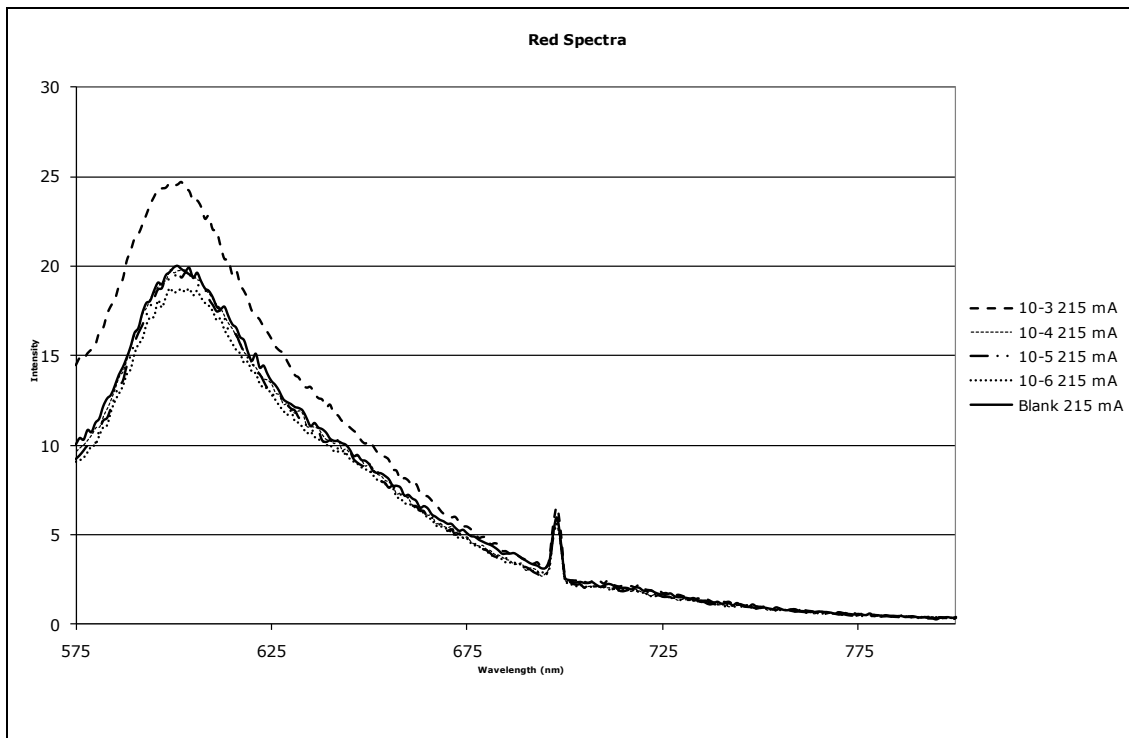


Figure 4.27 Emission spectra for dilutions 10^{-3} to 10^{-6} subjected to an LED intensity of 215 mA, compared to the Blank

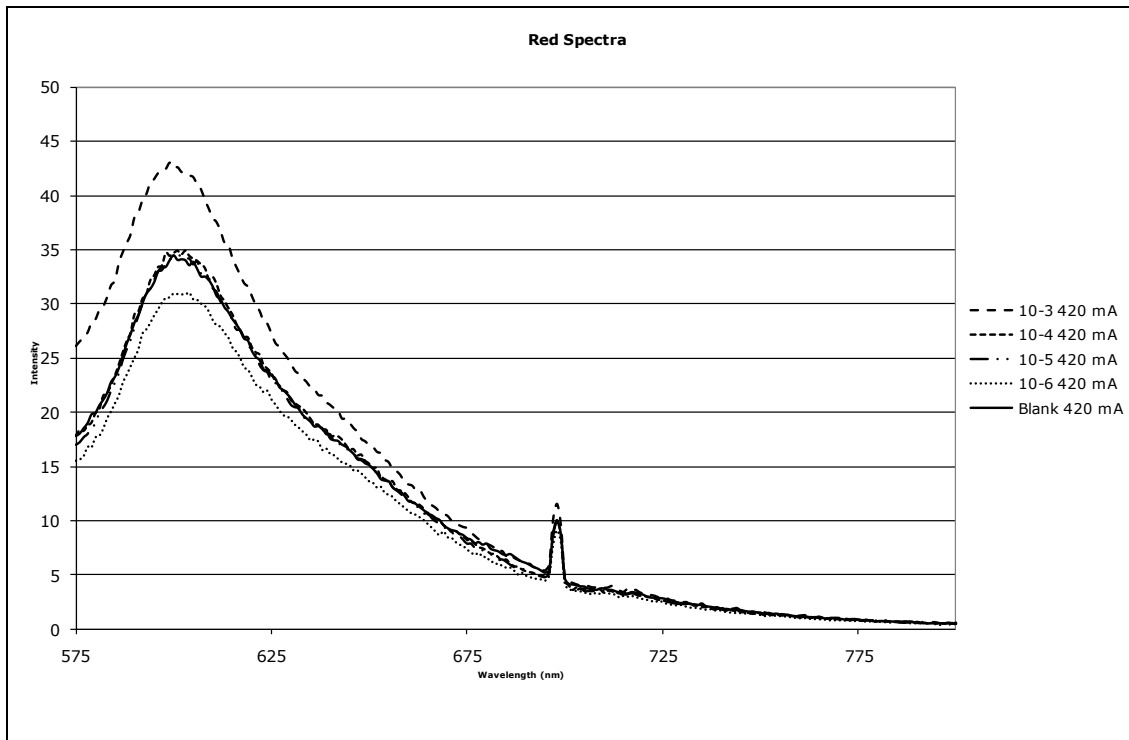


Figure 4.28 Emission spectra for dilutions 10^{-3} to 10^{-6} subjected to an LED intensity of 420 mA, compared to the Blank

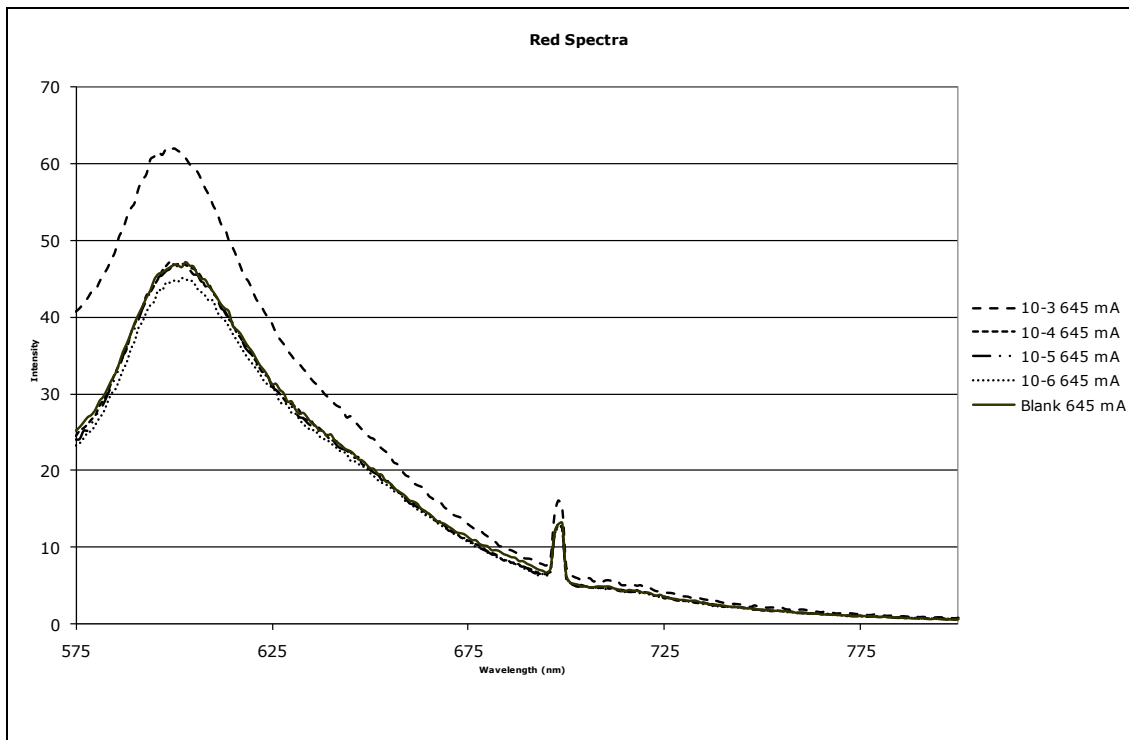


Figure 4.29 Emission spectra for dilutions 10^{-3} to 10^{-6} subjected to an LED intensity of 645 mA, compared to the Blank

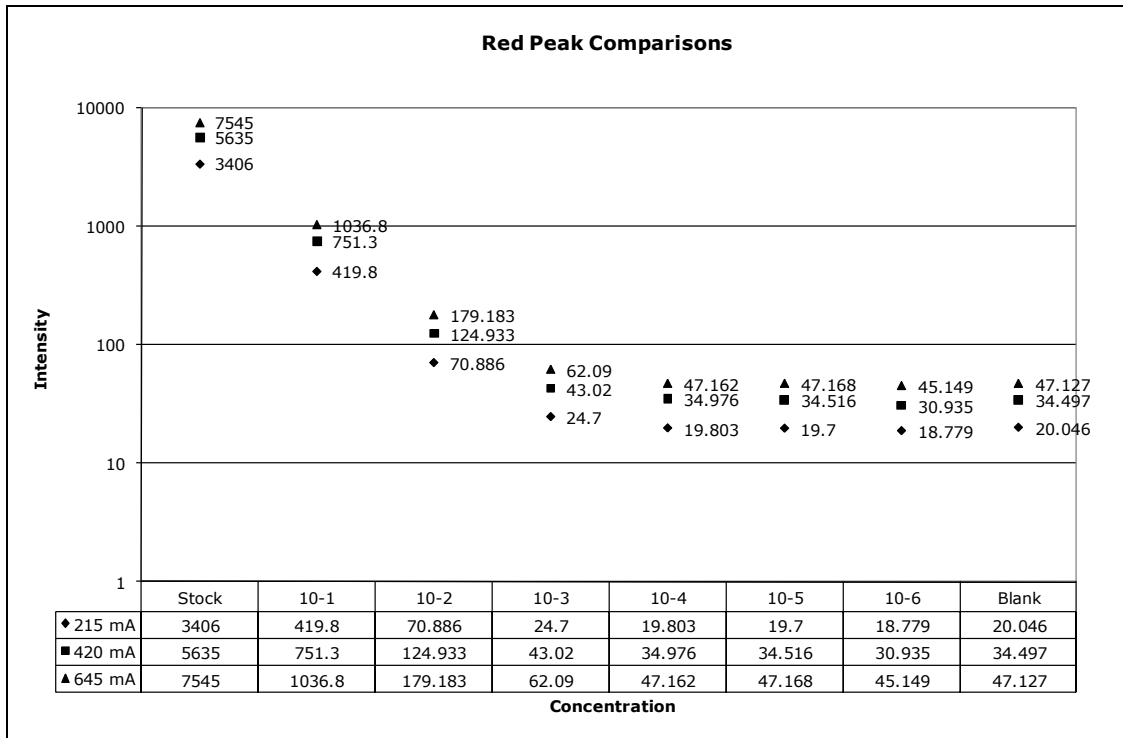


Figure 4.30 Comparison of peak emission intensities for dilutions at varying source intensities

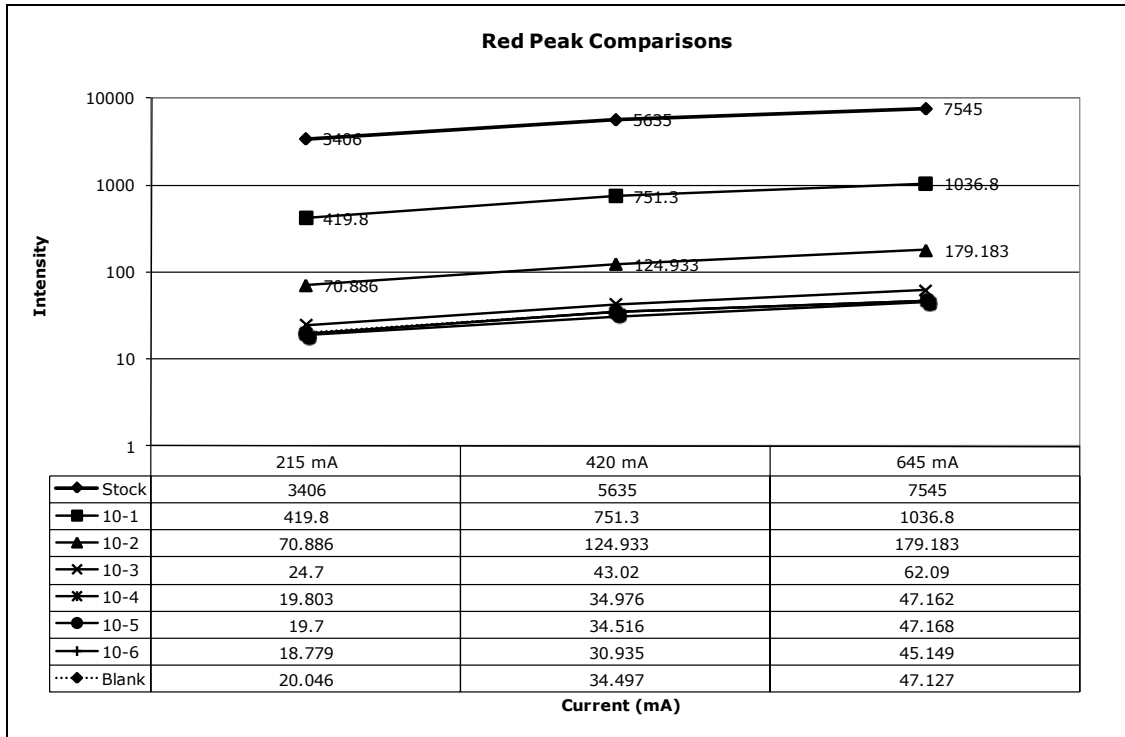


Figure 4.31 Comparison of peak emission intensities at increasing source intensities

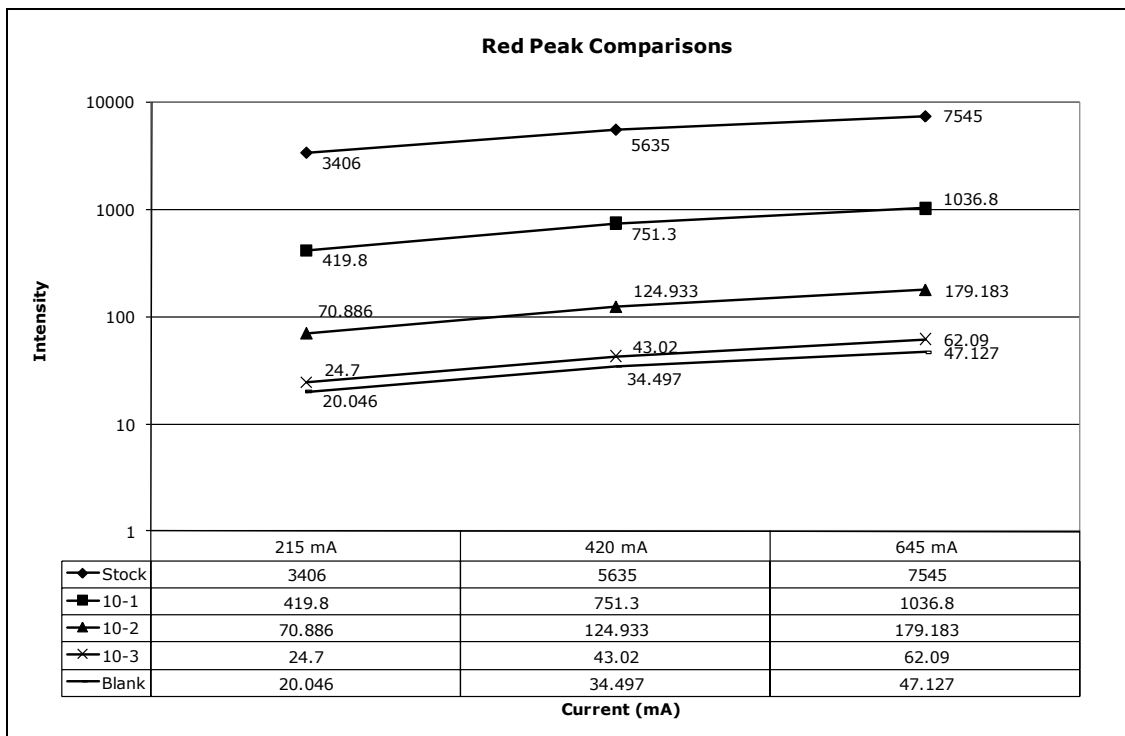


Figure 4.32 Comparison of peak emission intensities at increasing source intensities

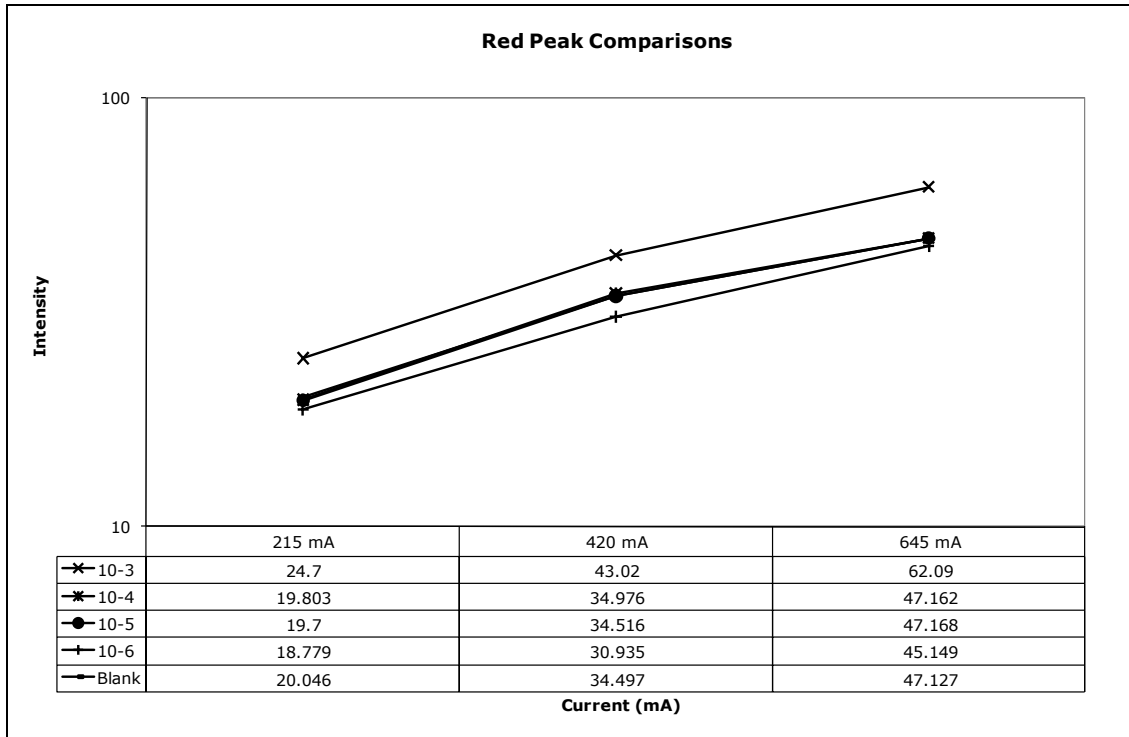


Figure 4.33 Comparison of peak emission intensities at increasing source intensities

Chapter 5 Discussion

5.1 Preliminary Studies

Preliminary studies comparing potential detection methods using colloidal gold to fluorescence suggested that using a fluorescence detection method would greatly improve on the detection limits achieved by the colloidal gold method. The means by which colloidal gold particles are detected differ from fluorescently labelled particles, as shown in the graphs shown in the preliminary experiments (Figure 4.1 to Figure 4.5).

In the colloidal gold studies, reflectance spectra were obtained for colloidal gold and colloidal gold-antibody conjugate samples. Both samples show peaks at 630 nm, which suggests that the reflected signals originate from the colloidal gold itself, i.e. no influence from the antibodies. If the presence of antibody on the gold surface, as in the case of the conjugate sample, had had any effect on the reflectance spectrum, then the conjugate sample's reflectance peak would differ from that of unbound gold, hence the deduction that the signals are solely the property of the gold microspheres. This is in accordance with literature, as discussed in Section 2.6.1. However, the intensity of the reflectance spectrum for the conjugate sample is greater than that of the colloidal gold sample. This can be attributed to the increased separation between the gold particles in the colloidal suspension due to the introduction of antibodies onto the gold particles, which reduces the absorption per unit volume and therefore increasing the intensity of the reflected signal.

Dilutions of the colloidal gold and colloidal gold-antibody conjugate samples subjected to white light illumination showed that at higher colloidal gold concentrations, the overall light intensity output is decreased and a red shift in the spectrum is introduced. The reduced light intensity at higher concentrations is due to the absorbing properties of gold. The increased red shift at higher concentrations is due to the size effect in reflection and to the fact that absorption is wavelength dependent (blue is more absorbing than red).

When using colloidal gold in detection systems, more gold present reflects a greater proportion of the red component of white light making the red colour more detectable. However, the absorption effect of the gold also becomes more significant. As the colloidal gold becomes more dilute, the red colour becomes less detectable as there are fewer particles to reflect the red light whilst absorbing the other components of white light. The detection limit when using colloidal gold is thus difficult to determine, as is shown in Figure 4.2, where the colloidal gold could no longer be detected after the first dilution as the spectrum becomes merged with the white light spectrum.

Originally, there were plans to combine the use of colloidal gold with fluorescent molecules in order to combine the benefits of colloidal gold's small size (40 nm) with the potentially powerful fluorescence detection methods. Therefore, it was necessary to choose a suitable fluorescent dye that had an emission peak at a wavelength corresponding to the reflectance spectrum of colloidal gold (630 nm). Lumogen Red F appeared to be a suitable candidate; therefore, preliminary experiments were performed on Lumogen Red to assess its suitability.

In the first experiment conducted on Lumogen Red, initially without applying any filter, fluorescence emission was detected at 180° to the LED light source and resulted in an emission peak at around 605 nm (Figure 4.3), which is shifted away from the red and towards the blue end of the spectrum. Speculation suggests that some of the green light from the LED may have been detected by the photodetector. After having applied a red filter to the set-up, the resulting graph (Figure 4.4) showed the maximum emission peak to be 630 nm, which suggests that the filter had absorbed the green light from the LED source and that the green part of the spectrum had been cancelled out, giving an emission peak that corresponds to the reflectance spectrum of colloidal gold, as predicted.

To back up the original plan of combining fluorescence with colloidal gold in order to enhance the detection signal and improve detection limits, it was thus concluded, from the results of the first experiment conducted on Lumogen Red, that Lumogen Red would be a suitable fluorescent dye to use with colloidal gold.

However, in light of the results obtained from the experiment conducted on colloidal gold and colloidal gold-antibody conjugate, it appeared that the use of colloidal gold was not so beneficial after all, taking into account the amount of light lost to absorption by the gold particles.

The major difference between using colloidal gold and fluorescent dyes is that colloidal gold contains light absorbing particles and may only be detected by light reflectance and scattering whereas fluorescent dyes may be excited by an energy source, or monochromatic light, at a particular wavelength causing it to emit light. The more energy introduced to the system, the more light will be emitted that may be detected. Thus, even at very small concentrations of dyes, there may be enough detectable light emitted provided the power of the light source is increased significantly.

In the second fluorescence experiment conducted on dilutions of Lumogen Red, without the application of a filter and where the emitted light was detected at right angles to the incident light, results in Figure 4.5 show that the emission wavelength is around 610 nm, which although is further towards the blue end of the electromagnetic spectrum than the predicted value of 630 nm is closer to the predicted value than the result obtained from the experiment conducted in a straight line. This shows that by rearranging the set-up in a 90° configuration not as much green light travels through the sample to the detector as in the straight-line set-up. However, even at right angles but without the use of a filter, some green light was still detected. This could be caused by reflection off the side of the sample holder, causing some of the green light to be detected. The experiment was not repeated with the application of a filter, but if it had been, it would be expected that the emission wavelength would be the predicted value of 630 nm.

With respect to the effectiveness of detection using fluorescence, it was surmised that the more dilute the sample, the less light would be absorbed by the particles, thus allowing more green light to travel through the sample. In the most diluted sample, where the concentration was of the order of 10^{-7} g l⁻¹ of the stock solution and with a source illumination current at only 34 mA, the light output detected was of the order of 10^3 .

It was observed that if the power of the light source were to be increased, smaller concentrations could be detectable. Contrary to the results observed for colloidal gold, the intensity of fluorescent light is linearly proportional to the intensity of the light source. It was therefore deduced that the detection limit could be predicted by stating the following: Assuming the detection limit is in orders of 10 (reading of fluorescence intensity) for fluorescent light, it can be estimated that the lowest concentration that would be detectable using a 34 mA light source would be 10^{-9} g l⁻¹. Increasing the LED power ten times would increase the detection limit ten times. Thus, using this method, a concentration of 10^{-10} g l⁻¹ should be detectable.

As a result of the findings from the experiments comparing dilutions of colloidal gold to dilutions of Lumogen Red, it was concluded that combining colloidal gold with fluorescence could result in significant shifts in the spectra, making the outcomes imprecise and indistinguishable. Thus, it was decided that it would perhaps be more beneficial to discard the use of colloidal gold altogether and replace it with polymer microspheres, which could be internally labelled with a fluorescent dye and detected by means of fluorescence instead of reflectance and scattering.

It was decided that a detection system utilising colloidal gold would perhaps not be the most effective system and was discarded as a result. However, upon reconsideration, additional illumination experiments on colloidal gold could perhaps have been carried out. Since white light is composed of multi-chromatic light, then altering the illumination source to a monochromatic light may have yielded different reflectance spectra from the ones shown in the graph in Figure 4.2. Whilst colloidal gold detection was not favourable using a white light illumination source, using a different type of illumination source may well prove otherwise.

5.2 Polymer Microspheres

PMMA was chosen because of its superior optical properties over polystyrene in addition to its known biocompatibility and structural integrity. Moreover, because it had been decided that colloidal gold would no longer be used, as a consequence of results obtained from the preliminary experiments, it was no longer necessary to use a fluorescent dye with a corresponding peak emission wavelength. Rhodamine B was chosen as an alternative, due to its high photostability and quantum yield as well as its solubility in both water and ethanol.

PMMA microspheres prepared by the emulsion polymerisation technique described in Section 3.2 yielded uniform spherical particles of around 200 nm for the uncoloured particles and larger uniform spherical particles of around 300 nm for the Rhodamine B-labelled particles, as shown by the AFM images in Figure 4.6 and Figure 4.11 respectively. This increase in particle size is to be expected, providing the particles were prepared under the same conditions but for the addition of the dye molecules, since the dye itself takes up volume and thus enlarging the overall molecular formation. This emulsion polymerisation technique is therefore considered to be an effective method for producing uniform PMMA microspheres.

Because chemical covalent coupling was being considered as a method of conjugating antibodies to the polymer microspheres, it was necessary to find a means of modifying the surface chemistry of the PMMA microspheres so that it contained a hydroxyl group, in order for the microsphere to be chemically attractive to the Fc region of the antibody. A potentially suitable method would be to copolymerise MMA with another monomer containing the required hydroxyl functional group. Therefore, it was decided that this theory would be tested by copolymerising methyl methacrylate with 2-hydroxyethyl methacrylate to create P(MMA-HEMA), using a combination of a modified version of the tried and effective emulsion polymerisation technique used in the PMMA microspheres production and the method described by Yavuz *et al* (2002).

It can be seen from the SEM images (Figure 4.17), however, that the copolymerisation did not yield uniform spherical particles as predicted and seem to have undergone some undesirable effects. From the images, it can be seen that the particles were nearly spherical but appeared flattened and somewhat stretched, as if they had either formed and were disintegrating or they had not properly formed. Aggregation of the particles also seems to have taken place.

What appears to have occurred is that, because HEMA is soluble in water, polymerisation conditions may not have been suitable or effective in allowing the HEMA molecules to copolymerise with MMA to form solid spheres. Another explanation may be that the spheres were formed but the bonds were not strong enough to maintain the solid sphere causing the spheres to swell and begin to dissolve in the aqueous medium. If the latter were the case, the images seen on the SEM would represent the degree to which the particles had dissolved when the water was removed by drying the sample onto the SEM stubs. This would also explain the aggregation of the particles.

Another possible explanation may be that upon copolymerisation, the HEMA constituent has led to a weakening of the originally hard PMMA structure, especially in an aqueous solvent, due to the swellable nature of PHEMA. This factor could be combined with the possibility that the monomers compositions were not optimised. If this is the case, it would suggest that the concentration of HEMA in the copolymerisation is too high. Using a combination of methods as discussed in Section 2.6.5 requires numerous trials and re-trials in order to achieve an optimised method suitable for a specific need. One apparent alteration would be to run a series of optimisation experiments with a range of monomer concentrations.

Also, the possibly weakened microsphere structure due to excess HEMA in the copolymer composition may be the reason why the particles were not spherical. They may also have been damaged by the sputter coating process in preparation for imaging using the SEM as well as by electron bombardment during the imaging process.

Because HEMA is highly soluble in water, it has become apparent that using an aqueous medium for polymerisation containing HEMA can be problematic, although its successful use has been reported in a number of cases (Denizli *et al* 1997; Yavuz *et al* 2002). Due to HEMA's high solubility in water, there is a possibility that a certain amount of solution polymerisation is taking place within the reaction system rather than emulsion polymerisation. Due to the complications that have arisen, possibility due to HEMA's solubility in water, a consideration would be to use a non-aqueous (possibly organic) solvent such as ethanol or toluene instead.

In addition to readjustments in monomer composition and a different type of polymerisation solvent, the monomer reactivity ratios would have to be obtained, as discussed in Section 2.6.3. It has been discussed that the choice of solvent can have a significant effect on reactivity ratios in systems involving monomers that are ionisable or form hydrogen bonds, of which HEMA is one, therefore the reactivity ratios would vary according to the solvent used, whether it was water, toluene, ethanol or some other solvent. The importance of the reactivity ratios could go some way to explaining the difficulties of copolymerising MMA and HEMA, as it may well show a significant difference in the rate of reaction of each of the monomers in the different solvents, which would in turn affect the particle formation and composition. Therefore, further analyses in addition to imaging would have to be done for this to be possible; ¹H-NMR spectroscopy would be needed in order to determine the polymer composition and the results from the spectroscopy then used to calculate the reactivity ratios.

As was discussed in Section 2.6.5, the hydrophilic nature of PHEMA and solubility of its monomer in water requires careful consideration of its polymerisation process and the stabilisers and initiators used. This factor clearly extends to considerations involving its use in copolymerisation. A hydrophobic monomer and its respective polymer require less careful consideration because there is no danger that the produced polymer or its monomer will become dissolved in the aqueous medium. However, despite the complications that can arise due to its hydrophilic nature, it still continues to be an attractive option for copolymerisation because of its other qualities.

AIBN was used as the initiator for the copolymerisation, following discussions in Section 2.6.5 that a persulphate initiator would not be suitable. However, since choice of initiator may also affect polymerisation systems involving HEMA, this factor should not be ignored. An alternative initiator that may be considered is benzoyl peroxide.

Instead of trying out the combination of methods as discussed in Section 2.6.5 as the initial copolymerisation step, it would perhaps have been beneficial to first experiment further with the method described in Section 3.2, a method that was used to successfully produce monodisperse and uniform PMMA particles. Using this tested method, whilst maintaining the same reaction conditions that were used to produce PMMA, varying amounts of HEMA could be added to the system without introducing any other new variables.

5.3 Antibody-Microsphere Conjugation

It has been reported in a number of literature that the conjugation of antibodies to polymer microspheres by passive adsorption is a generally sufficient method for immobilisation but that in certain cases other immobilisation techniques such as complex adsorption and chemical covalent coupling may be required (Bangs Labs 1999a, 1999b). Because of the apparent simplicity and reproducibility of passive adsorption, this method of antibody-microsphere conjugation was investigated and it was therefore expected that the method of passive adsorption of antibodies onto PMMA microspheres would yield favourable results. The outcome of experimentation utilising this method, as shown by the results obtained in Section 4.5, did not, however, reflect the apparent simplicity and reproducibility expected of this method. This is discussed in more detail later on in this section.

Prior to the actual conjugation steps carried out in Section 3.5.2, the antibodies were prepared, as described in Section 3.4. Results shown in Figure 4.18 correspond to the theoretical graph (Figure 2.8) for the purification of IgG using affinity chromatography. It can therefore be confirmed that no complications or unexpected outcomes had occurred in preparing the antibodies for use in microsphere conjugation and that the results are satisfactory thus far.

Images of the microspheres were taken in water and after they were suspended in their binding buffer in order to show any discrepancies. The SEM images of PMMA microspheres in phosphate buffer show that the microspheres maintained their uniform size of around 300 nm, which corresponds to the results for PMMA microspheres in water and shows that steps used to prepare the PMMA microspheres in the phosphate buffer did not result in any visible undesired effects on the microspheres themselves.

However, after the steps to conjugate the antibodies to the microspheres were taken and images of the conjugates were obtained, the images show aggregation of the particles and show that they are no longer uniform in size.

Possible reasons for this unexpected outcome may be that the binding conditions may have altered due to the addition of antibodies to the microspheres in the buffer. Although the pH or temperature was not expected to change, one or both of them may have done so. pH readings and temperature measurements were not taken after the adsorption procedures but probably should have been; the case may be that the environmental conditions in the system had somehow become altered.

Another explanation as to why the particles appear to have coagulated may lie in the fact that the conjugated sample was washed using centrifugation. Using centrifugation at a high rotation speed may be sufficient to clean PMMA microspheres because they are less likely to be damaged by the process than a sample containing proteins. In addition, centrifugation at excessive rotation speed may cause the adsorbed antibodies to become unbound from the microsphere surface. On the other hand, if the centrifugation speed is not high enough, then washing may not be efficient enough, leaving the sample with unbound antibodies, loosely bound antibodies and antibodies adsorbed in unfavourable orientations. The presence of unbound, loosely bound and wrongly oriented antibodies may result in additional attractive intermolecular forces between the particles other than those required for the conjugated particles to remain in a stable colloidal suspension, causing them to flocculate.

Diffusion experiments were performed on colloidal gold, colloidal gold-antibody conjugate and Rhodamine B-labelled PMMA microspheres for the purpose of comparing the diffusion rates of the three colloidal suspensions along a nitrocellulose strip. However, diffusion of Rhodamine B-labelled PMMA-antibody conjugate was not carried out due to the unexpected aggregation and non-uniformity of the microsphere-antibody conjugate. In order for the diffusion experiment to be considered valid for the microsphere-antibody conjugate the colloidal suspension would have had to contain uniform, monodisperse particles sans aggregation.

Using the passive adsorption method described in this thesis, the particles had undergone a considerable amount of ‘clumping’, which is not the desired effect. It seems that batch operations of adsorption, simply by mixing the particles by gentle agitation, are not adequate to produce monodisperse microsphere-antibody conjugates. Literature has shown that more effective, albeit more complex and more

costly, methods exist, which include the employment of tangential flow filtration (to be used as a microsphere cleaning technique as well as during the conjugation process) and chemical covalent coupling of the antibodies to the microsphere surface, as discussed in sections 2.6.6 and 2.8.3. However, it has been suggested that in order to effectively conjugate the particles by chemical covalent coupling, the microsphere surface needs to have a suitable functional group to bind to the Fc region of the antibody. As was shown in these works, P(MMA-HEMA) seemed to have been a strong candidate for such a chemical coupling. Regrettably, the successful production of monodisperse and monosized P(MMA-HEMA) microspheres was not achieved, possibly due to a number of factors discussed previously in Section 5.2.

5.4 Imaging Techniques

A number of imaging techniques for microsphere analysis were evaluated. Due to access limitation constraints, however, it was not possible for all of the samples to be imaged using each type of imaging technique. Initially, PMMA microspheres were imaged using a Cambridge Instruments stereo-scan SEM. Whilst the images obtained using the Cambridge were of reasonable quality, those obtained by the more sophisticated cold field emission SEM were of a noticeably higher quality. However, it is unclear whether preparation steps using the sputter coater or, indeed, the use of the SEM itself could have damaged the possibly weakened P(MMA-HEMA) microparticles. It would be useful to be able to obtain images of the P(MMA-HEMA) particles under an AFM in order to compare the image analyses.

The use of an AFM was briefly available courtesy of Edinburgh University and some images of the PMMA microspheres were obtained. Using the AFM, it was possible to obtain images of much higher resolutions than those obtained using either the Cambridge or the field emission SEM. Using tapping mode AFM, it is possible to obtain images of soft particles with minimal damage to the particle surfaces. Hence, the use of an AFM to analyse the copolymer particles would have been beneficial.

An attempt was made to introduce a third imaging technology as part of the microsphere analyses by utilising the confocal microscope, which is widely used to image cells and other biological macromolecules. However, no meaningful results were produced and therefore the use of the confocal microscope was promptly abandoned.

5.5 Detection Limits

Results in Section 4.7 show a linear correlation between peak intensity output values and concentration, as expected. However, while the detection limit for dilutions of Rhodamine B-labelled PMMA microspheres was expected to be of the order of 10^{-9} or lower, it was found from the results that a detection limit of only 10^{-3} was achieved. While this value seems to be well short of the expected detection limit, there are several possible explanations as to why this is so.

When preparing the dilutions for detection, it was necessary to prepare each dilution from a common stock solution rather than by using a series of dilutions, using the serial dilution method, in order to ensure that each dilution did indeed contain the amount of PMMA microspheres required. However, despite this, for the more diluted samples, larger vessels were required to accommodate the sample. It was only possible to pipette out very small amounts of the required volume of stock sample, in so far as the smallest pipette size was available. The smallest volume able to be pipetted was 2.0 μl . This meant that, in order to prepare a dilution of 10^{-6} of the stock solution, a total volume of 2 l was required. It was known that in the prepared sample, the concentration was as required. However, in order to perform the detection experiment, it was necessary to decant the sample into a cuvette in order to be read by the spectrophotometer. In decanting the prepared sample into the cuvette, it is possible that the cuvette then no longer contained any PMMA microspheres and therefore the spectrophotometer was not able to detect any, thus showing the result to be similar to the blank.

Chapter 6 Conclusions

This research study has investigated the importance of biosensors in the field of microbial detection, with special emphasis given to a particular method of detection, the immunochromatographic assay, due to its small size, ability for rapid visual detection and simplicity of use. Microspheres, which are an integral material component in an immunochromatographic assay, have been examined by comparing detection using colloidal gold microspheres to detection using polymer microspheres. In addition, an extensive review of literature has been carried out, detailing the developments in the field of microbial detection and discussing the various technologies involved.

Experimental evaluation of existing technology, using colloidal gold, and an attempt to improve on the immobilisation of antibodies to the microspheres and improve detection limits by implementing the use of internally labelled polymer and co-polymer microspheres have been carried out, as described in Chapter 3, the results of which have been shown and discussed in Chapter 4 and Chapter 5 respectively, and the outcomes of which are summarised as follows.

The production of PMMA microspheres by the emulsion polymerisation method described in Chapter 3 resulted in monodisperse spherical particles of around 200 nm for particles prepared without the addition of any fluorescent dye and 300 nm for particles internally labelled with the fluorescent dye Rhodamine B.

The production of P(MMA-HEMA) using the emulsion polymerisation method described in Chapter 3 did not result in uniform spherical particles. In addition, P(MMA-HEMA) was found to coagulate using this method.

The conjugation of Immunoglobulin G to Rhodamine B-labelled PMMA microspheres by the passive adsorption method described in Chapter 3 resulted in agglutination of the conjugate particles.

The diffusion of Rhodamine B-labelled PMMA along a nitrocellulose strip, as carried out using the method in Chapter 3, was found to be 42% slower than the diffusion of colloidal gold along a nitrocellulose strip.

Starting with a stock solution of 1% w/v of Rhodamine B-labelled PMMA microspheres in suspension, the detection limit, using the detection method carried out as described in Chapter 3, was found to be of the order of 10^{-3} .

Chapter 7 Recommendations for Future Work

It has been shown by the results obtained that some of the methods used in this study require further development and if improved upon, by adjusting certain parameters or employing more sophisticated methods, may yield outcomes that are closer to predictions. In addition, due to time and cost constraints associated with this study, some of the proposed investigations discussed in the review of literature were not able to be experimentally carried out. Further work to improve on methods investigated in this study would therefore be beneficial; some recommendations are proposed and summarised as follows:

1. Production of P(MMA-HEMA) microspheres using a non-aqueous (organic) solvent.
2. Following successful production of P(MMA-HEMA) microspheres of around 200 nm, use them for the chemical covalent coupling of antibodies.
3. Utilise tangential flow filtration when cleaning microspheres and immobilising antibodies onto microsphere surfaces in order to increase efficiency of cleaning and immobilisation and prevent particle aggregation.
4. Incorporate a lock-in amplifier into the design of the detection device to attempt to improve detection limit.

7.1 Recommendation for production of P(MMA-HEMA)

As was discussed in Section 5.2, there are a number of possible reasons why the method used for the copolymerisation of MMA and HEMA did not successfully yield monodisperse and uniform copolymer microspheres. A considerable number of small adjustments to the experimental methods would be required in order to determine a suitable solvent, if water is indeed not the ideal solvent, and optimum monomer and comonomer concentrations.

As a recommendation for further work, a series of copolymerisation reactions would be carried out using the method described in Section 3.2 with no other new parameter introduced to the system except for the range of concentrations of HEMA. This would include retaining water as the polymerisation medium.

Other possible trials may be to try to adjust certain parameters within the method described in Section 3.3. Such parameters include the use of a non-aqueous solvent such as toluene or ethanol, a range of concentrations of HEMA and possibly a different initiator such as benzoyl peroxide.

¹H-NMR spectroscopy should be carried out in addition to SEM and AFM analyses in order to determine polymer compositions and calculate the reactivity ratios for the monomer and comonomer.

Carrying out extra experimentation on P(MMA-HEMA) copolymerisation as recommended in this section would in all probability be able to ascertain the deductions made in Section 5.2 or establish more accurate explanations. In addition, refining the parameters should, with little doubt, lead to successful copolymerisation of P(MMA-HEMA) suitable for covalent bioconjugation.

In addition to optimising polymerisation conditions in order to achieve suitable copolymer microspheres, further analyses on the copolymers may be done to characterise the microsphere surfaces. However, studies on surface chemistry and

surface characterisation can be extensive and very detailed, and should perhaps therefore be considered as a basis for a separate research project.

7.2 Recommendation for covalent chemical coupling

Provided successful copolymerisation of MMA and HEMA, the next logical step would be to use them in covalent chemical coupling experiments. Chemical coupling protocols would be required to be considered and evaluated through experimentation in order to determine a suitable method for attaching antibodies to P(MMA-HEMA) microspheres. Colloidal stability should be tested over a number of years; in addition, binding strength should be tested by subjecting the conjugated particles to changes in various environmental conditions such as pH, temperature and the introduction of competing species.

Other optimisation experiments may include amount of antibodies used and concentration of the microspheres colloidal suspension.

7.3 Recommendation for microsphere cleaning and separation

As discussed in sections 2.6.7 and 5.3, conventional methods of cleaning and separation of microspheres using centrifugation and normal flow filtration may not be sufficient when handling microspheres, especially copolymer microspheres and bioconjugated microspheres. Incorporated into recommendations 1 and 2 above should be the employment of a tangential flow filtration unit for the purpose of cleaning and separating the microparticles, but also to facilitate the conjugation process, as discussed in Section 2.6.7.

7.4 Recommendation for lock-in amplification

Because signal recovery involving very dilute samples can be problematic due to the increased significance of noise at these levels, there needs to be a way of isolating the required signal and amplifying it so that meaningful results could be obtained and not cluttered with undesirable noise signals. As discussed in Section 2.10, a possible way to achieve this would be the introduction of an optical chopper and a lock-in amplifier to 'home in' on the required signal. The recommendation for work regarding signal recovery would be to incorporate a lock-in amplifier into the detection system and carry out experiments to determine the frequency at which the optical chopper should operate.

References

Abbas AK (2000). Antibodies and Antigens. *Cell and Molecular Immunology*. Fourth Ed. **Saunders Company, USA**. Ch 3, 41-62.

Ahlin P, Kristl J, Kristl A and Vrecer F (2002). Investigation of polymeric nanoparticles as carriers of enalaprilat for oral administration. *International Journal of Pharmaceutics* **239**(1-2): 113-120.

Araujo L, Sheppard M, Lobenberg R and Kreuter J (1999). Uptake of PMMA nanoparticles from the gastrointestinal tract after oral administration to rats: modification of the body distribution after suspension in surfactant solutions and in oil vehicles. *International Journal of Pharmaceutics* **176**(2): 209-224.

Arica MY (2000). Epoxy-derived pHEMA membrane for use bioactive macromolecules immobilization: Covalently bound urease in a continuous model system. *Journal of Applied Polymer Science* **77**(9): 2000-2008.

Arica MY, Denizli A, Salih B, Piskin E and Hasirci V (1997). Catalase adsorption onto Cibacron Blue F3GA and Fe(III)-derivatized poly(hydroxyethyl methacrylate) membranes and application to a continuous system. *Journal of Membrane Science* **129**(1): 65-76.

Ayhan H (2002). Model Protein BSA Adsorption and Covalent Coupling onto Methyl Methacrylate Based Latex Particles with Different Surface Properties. *Journal of Bioactive and Compatible Polymers* **17**(4): 271-283.

Bangs Labs (1999a). **Adsorption to Microspheres**. *Beads Above the Rest: Technical Notes*. **Bangs Laboratories**. Retrieved <http://www.bangslabs.com/literature/technotes>.

Bangs Labs (1999b). **Lateral Flow Tests**. *Beads Above the Rest: Technical Notes*. **Bangs Laboratories**. Retrieved <http://www.bangslabs.com/literature/technotes>.

Bangs Labs (2002). **Working with Microspheres**. *Beads Above the Rest: Technical Notes*. **Bangs Laboratories**. Retrieved <http://www.bangslabs.com/literature/technotes>.

Baptista RP, Santos AM, Fedorov A, Martinho JMG, Pichot C, Elaissari A, Cabral JMS and Taipa MA (2003). Activity, conformation and dynamics of cutinase adsorbed on poly(methyl methacrylate) latex particles. *Journal of Biotechnology* **102**(3): 241-249.

Beesley JE (1989). *Colloidal Gold: A New Perspective for Cytochemical Marking*. **Oxford University Press: New York**.

Bell TE (2003). Technologies Developed by NASA's Office of Biological and Physical Research to Keep Air, Water, and Food Safe for Astronauts in Space Can also Help Protect People on Earth from Bioterrorism. *spaceresearch.nasa.gov*.

Biacore (2001). **Surface Plasmon Resonance**. *Technical Notes*. **Biacore**. Retrieved www.biacore.com/pdf/TN/TN_1.pdf

Borchard G, Audus KL, Shi F and Kreuter J (1994). Uptake of surfactant-coated poly(methyl methacrylate)-nanoparticles by bovine brain microvessel endothelial cell monolayers. *International Journal of Pharmaceutics* **110**(1): 29-35.

Boury F, Marchais H, Benoit JP and Proust JE (1997). Surface characterization of poly([alpha]-hydroxy acid) microspheres prepared by a solvent evaporation/extraction process. *Biomaterials* **18**(2): 125-136.

Campbell AI and Bartlett P (2002). Fluorescent hard-sphere polymer colloids for confocal microscopy. *Journal of Colloid and Interface Science* **256**(2): 325-330.

Capua I and Alexander DJ (2002). Avian influenza and human health. *Acta Tropica* **83**(1): 1-6.

Chandler J (2000). The Place of Gold in Rapid Tests. www.devicelink.com. **Medical Device Link**.

Chen X, Cui Z, Chen Z, Zhang K, Lu G, Zhang G and Yang B (2002). The synthesis and characterizations of monodisperse cross-linked polymer microspheres with carboxyl on the surface. *Polymer* **43**(15): 4147-4152.

Cox NJ, Tamblyn SE and Tam T (2003). Influenza pandemic planning. *Vaccine* **21**(16): 1801-1803.

Denizli A, Köktürk G, Salih B, Kozluca A and Pişkin E (1997). Congo red- and Zn(II)-derivatized monosize poly(MMA-HEMA) microspheres as specific sorbent in metal chelate affinity of albumin. *Journal of Applied Polymer Science* **63**(1): 27-33.

Denizli A, Yavuz H, Garipcan B and Arica MY (2000). Nonporous monosize polymeric sorbents: Dye and metal chelate affinity separation of lysozyme. *Journal of Applied Polymer Science* **76**(2): 115-124.

dictionary.com (2007). **sensor**. *The American Heritage® Dictionary of the English Language*. Retrieved 14 May 2007. <http://dictionary.reference.com/browse/sensor>.

Duke Scientific Corp (2004). **Reagent Microspheres-Surface Properties and Conjugation Methods**. *Technical Note 013C*. Retrieved

Ercole C, Gallo MD, Pantalone M, Santucci S, Mosiello L, Laconi C and Lepidi A (2002). A biosensor for Escherichia coli based on a potentiometric alternating biosensing (PAB) transducer. *Sensors and Actuators B: Chemical* **83**(1-3): 48-52.

Freiberg S and Zhu XX (2004). Polymer microspheres for controlled drug release. *International Journal of Pharmaceutics* **282**(1-2): 1-18.

Fried JR (2003). *Polymer Science and Technology. Second Ed.* **Prentice Hall:** Upper Saddle River, NJ.

Gella FJ, Serra J and Gener J (1991). Latex agglutination procedures in immunodiagnosis. *Pure and Applied Chemistry* **63**(8): 1131-1134.

Hale WG, Margham JP and Saunders VA, Eds. (1995). *Collins Dictionary of Biology.* **Harper Collins:** Glasgow.

Hall M, Kazakova I and Yao YM (1999). High sensitivity immunoassays using particulate fluorescent labels. *Analytical Biochemistry* **272**(2): 165-170.

Hegemann D, Brunner H and Oehr C (2003). Plasma treatment of polymers for surface and adhesion improvement. *Nuclear Instruments and Methods in Physics Research Section B: Beam Interactions with Materials and Atoms* **208**: 281-286.

Hermanson GT (1996). *Bioconjugate Techniques.* **Academic Press, Inc:** San Diego.

Hobson NS, Tothill I and Turner APF (1996). Microbial detection. *Biosensors and Bioelectronics* **11**(5): 455-477.

Huse K, Bohme HJ and Scholz GH (2002). Purification of antibodies by affinity chromatography. *Journal of Biochemical and Biophysical Methods* **51**(3): 217-231.

IUPAC (1997). **van der Waals forces.** *IUPAC Compendium of Chemical Terminology - the Gold Book.* **Blackwell Scientific Publications, Oxford.** Retrieved 23 August 2009. <http://goldbook.iupac.org/V06597.html>.

Jandt KD (2001). Atomic force microscopy of biomaterials surfaces and interfaces. *Surface Science* **491**(3): 303-332.

Jodar-Reyes AB, Martin-Rodriguez A and Ortega-Vinuesa JL (2006). Effect of the ionic surfactant concentration on the stabilization/destabilization of polystyrene colloidal particles. *Journal of Colloid and Interface Science* **298**(1): 248-257.

Jodar-Reyes AB, Ortega-Vinuesa JL and Martin-Rodriguez A (2005). Adsorption of different amphiphilic molecules onto polystyrene latices. *Journal of Colloid and Interface Science* **282**(2): 439-447.

Jodar-Reyes AB, Ortega-Vinuesa JL and Martin-Rodriguez A (2006). Electrokinetic behavior and colloidal stability of polystyrene latex coated with ionic surfactants. *Journal of Colloid and Interface Science* **297**(1): 170-181.

Kamei S, Okubo M, Matsuda T and Matsumoto T (1986). Adsorption of trypsin onto styrene-2-hydroxyethyl methacrylate copolymer microspheres and its enzymatic activity *Colloid & Polymer Science* **264**(9): 743-747.

Kinloch AJ (1987). *Adhesion and Adhesives: Science and Technology*. **Chapman and Hall**.

Köhler G and Milstein C (1975). Continuous cultures of fused cells secreting antibody of predefined specificity. *Nature* **256**: 496-497.

Kristensson K (2006). Avian influenza and the brain--Comments on the occasion of resurrection of the Spanish flu virus. *Brain Research Bulletin* **68**(6): 406-413.

Lehenkari PP, Charras GT, Nesbitt SA and Horton MA (2000). New technologies in scanning probe microscopy for studying molecular interactions in cells. *Expert Reviews in Molecular Medicine* **8** March(<http://www.expertreviews.org/00001575h.htm>).

Leonard P, Hearty S, Brennan J, Dunne L, Quinn J, Chakraborty T and O'Kennedy R (2003). Advances in biosensors for detection of pathogens in food and water. *Enzyme and Microbial Technology* **32**(1): 3-13.

Li S, Hu J and Liu B (2004). Use of chemically modified PMMA microspheres for enzyme immobilization. *Biosystems* **77**(1-3): 25-32.

Licker MD, Geller E, Weil J, Blumel D and Rappaport A, *Eds.* (2003). *McGraw-Hill Dictionary of Physics*. **McGraw-Hill**.

Liu Q, Hedberg EL, Liu Z, Bahulekar R, Meszlenyi RK and Mikos AG (2000). Preparation of macroporous poly(2-hydroxyethyl methacrylate) hydrogels by enhanced phase separation. *Biomaterials* **21**(21): 2163-2169.

López-León T, Jodar-Reyes AB, Ortega-Vinuesa JL and Bastos-Gonzalez D (2005). Hofmeister effects on the colloidal stability of an IgG-coated polystyrene latex. *Journal of Colloid and Interface Science* **284**(1): 139-148.

Lubarsky GV, Davidson MR and Bradley RH (2004). Characterisation of polystyrene microspheres surface-modified using a novel UV-ozone/fluidised-bed reactor. *Applied Surface Science* **227**(1-4): 268-274.

Magner E (1998). Trends in electrochemical biosensors. *Analyst* **123**: 1967-1970.

Martín-Rodríguez A, Cabrerizo-Vílchez MA and Hidalgo-Álvarez R (1996). Surface characterization of latexes with different interfacial properties. *Colloids and Surfaces A: Physicochemical and Engineering Aspects* **108**(2-3): 263-271.

Millipore (2003). **Protein concentration and diafiltration by tangential flow filtration** (Technical Brief). **Millipore**. Retrieved www.millipore.com/techpublications.

Moad G and Solomon DH (2006). *The Chemistry of Radical Polymerization*. 2nd Ed. **Elsevier Ltd**.

Müller M, Zentel R, Maka T, Romanov SG and Sotomayor Torres CM (2000). Dye-Containing Polymer Beads as Photonic Crystals. *Chemistry of Materials* **12**(8): 2508-2512.

Nicholson JW (1997). *The Chemistry of Polymers. 2nd Ed.* **The Royal Society of Chemistry.**

Odian G (2004). *Principles of Polymerization. Fourth Ed.* **John Wiley & Sons, Inc.**

Okubo M, Yamamoto Y and Kamei S (1989). XPS analysis (ESCA) of the surface composition of poly(styrene/2-hydroxyethyl methacrylate) microspheres produced by emulsifier-free emulsion polymerization. *Colloid & Polymer Science* **267**(10): 861-865.

Okubo M, Yamamoto Y, Uno M, Kamei S and Matsumoto T (1987). Immunoactivity of polymer microspheres with their hydrophilic/hydrophobic heterogeneous surface sensitized with an antibody. *Colloid and Polymer Science* **265**(12): 1061-1066.

Olal AD (1990). A Surface and Colloid Chemical Study of the Interaction of Proteins with Polystyrene Latex (PSL). *PhD Thesis.* **The University of British Columbia, Canada.**

Ortega-Vinuesa JL, Bastos-González D and Hidalgo-Alvarez R (1995). Comparative Studies on Physically Adsorbed and Chemically Bound IgG to Carboxylated Latexes, II. *Journal of Colloid and Interface Science* **176**(1): 240-247.

Ortega-Vinuesa JL and Hidalgo-Alvarez R (1993). Study of the adsorption of F(ab')₂ onto polystyrene latex beads. *Colloids and Surfaces B: Biointerfaces* **1**(6): 365-372.

Ortega-Vinuesa JL, Hidalgo-Alvarez R, las Nieves FJ, Davey CL, Newman DJ and Price CP (1998). Characterization of immunoglobulin G bound to latex particles using surface plasmon resonance and electrophoretic mobility. *Journal of Colloid and Interface Science* **204**(2): 300-311.

Paek SH, Lee SH, Cho JH and Kim YS (2000). Development of rapid one-step immunochromatographic assay. *Methods* **22**(1): 53-60.

Piirma I, Ed. (1982). *Emulsion Polymerization.* **Academic Press, Inc.:** New York.

Plotz CM and Singer JM (1956a). The latex fixation test. I. Application to the serologic diagnosis of rheumatoid arthritis. *American Journal of Medicine* **21**(6): 888-892.

Plotz CM and Singer JM (1956b). The latex fixation test. II. Results in rheumatoid arthritis. *American Journal of Medicine* **21**(6): 893-896.

Rich RL and Myszka DG (2003). Spying on HIV with SPR. *Trends in Microbiology* **11**(3): 124-133.

- Romanov SG, Maka T, Torres CMS, Müller M and Zentel R (2001). Thin film photonic crystals. *Synthetic Metals* **116**(1-3): 475-479.
- Rudin A (1999). *The Elements of Polymer Science and Engineering. Second Ed. Academic Press.*
- Schultz J and Nardin M (2003). Theories and Mechanisms of Adhesion. *Handbook of Adhesive Technology. 2nd Ed. Marcel Dekker, Inc.* Ch 3, 53-67.
- Seradyn (1999). **Polystyrene and carboxylate-modified microparticles.** *Technical Notes.* Retrieved www.seradyn.com/technical/pdf/polystyrene.pdf.
- Shyu RH, Shyu HF, Liu HW and Tang SS (2002). Colloidal gold-based immunochromatographic assay for detection of ricin. *Toxicon* **40**(3): 255-258.
- Siiman O, Burshteyn A and Insausti ME (2001). Covalently Bound Antibody on Polystyrene Latex Beads: Formation, Stability, and Use in Analyses of White Blood Cell Populations. *Journal of Colloid and Interface Science* **234**(1): 44-58.
- Tauer K, Imroz Ali AM and Sedlak M (2005). On the preparation of stable poly(2-hydroxyethyl methacrylate) nanoparticles. *Colloid & Polymer Science* **283**(4): 351-358.
- Taylor AD, Yu Q, Chen S, Homola J and Jiang S (2005). Comparison of E. coli O157:H7 preparation methods used for detection with surface plasmon resonance sensor. *Sensors and Actuators B: Chemical* **107**(1): 202-208.
- Thévenot D, Toth K, Durst R and Wilson G (1999). Electrochemical biosensors: Recommended definitions and classification (Technical Report). *Pure and Applied Chemistry* **71**(12): 2333-2348.
- Unilever PLC GB (1988). Immunoassays and Devices Therefor. **Patent No. WO 88/08534.**
- University of Newcastle upon Tyne (1999). **Online Medical Dictionary.** Retrieved <http://cancerweb.ncl.ac.uk/cgi-bin/omd?biosensor>.
- Uzun L, Odabaşı M, Arıca Y and Denizli A (2005). Poly(Styrene-Hydroxyethyl Methacrylate) Monodisperse Microspheres as Specific Sorbent in Dye Affinity Adsorption of Albumin. *Separation Science and Technology* **39**(10): 2401 - 2418.
- Wang DQ, Liu BL, Hu J, Lin XQ and Zhang M (2004). A novel method for preparing approximately micron-sized polymethyl methacrylate microspheres with clear surface. *Chinese Chemical Letters* **15**(3): 371-374.
- Weiser HB (1933). *Inorganic Colloid Chemistry Volume I: The Colloidal Elements. John Wiley and Sons, Inc.:* New York.
- West P (2007). **Introduction to Atomic Force Microscopy: Theory, Practice and Applications. Pacific Nanotechnology.** Retrieved April. www.afmuniversity.org.

Wong SS (1993). *Chemistry of Protein Conjugation and Cross-Linking*. **CRC Press, Inc.**

Wu L, Zhang Q, Su L, Huang M, Zhao J and Yang M (2007). Effects of small molecular inhibitors on the binding between HIV-1 reverse transcriptase and DNA as revealed by SPR biosensor. *Sensors and Actuators B: Chemical* **122**(1): 243-252.

Xu X, Jin M, Yu Z, Li H, Qiu D, Tan Y and Chen H (2005). Latex Agglutination Test for Monitoring Antibodies to Avian Influenza Virus Subtype H5N1. *J. Clin. Microbiol.* **43**(4): 1953-1955.

Yavuz H, Bayramoglu G, Kacar Y, Denizli A and Yakup Arica M (2002). Congo Red attached monosize poly(HEMA-co-MMA) microspheres for use in reversible enzyme immobilisation. *Biochemical Engineering Journal* **10**(1): 1-8.

APPENDIX I Sample Calculations

Appendix I-A Calculating % w/v of Microspheres in an Aqueous Suspension

Defining Variables

m_g = mass of beaker or watch glass (g)

m_{wt} = total mass of beaker + wet sample (g)

m_{dt} = total mass of beaker + dry sample (g)

Equations

$$\text{mass of wet sample, } m_{ws} = m_{wt} - m_g \quad (\text{g}) \quad (\text{I.A.1})$$

$$\text{mass of dry sample, } m_{ds} = m_{dt} - m_g \quad (\text{g}) \quad (\text{I.A.2})$$

$$\begin{aligned} \text{mass of water in suspension, } m_w &= m_{ws} - m_{ds} \quad (\text{g}) \\ \text{volume of water in suspension, } V_w &= m_w \quad (\text{g}) \end{aligned} \quad (\text{I.A.3})$$

$$\begin{aligned} \text{concentration of sample, } c_1 &= \frac{m_{ds}}{m_w} \quad (\text{g } l^{-1}) \\ \% \text{ w/v} &= c_1 \times 100\% \quad (\% \text{ w/v}) \text{ or } (\% \text{ solids}) \end{aligned} \quad (\text{I.A.4})$$

Sample Calculations

$$m_g = 6.4348 \text{ g}$$

$$m_{wt} = 8.4761 \text{ g}$$

$$m_{dt} = 6.6090 \text{ g}$$

$$\begin{aligned} m_{ws} &= m_{wt} - m_g \\ &= 8.4761 - 6.4348 \\ &= 2.0413 \text{ g} \end{aligned}$$

$$\begin{aligned}m_{ds} &= m_{dt} - m_g \\ &= 6.6090 - 6.4348 \\ &= 0.1742 \text{ g}\end{aligned}$$

$$\begin{aligned}m_w &= m_{ws} - m_{ds} \\ &= 2.0413 - 0.1742 \\ &= 1.8671 \text{ g}\end{aligned}$$

$$\begin{aligned}c_1 &= \frac{m_{ds}}{m_w} \\ &= \frac{0.1742}{1.8671} \\ &= 0.0933 \text{ g ml}^{-1}\end{aligned}$$

$$\begin{aligned}\% \text{ w/v} &= c_1 \times 100\% \\ &= 9.3\% \text{ solids}\end{aligned} \tag{I.A.5}$$

Appendix I-B Preparation of a Required Concentration, c_2 , of Microspheres in a Specified Total Volume, V_T , using the Sample from Appendix I-A

Let

c_1 = concentration of available sample ($g\ ml^{-1}$)

c_2 = required concentration ($g\ ml^{-1}$)

m = mass of microsphere in sample of required concentration (g)

V_T = specified total volume (ml)

$$\text{volume of water required, } V_w = m \left(\frac{1}{c_2} - \frac{1}{c_1} \right) \quad (ml) \quad (\text{I.B.1})$$

$$\text{volume of original sample required, } V_s = V_T - V_w \quad (ml) \quad (\text{I.B.2})$$

To prepare 100 ml of 0.01 $g\ ml^{-1}$ (1% w/v) microsphere suspension:

$c_1 = 0.093\ g\ ml^{-1}$ (calculated in Appendix I-A)

$c_2 = 0.01\ g\ ml^{-1}$

$V_T = 100\ ml$

Mass of microspheres in 100 ml of 0.01 $g\ ml^{-1}$ microsphere suspension

$$m = c_2 \times V_T = 0.01 \times 100 = 1\ g$$

$$V_w = m \left(\frac{1}{c_2} - \frac{1}{c_1} \right) = \frac{1}{0.01} - \frac{1}{0.093} = 89.25\ ml$$

$$V_s = V_T - V_w = 100 - 89.25 = 10.75\ ml$$